

---

## **Vulnerability of structures to collapse during the decay phase of a fire**

**Auteur** : Gamba, Antonio

**Promoteur(s)** : Gernay, Thomas

**Faculté** : Faculté des Sciences appliquées

**Diplôme** : Master en ingénieur civil des constructions, à finalité spécialisée en "civil engineering"

**Année académique** : 2016-2017

**URI/URL** : <http://hdl.handle.net/2268.2/2561>

---

### *Avertissement à l'attention des usagers :*

*Tous les documents placés en accès ouvert sur le site le site MatheO sont protégés par le droit d'auteur. Conformément aux principes énoncés par la "Budapest Open Access Initiative"(BOAI, 2002), l'utilisateur du site peut lire, télécharger, copier, transmettre, imprimer, chercher ou faire un lien vers le texte intégral de ces documents, les disséquer pour les indexer, s'en servir de données pour un logiciel, ou s'en servir à toute autre fin légale (ou prévue par la réglementation relative au droit d'auteur). Toute utilisation du document à des fins commerciales est strictement interdite.*

*Par ailleurs, l'utilisateur s'engage à respecter les droits moraux de l'auteur, principalement le droit à l'intégrité de l'oeuvre et le droit de paternité et ce dans toute utilisation que l'utilisateur entreprend. Ainsi, à titre d'exemple, lorsqu'il reproduira un document par extrait ou dans son intégralité, l'utilisateur citera de manière complète les sources telles que mentionnées ci-dessus. Toute utilisation non explicitement autorisée ci-avant (telle que par exemple, la modification du document ou son résumé) nécessite l'autorisation préalable et expresse des auteurs ou de leurs ayants droit.*

---



Université de Liège – Faculté des sciences appliquées

---

VULNERABILITY OF STRUCTURES TO COLLAPSE  
DURING THE DECAY PHASE OF A FIRE

---

Travail de fin d'études réalisé par  
GAMBA Antonio  
en vue de l'obtention du grade de Master en  
Ingénieur civil des constructions, à finalité approfondie

MEMBRES DU JURY

Gernay Thomas (promoteur)

Franssen Jean Marc

Demonceau Jean-François

Felicetti Roberto

Année académique 2016-2017.



# Summary

**Title:** Vulnerability of structures to collapse during the decay phase of a fire

**Author:** Gamba Antonio, Second year master student in civil engineering

**Academic Year:** 2016-2017

When a fire develops in a building, it leads to an increase in the temperature until reaching a peak and then is followed by a decrease and return to ambient temperature. Until now fire engineering has mainly focused on the effect of heating phase on structures, using standardize fire models that consist of continuously increasing temperature over time. As a direct consequence, the knowledge about the structural behavior during the cooling phase of a fire is very limited.

The objective of this work is the investigation of the behavior of structures when subjected to the full course of natural fires, until burnout, in particular referred to their response based on the variation of certain parameters such as fire severity, applied load and element geometry. The study aim it is addressed by performing different parametric analysis upon frames made of different typology and constituting material such as Steel and Concrete. The nonlinear finite element software used to perform the numerical analysis it is validated using data from a study upon a real steel tested structure.

The work is mainly focused on steel structure for which there were a support of data from a real tested structure respect to concrete. The main founding regarding the structural response during the decay phase of the fire, are enhancing the actual knowledge on the topic, showing for example how based on the structure geometry it is possible to have different structural response that lead to local or global structural failure. The different ways to fail and behave underlining the structural vulnerability related to the parameter adopted.



## Acknowledgments

I would first to thank my thesis advisor Thomas Gernay his door's office was always open whenever I ran into a trouble spot or had a question about my research. He consistently allowed this paper to be my own work, but steered me in the right direction whenever I needed.

During those academic years I had the pleasure to meet different professors in different country, I would like to acknowledge every one for sharing their knowledge enhancing my professional luggage and preparation. In particular to Professor J.M. Franssen and my advisor Thomas Gernay, thanks to them I discovered fire safety engineering that for me was a totally new field. If I fall captured for this subject it is also their achievement.

Then I would like to thanks the members of my theses committee for the time spent to read my work.

Durante questo avvincente viaggio ho avuto il piacere di essere circondato da tante persone che mi sono state vicine ed hanno contribuito ad arricchire la mia vita in mille modi diversi. Ringrazio tutti i miei amici che anche dall'Italia hanno avuto il tempo di venirmi a trovare fin qui in Belgio, ringrazio i ragazzi del B52, Laura, Marina, Alessia , Tommaso, Joao e Jocelyn.

Ringrazio la mia famiglia, mio nonno Giovanni e la mia compagna per il continuo supporto e vicinanza.

Ultimi ma non per importanza ringrazio i miei genitori, le persone a me più care, le quali hanno sempre creduto nelle mie doti e capacità, senza il loro supporto tutto questo non sarebbe stato possibile.



# TABLE OF CONTENTS

<b>SUMMARY</b> .....	<b>II</b>
<b>ACKNOWLEDGMENTS</b> .....	<b>IV</b>
<b>TABLE OF CONTENTS</b> .....	
<b>1. INTRODUCTION</b> .....	<b>1</b>
1.1 MOTIVATION OF THE STUDY .....	1
1.2 OBJECTIVES .....	2
1.3 STRUCTURE .....	2
<b>2. STATE OF THE ART</b> .....	<b>3</b>
2.1 FIRE MODELS .....	3
2.1.1 <i>Definition of ISO standard fire curve</i> .....	3
2.1.2 <i>Definition of Natural fire curve</i> .....	4
2.2 MATERIAL BEHAVIOR UNDER NATURAL FIRE .....	5
2.2.1 <i>Concrete behavior under natural fire</i> .....	5
2.2.2 <i>Steel behavior under natural fire</i> .....	6
2.3 STRUCTURAL BEHAVIOR UNDER NATURAL FIRE .....	7
2.3.1 <i>Duration Heating Phase concept (DHP)</i> .....	7
2.4 CONCLUSION .....	8
<b>3. EXPERIMENTAL TEST – STEEL STRUCTURE</b> .....	<b>9</b>
3.1 TEST SET-UP AND PROCEDURE.....	9
3.2 GEOMETRY.....	9
3.3 MATERIALS .....	10
3.4 APPLIED LOADS .....	11
3.5 FIRE CURVES ADOPTED .....	12
3.6 RESULTS.....	14
3.6.1 <i>Test Frame Temperature Evolution</i> .....	14
3.6.2 <i>Displacements</i> .....	17
3.6.3 <i>Strains</i> .....	20
<b>4. DESCRIPTION AND VALIDATION OF THE NUMERICAL MODEL – SAFIR VALIDATION</b> <b>23</b>	
4.1 SAFIR® - OVERVIEW .....	23
4.2 PROBLEM DATA .....	24
4.2.1 <i>Geometry, Conditions and Material</i> .....	24
4.2.2 <i>Boundary Conditions</i> .....	28
4.2.3 <i>Applied Loads</i> .....	29
4.2.4 <i>Elements Properties</i> .....	30
4.3 RESULTS.....	31
4.3.1 <i>Temperature in the heated column</i> .....	31

4.3.2 Displacements.....	34
4.3.3 Load Transfer.....	37
<b>5. VULNERABILITY OF STEEL STRUCTURE UNDER NATURAL FIRE.....</b>	<b>39</b>
5.1 REFERENCE MODEL.....	39
5.1.1 Materials.....	40
5.2 PARAMETRIC ANALYSIS.....	40
5.2.1 Beams Cross-section.....	40
5.2.2 Load Ratio.....	42
5.2.3 Fire Curves.....	43
5.2.4 Conclusion.....	44
5.3 RESULTS.....	44
5.3.1 General Overview.....	44
5.3.2 Frame 1.....	46
5.3.3 Frame 2.....	49
5.3.4 Frame 3.....	54
5.4 CONCLUSIONS.....	62
<b>6. VULNERABILITY OF REINFORCED CONCRETE STRUCTURE UNDER NATURAL FIRE..</b>	<b>66</b>
6.1 GENERAL DESIGN.....	66
6.1.1 Geometry.....	66
6.1.2 Columns & Beams.....	67
6.1.3 Material properties.....	68
6.2 PARAMETRIC ANALYSIS.....	70
6.2.1 Applied Load.....	70
6.2.2 Fire curves.....	71
6.2.3 Convergence criteria and settings.....	72
6.3 RESULTS.....	73
6.3.1 General Overview.....	73
6.3.2 Frame 1.....	74
6.3.3 Frame 2 & 3.....	77
<b>7. CONCLUSION.....</b>	<b>81</b>
<b>8. APPENDIX.....</b>	<b>83</b>
8.1 PARAMETRIC TEMPERATURE-FIRE CURVES.....	83
8.2 DURATION OF HEATING PHASE (DHP).....	84
8.3 MAXIMUM LOAD CAPACITY AT AMBIENT TEMPERATURE.....	86
<b>LIST OF FIGURES.....</b>	<b>A</b>
<b>LISTS OF TABLES.....</b>	<b>C</b>
<b>BIBLIOGRAPHY.....</b>	<b>D</b>



# 1. INTRODUCTION

The title of my master thesis: “Vulnerability of structures to collapse during the decay phase of a fire” involves different concepts. First of all it is possible to understand the main field of the studied topic, fire safety engineering. Furthermore it is underlined the importance of the vulnerability concept under certain condition, for instance a decay phase of a fire.

## 1.1 Motivation of the study

When a fire develops in a building, it leads to an increase in the temperature until reaching a peak and then is followed by a decrease and return to ambient temperature. Until now fire engineering has mainly focused on the effect of heating phase on structures, using standardize fire models that consist of continuously increasing temperature over time. As a direct consequence, the knowledge about the structural behavior during the cooling phase of a fire is very limited.

The recent past underlined the gap of knowledge between the two fire phases (heating and cooling) above mentioned, with different cases of structural collapse during the cooling phase of a fire. An example is the delayed failure of an underground car park in Switzerland where seven member of the fire brigade lost their lives. Those men were in the car park after having successfully fought the fire when the concrete structure suddenly collapsed (1). A more recent tragedy happens in Iran, precisely in the city of Tehran where the Plasco Building collapsed the 19<sup>th</sup> January 2017. This high raise multi storey concrete building, was one among the tallest structure in the country with 17 floors. Firefighters battled the blaze for several hours before the building, just north of the capital’s sprawling bazaar, fell. Police tried to keep out shopkeepers and other wanting to rush back in order to collect their valuables, having seen the flame burnout. The building came down in a matter of seconds after several hours and 20 firefighters have died in the tragic event (2).

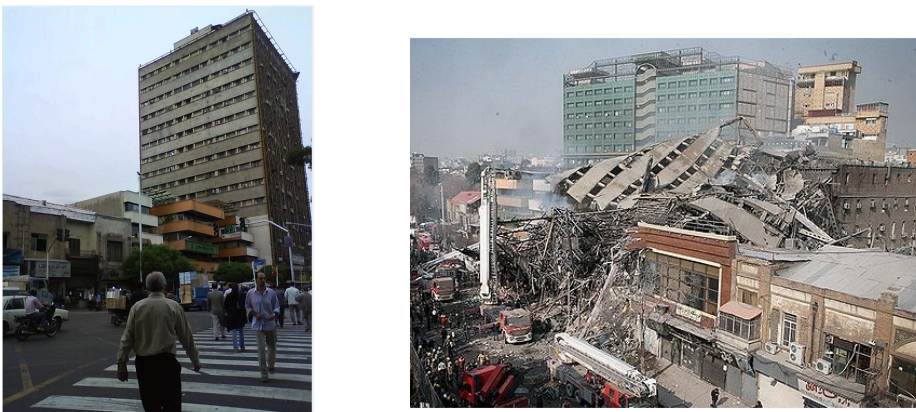


Figure 1 - Plasco Building before and after the event.

## **1.2 Objectives**

Herein above it has been showed some tragic events, underlining the point that a structure may collapse after the time of maximum fire temperature in a compartment. The fact that safety of structures is not ensured during the cooling phase is due to a conjunction of different factors, which makes this problem both complex and fascinating. The aim of this work is principally the investigation of the structures behavior when subjected to the full course of the natural fires until the complete burnout. More specifically it is tried to identify the key mechanism influencing the response of structures during the decay phase of a fire and quantifying the vulnerabilities as a function of their typology and constituting materials.

The way in which it is handled the problem is by means of numerical simulations sustained from physical reasoning. Simulation of both steel and concrete structure are run under natural fire models, in order to understand which are the parameters and the mechanisms influencing the response of structure during the course of the decay phase of a fire. The nonlinear finite element software SAFIR developed in the university of Liège by J.M. Franssen and T.Gernay, is adopted in order to performs the numerical simulation and problem modeling.

## **1.3 Structure**

The study has been organized in six main chapters, after the introduction a general overview of the state of the art is given. The aim is to make the reader aware of the most important basic concept related to the fire safety engineering and at the same time gives a general outlook on the progress made about this topic, which is a very fresh one. After that it will be presented the input study that triggered all of this research, it consists in an experimental test made upon a steel frame under natural fire. Real tested structures under natural fire are rare, and this one in particular gives precious information concerning the behavior of structures under natural fire valuable for my study purpose. Since the majority of the work is realized by using nonlinear finite element software, the tested frame mentioned before, is taken in order to validate the software used for further analysis. After the software validation, a steel reference frame is chosen and different numerical simulations are done in order to address the proposed objectives. Furthermore in order to have a comparison of the structural behavior among more than one material, the same it is done for a concrete frame. I would like to specify that more time have been dedicated to the steel structure just because the input study on which it was made the software validation was made of steel; as a consequence there are more data about the steel frame respect to the concrete.

## 2. STATE OF THE ART

### 2.1 Fire Models

As it was mentioned, this work involves the fire safety-engineering field and in particular the concept of vulnerability of structure under a cooling phase. For this reason it is necessary deliver some of the key point definition about standard and natural fire curves. Where the aim is pointed to understand the two different fire approach and the very basic concept in the fire engineering to facilitate the understanding of the paper.

#### 2.1.1 Definition of ISO standard fire curve

The fire action on a structure can be represented using models, by adopting a prescriptive approach it is implicitly chosen to adopt a standardized fire curve. The concept behind this kind of curve is the possibility to have a standard representation that is useful for comparison and classification between the different tested elements. The fire resistance criterion is to ensure the required function during the prescribed duration. The construction does not require additional data; the equation is only in function of the time and it is proposed in EN1991-1-2 (3).

The ISO curve follows these simple assumptions:

- It is applied to the whole compartment even if it is large
- Does not have a cooling down phase and never decrease
- Does not consider the Pre-Flashover phase
- Does not depend on the fire load and the ventilation conditions

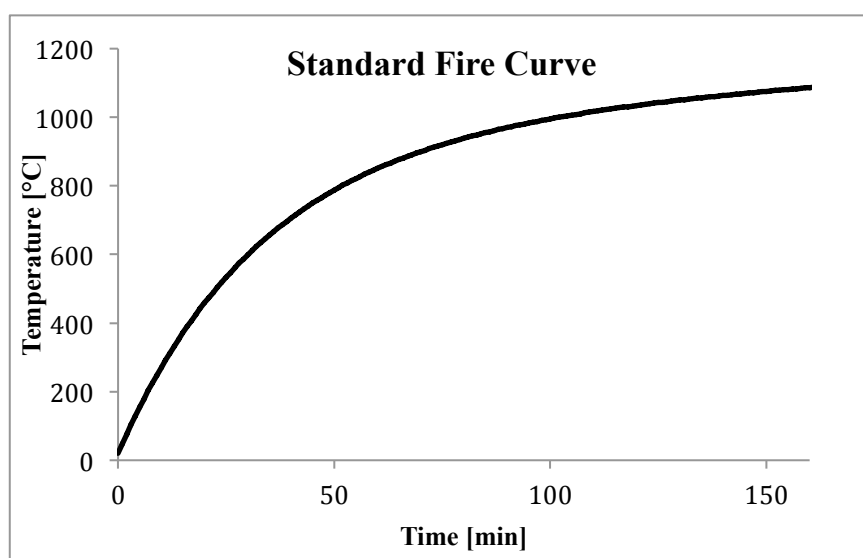


Figure 2 - ISO standard fire curve EN1991-1-2

### 2.1.2 Definition of Natural fire curve

When the designer decides to adopt a natural fire curve in order to make the study, he implicitly chooses to deal with a performance-based approach. The objective of this kind of study is to have a realistic representation of the temperature evolution based on physics. Furthermore the resistance criterion is not anymore the one to ensure a required function during prescribed time duration, instead is the one to ensure the required function during the whole fire duration, including decay and extinction. The natural fire model are divided in two main categories, on one side there are the so-called simplified fire model, and on the other the advanced fire model. For what concern the simplified fire model it is possible to have localized and full compartment fire, instead the others enclose Two-zone, One-zone model and CFD. The common feature among all of them is that for every natural fire model is required an exact geometry of the problem and other data input such as fire surface, fire load, boundary properties and opening.

Here below an example of a full compartment parametric fire, the construction it is done by following the Annex A in EN1991-1-2 (3) with an heating phase of 90 minutes and a total duration of almost 250 minutes. In the appendix, chapter 8.1 it is explained how to build such kind of fire.

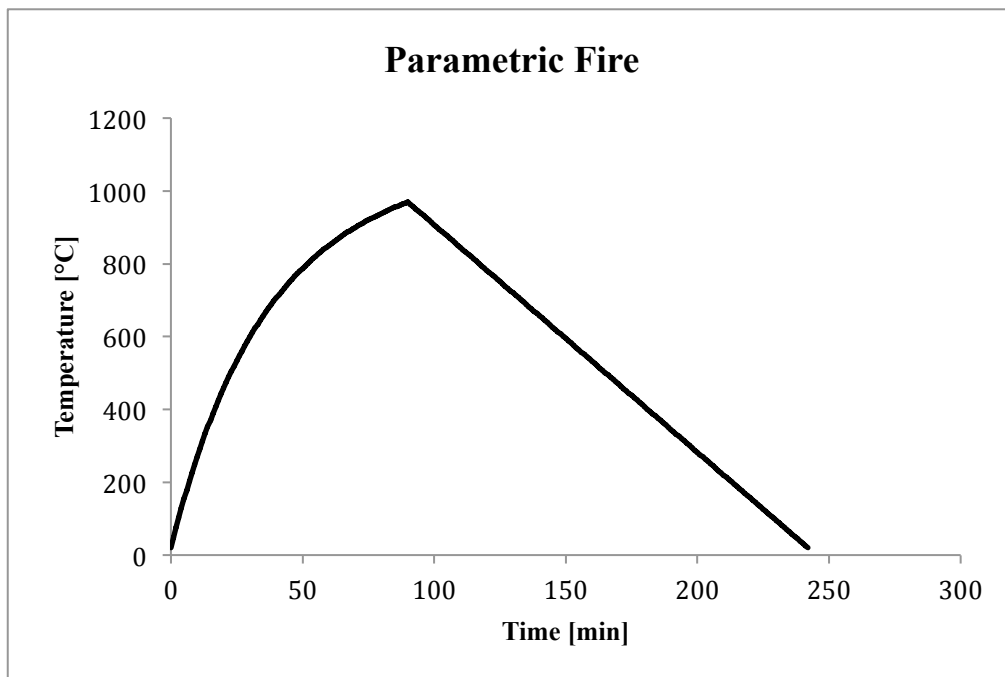


Figure 3 - Parametric fire curve Appendix A of EN1991-1-2 (3)

## 2.2 Material behavior under natural fire

The researches available related to the vulnerability of structures under a natural fire are almost entirely focused on the parameters and intrinsic properties of the various materials. This is why, it is a fresh topic and the authors needed to understand how the main construction materials (concrete, steel) behave under a totally new conditions such as the one given in the cooling phase. Then during the recent past other authors started to study the phenomena at the element level and also proposed a performance indicator for structure under natural fire, the so-called DHP.

### 2.2.1 Concrete behavior under natural fire

According to Yi-Hai L, Franssen J. M. (4), study in which were gathered more than 900 concrete samples, tested under the same condition, hence comparable between each others, it was possible to define correctly the concrete behavior under natural fire, in particular referred to its compressive strength during the heating and cooling phase. The results for the heating phase of the fire, confirmed the proposal model from (5) that establish a gradual decrease of compressive strength of the concrete during the first phase of the fire.

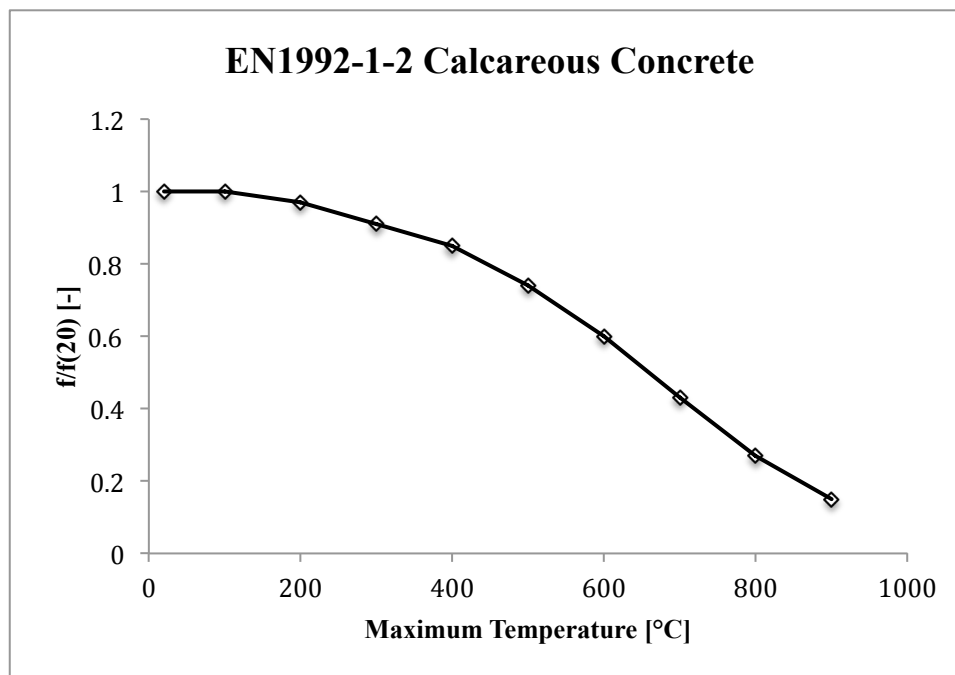


Figure 4 - Calcareous concrete compressive strength behavior during heating according to EN1992-1-2 (5)

The vertical axe represents the compressive strength ratio between the one depending on temperature and the other at ambient temperature. The horizontal axe shows the temperature evolution.

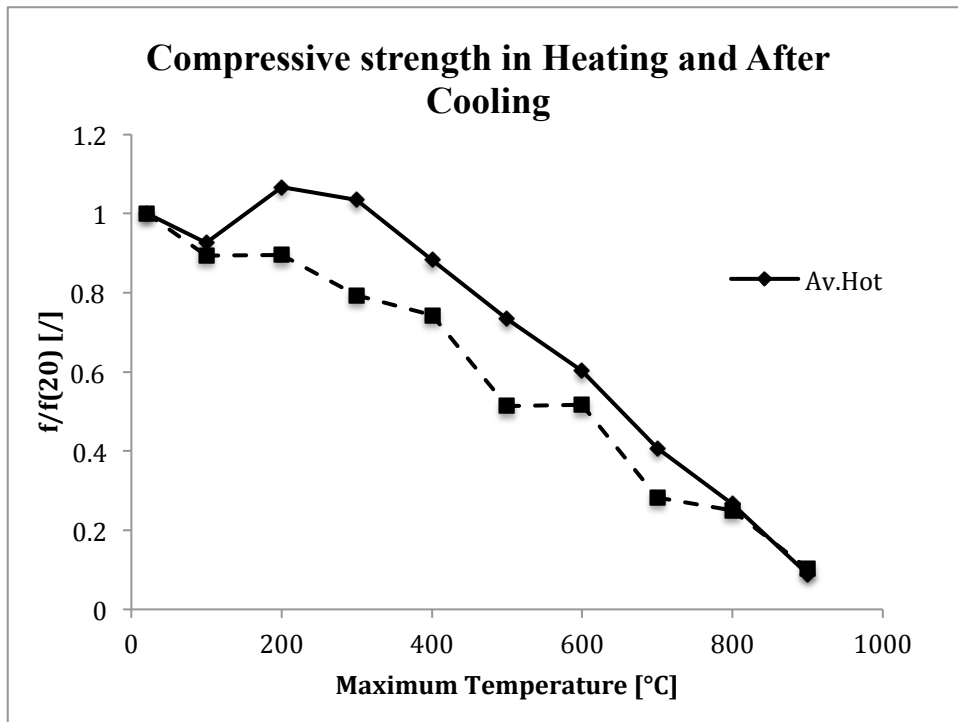


Figure 5 - Comparison between Hot and Residual Compressive Strength, from (4)

The most important output of the research, concern the behavior of the concrete under the cooling phase of the fire, in fact it has shown to experience an additional decreasing in the compressive strength (see Figure 5), quantified from the authors as far above 10% while the gas temperature came back to the ambient temperature. This is an important point able to underline a potential cause of the vulnerability during the cooling phase of a fire for concrete structures. As a remark, within the EN1994-1-2 (6) it is possible to find suggestion about this additional lost of strength during the cooling phase but nothing is stated in EN1992-1-2 (5).

### 2.2.2 Steel behavior under natural fire

Regarding the structural steel behavior under natural fire condition it is possible to say that it has a different way to behave compared to the concrete. In particular, an hypothesis often quoted on the mechanical behavior of steel under natural fire, consist in consider the tensile strength as reversible under a limit temperature of 600°C (7). To summarize, if the temperature does not exceed 600°C, the steel strength is considered reversible, as a

consequence the material will fully recover the strength until the initial value. Otherwise if the material is heated beyond 600°C a loss of residual yield strength should be considered.

## **2.3 Structural behavior under natural fire**

For the author's knowledge, researches on the behavior under natural fire are very scarce in literature. An important contribution can be found in (8) where the authors investigated on the behavior of different structural element such as steel, concrete, wood columns and beams, by proposing a performance indicator able to characterize the behavior of structures under natural fire (DHP).

### ***2.3.1 Duration Heating Phase concept (DHP)***

The fire resistance rating (R) has been adopted as a reference indicator in order to assess the performance of structure in fire. It is defined as the duration of time in which a structural component is able to fulfill predefined criteria such as integrity, stability and heat transmission under standardized fire condition (9). On the other hand, in a performance-based approach the fact that structure shows stability during the time of maximum temperature does not guarantee stability against latter failure. It is clear how the (R) indicator is not suitable in order to characterize a structure sensitivity to delayed failure since it is based on a monotonically increasing fire curve (8). It is proposed from the authors of the previous quoted study an indicator able to suit the description of the performance under a performed based environment.

DHP or Duration of the Heating Phase, “by definition it represents the minimum exposure time to standard ISO fire followed by cooling phase in accordance with EN1991-1-2 that will eventually result in a failure of the structural component (either be it in the heating phase, in the cooling phase or after at the termination of the fire)” (8).

The main features of this indicator are:

- It is unique, because associated to the ( $\Gamma=1$ ) of EN1991-1-2 parametric fire model Annex A. This leads to have for a given  $t_{max}$  a well-defined temperature evolution for both heating and cooling phases. (See 8.1)
- The DHP is an unequivocal characterization of a certain performance given a certain load level and structural component.
- It is able to make comparison between different structural systems under natural fire.
- DHP does not give any indication about time of collapse.

## **2.4 Conclusion**

The state of the art shows us how there are two different approaches in order to model a fire. The performance based is often indicated as the most suitable if we want to take into account the vulnerability of the structure in all of the fire phases. Furthermore the studies made on the vulnerability of structure during the cooling phase are scarce, and most of them are focused on the mechanical propriety of the material during cooling. It is possible to find some studies regarding the vulnerability in terms of element behavior such as columns and beams made of steel, concrete and wood but not much it is done at the structural level. This is one among the reasons why this research will investigate about the behavior at the structural level. The DHP indicator will be used in order to characterize and compare the obtained results, it is a key indicator for the research and it is possible know more in appendix chapter 8.2, where it is explained how it is possible to find it.

### **3. EXPERIMENTAL TEST – STEEL STRUCTURE**

The authors Binhui Jiang, Guo-Qiang Li, Liulian Li, B.A. Izzuddin in (10), were able to perform a test on 3 different structures with the same geometry, applying to the central column three different natural fires. Furthermore using different measurement instrumentations such as thermocouple and displacement gauges, obtained interesting data output. This research is very significant, because experimental researches on structures under natural fire are very scarce, so the authors give very important data to all the research community. Furthermore from the output of the experimental tests performed, it was possible to notice an interesting load transfer phenomena during the cooling phase of the fire, from the heated column to the side one not even heated. This particular fact is one among the leading reasons for which this research it has been chosen as starting point of my study, by thinking that it might be a correlation between the phenomena observed and the vulnerability of the structure under the decay phase of the fire. Here in this chapter the study made (10) is explained and in the next chapter it will be done a validation of the software used for the further numerical analysis. The aim of the validation is mostly the one to being sure that SAFIR® is able to capture the main output results given from the tested frame.

#### **3.1 Test Set-Up and Procedure**

The central column at the ground floor of each different test frame was heated through a particular electrical furnace. The middle part of the furnace is designed in such a way to hang on the beams of the test frames, allowing the vertical deformation of the structure, so the vertical deflection is allowed.

The test were conducted following each time the same procedure: set in place the test frame; installation of the safety system; load positioning; installation of measures instrumentation; turned on the measurement systems, then as last step turn on the electrical furnace.

#### **3.2 Geometry**

The test frame is made of four bays and two stories, the span length of the two middle bays is 2.2 m each and the two side bays 2.0 m each, the heights of the columns are 1.3 m and 1.2 m for the first and second storey respectively.

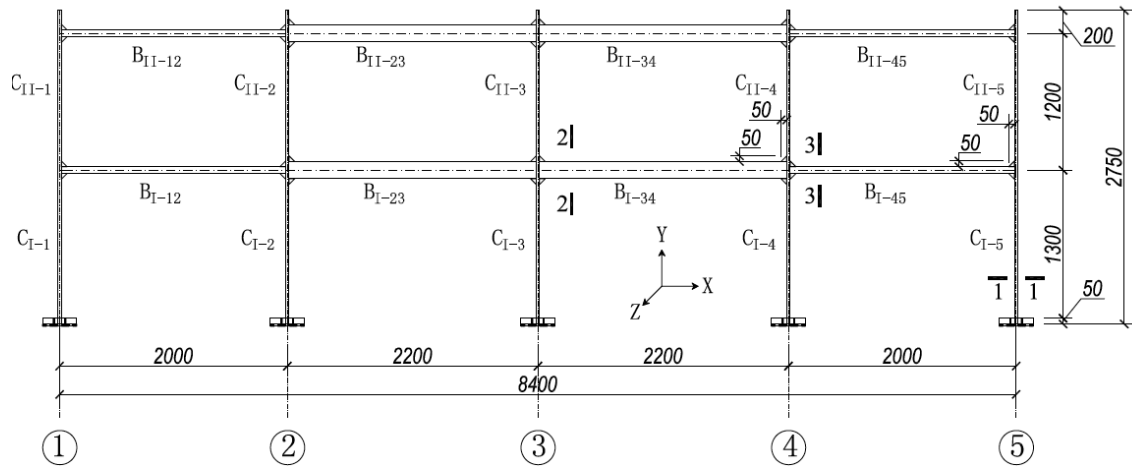


Figure 6 - Test Geometry, image takes from (10)

At the sectional level, the frame is made of rectangular tubular sections for the columns and beams of the all test frames.

FRAME No.	Column	Middle beam	Side Beam
1	50x30x3	150x50x5	60x40x3,5
2	50x30x3	60x40x3,5	60x40x3,5
3	50x30x3	60x40x3,5	60x40x3,5

Table 1 - Details of member sections (mm)

### 3.3 Materials

The material is steel for all the column and beams; the following table summarizes the material proprieties through specimen test.

Tube Section	Depth (mm)	$E_s$ (Gpa)	$\sigma_y$ (Mpa)	$\sigma_u$ (Mpa)	$\epsilon_u$
150x50x5	5	205,04	310,8	563,23	0,2
60x40x3,5	3,5	208,27	290,03	519,25	0,18
50x30x3	3	208,23	360,78	534,78	0,16

Table 2 - Material Proprieties

### 3.4 Applied Loads

The authors noticed that by applying a constant load by using hydraulic jack might cause difficulties in simulating constant gravity load during the whole test duration, in particular at the moment of column buckling. For this reason real gravity load were applied on the test frame by using metal lumps, which were contained in steel boxes fixed in each beams. Since gravity load were used to load the test frames, a safety system was needed to prevent damage to the test devices and reduce risk to human operators. So four steel cables, connected to the restraint frames, were used to prevent too large vertical deflection and other four steel cables were used in order to prevent too large lateral displacement as well.

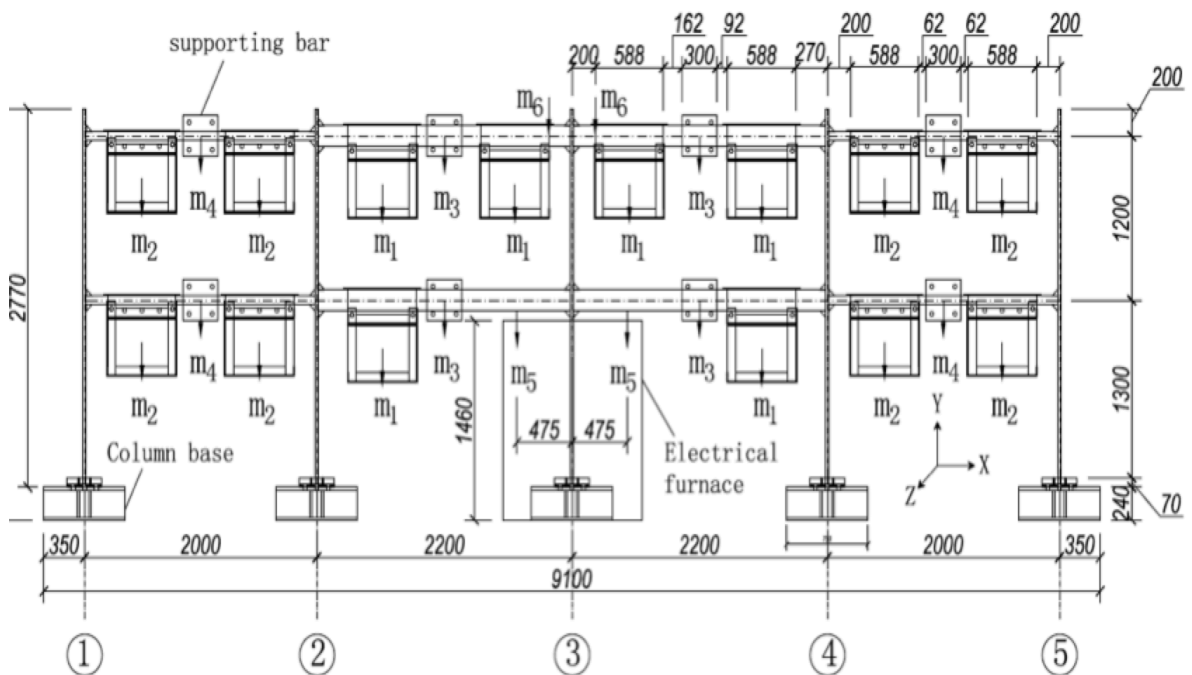


Figure 7 - Mass Distribution, images taken from (10)

In the figure shown above it is possible to see how the mass are distributed on the structural frame. In particular:

FRAME No.	m1 (kg)	m2 (kg)	m3 (kg)	m4 (kg)	m5 (kg)
1	296,94	179,66	71,56	7,54	7,55
2	476,26	235,96	76,54	7,11	8,34
3	754,44	379,25	76,54	7,11	10,58

Table 3 - Details of weight carried by the Test Frame

The masses m3 and m4 represents the weight of each supporting bar for the out-of-plane restraint adopted on the beams.

### 3.5 Fire Curves adopted

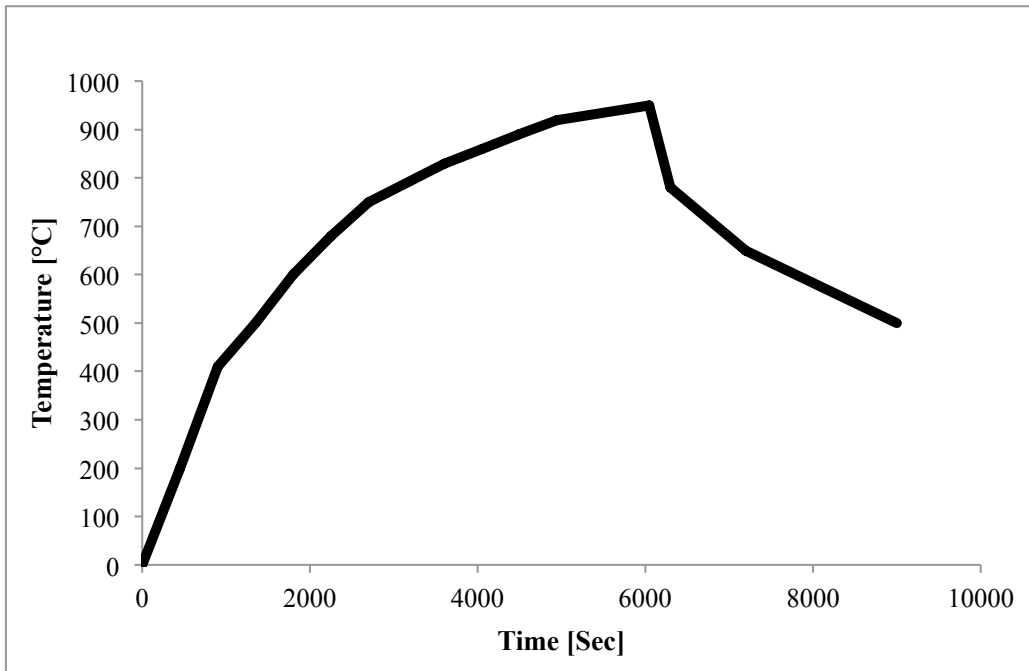


Figure 8 - Fire Curve Tested Frame I

The heating phase of a fire stands until the gas temperature reach 920 °C at 4950 seconds. The observed cooling has a time of 50 minutes.

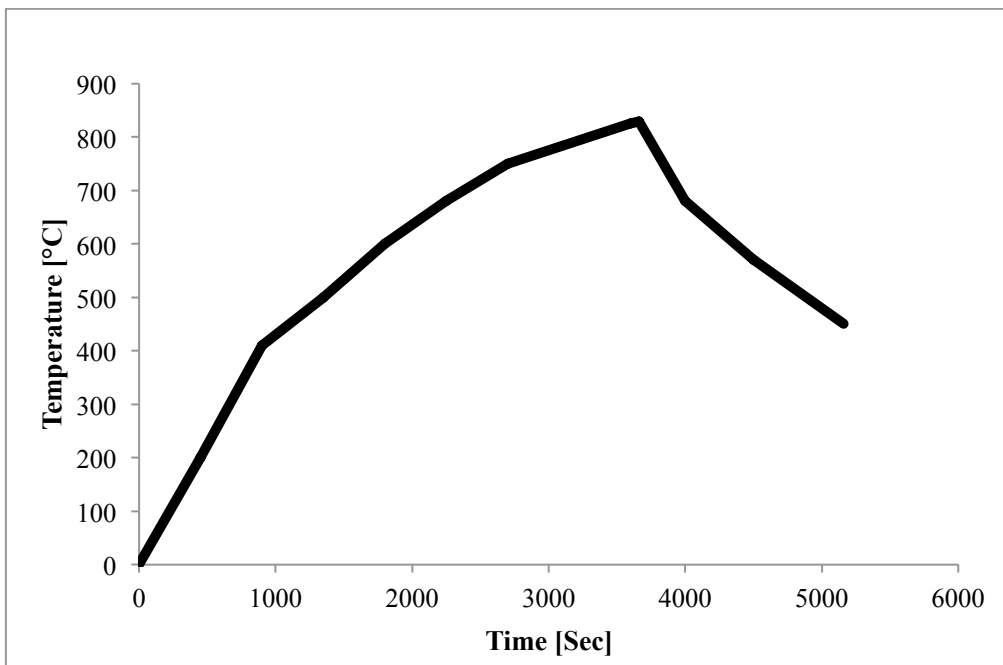
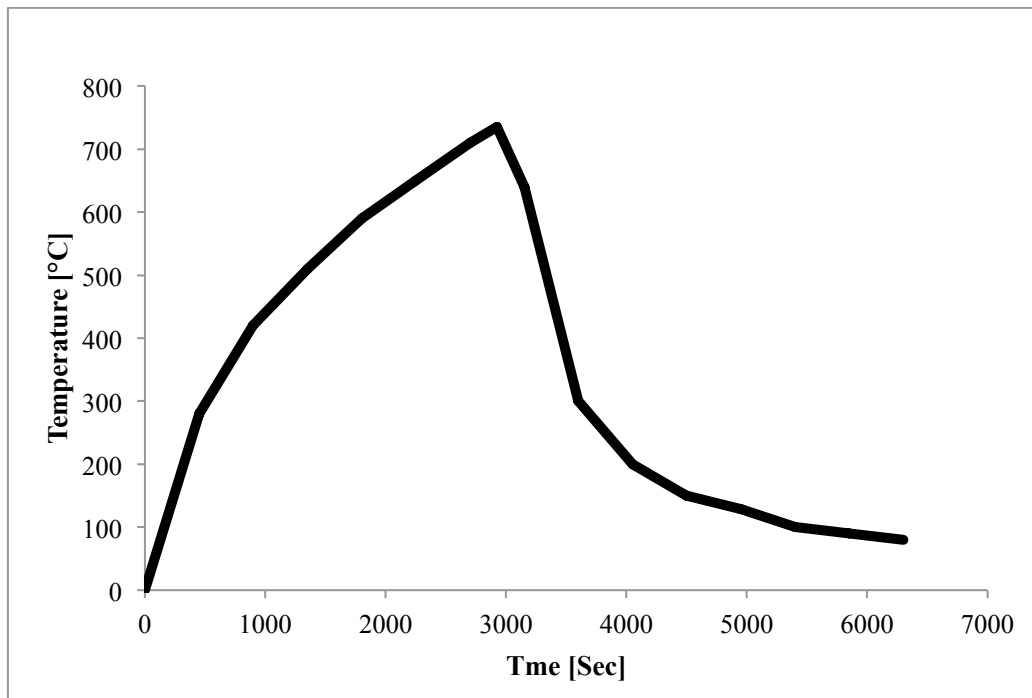


Figure 9 – Fire Curve Tested Frame II

The heating phase has a max temperature of 829°C when the furnace is turned off at 3660 seconds. The duration of cooling is 1500 seconds and the total observation time is 5000 seconds.



**Figure 10 - Fire Curve Tested Frame III**

Maximum temperature during heating 735°C at 2922 sec. followed from the longest observation time during cooling respect to the other frames until 6300 sec.

It is also possible to notice how the heating phase of the 3 different fire curves is almost the same; the only parameter that changes is the max temperature reached (920°C) and the duration of cooling phase. In the Frame I, there is the highest gas temperature reached and in the Frame III the longest cooling phase (55 minutes).

Those fire curves are applied for the three different test frames (see table 1) in the central ground column.

### 3.6 Results

The results are given in terms of temperature, displacement and strains.

#### 3.6.1 Test Frame Temperature Evolution

There are gathered the result for the different frame tested showing the temperature time behavior along the heated column section.

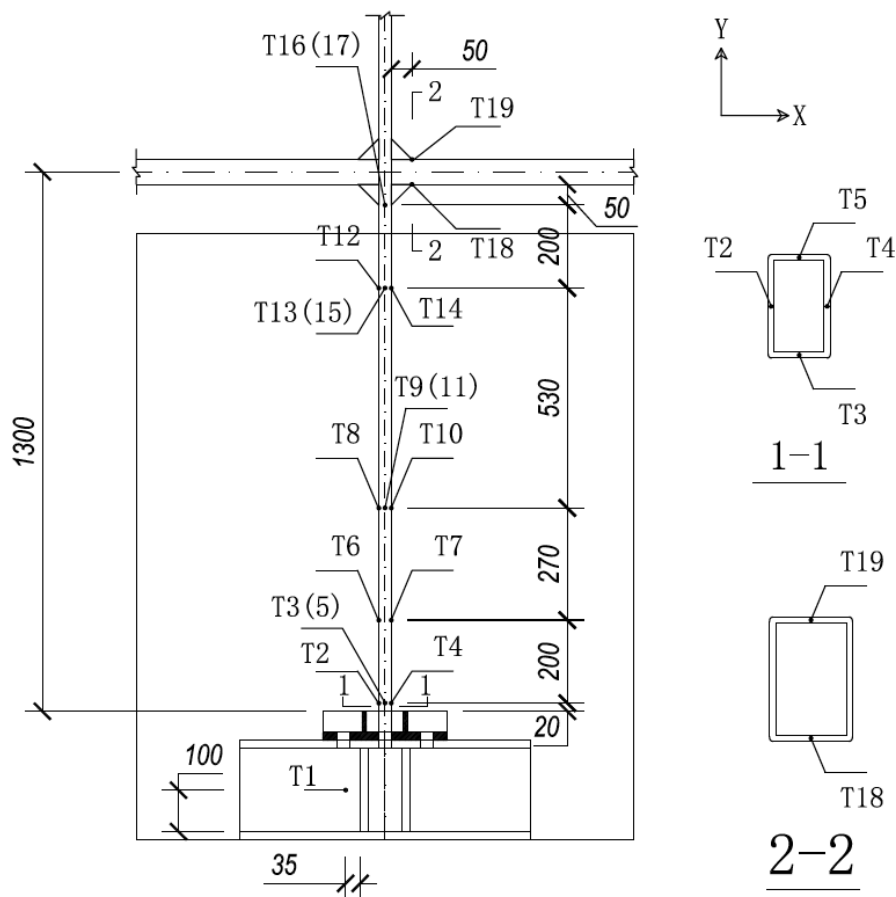


Figure 11 - Thermocouples Location, image takes from (10)

Figure 11 represents the central column, in particular where the thermocouple are positioned along the whole length of the column and in some point on the top beam.

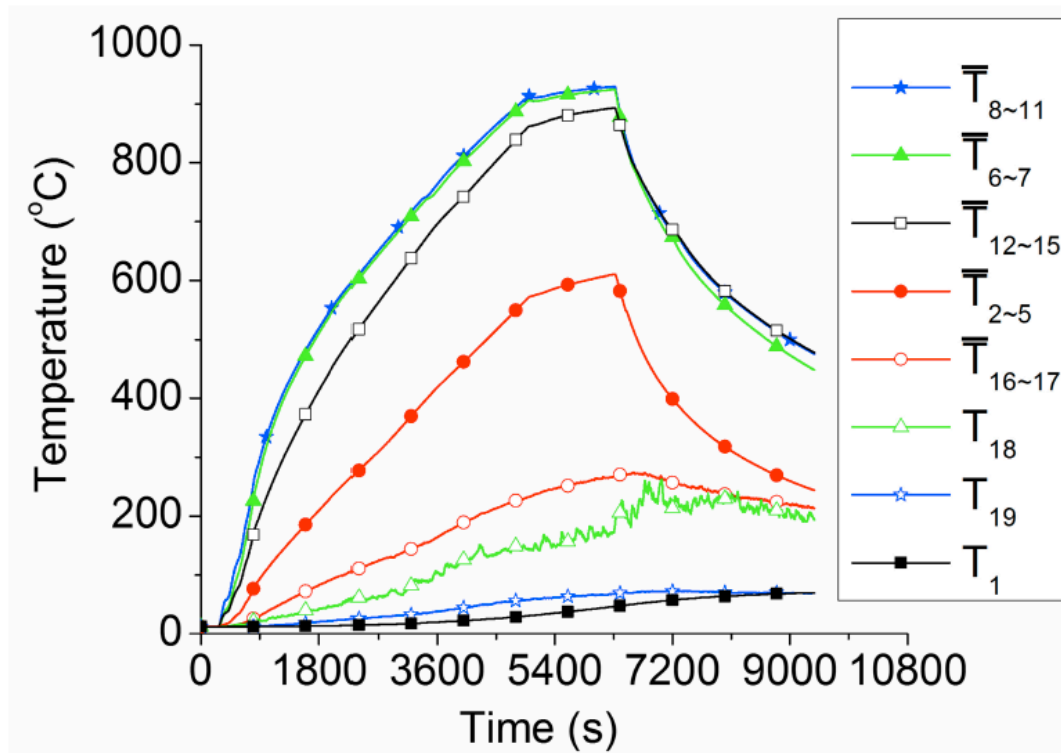


Figure 12 - Temperature evolution Heated column Frame I, image takes from (10)

From the results, where the zero point represent the moment in which the furnace is turned on, it is possible to see how the novel electrical furnace developed from the author (10) gives a uniformly temperature distribution along the section. It is possible to observe the thermocouples T 2-5 and T 16-17 located at the very start and end of the column show a different behavior respect to the ones located in the middle of the section T8-11 T6-7 T12-15 that seem to have approximately the same temperature-time curve. The fact that thermocouples located at the very end and at the bottom of the beams present a different temperature evolution, worth nothing because they represent 5 cm of a total length of 130 cm (figure 11). For this reasons it is possible to say that the global temperature behavior of the column is well represented from the thermocouples T8 to T15. For as regarding the top beam associated at the thermocouple T 18 reach a maximum temperature of 200°C due to the hot gasses coming from the furnace.

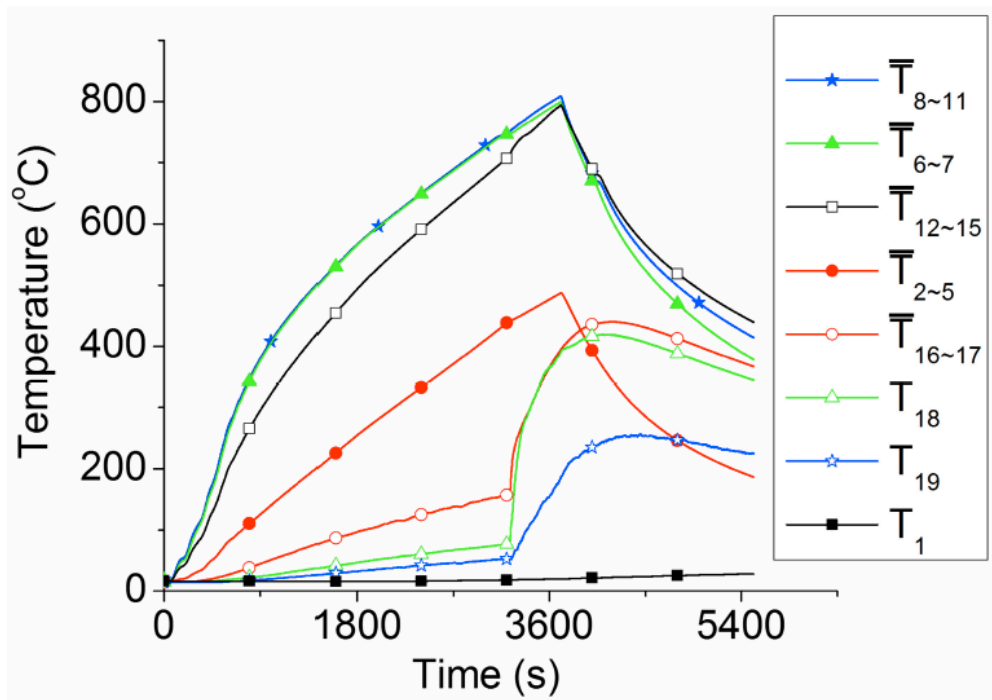


Figure 13 - Temperature evolution Heated column Frame II, takes from (10)

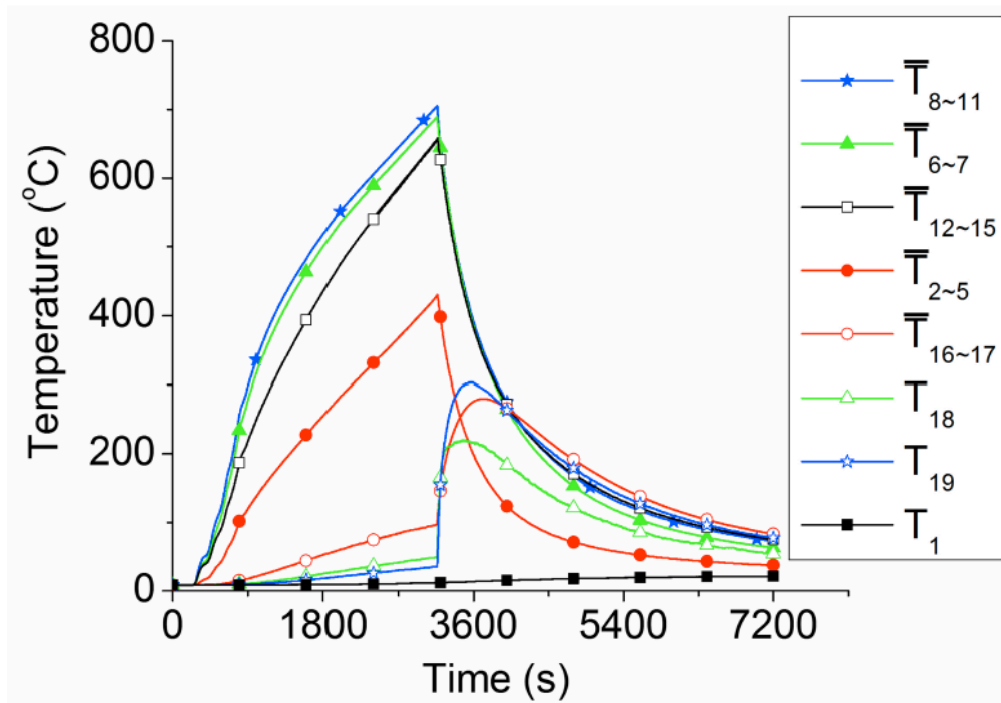


Figure 14 - Temperature evolution Heated column Frame III, takes from (10)

The temperature behaviors for test frame II and III are shown together, it is possible to notice also here the ascending rate almost the same in the middle part of the section T8-11, T6-7, T12-15 and the difference in temperature at the base of the column T12-15. The most important difference it can be noticed for the temperature behavior related to the beam connected at the column, where for test frame I were not relevant For test frame II and III the temperature in this part T18 increasing significantly starting from 3169 sec and 2992 sec respectively. That is a consequence of the buckling experienced from the column; it induced a significant vertical deflection that triggered the escape of significant hot gasses from the furnace toward the top beam. In test frame III the effect is even more pronounced because the beams dropped into the furnace due to a large vertical displacement.

### 3.6.2 Displacements

The displacement gauges are positioned among the whole structure as showed here below.

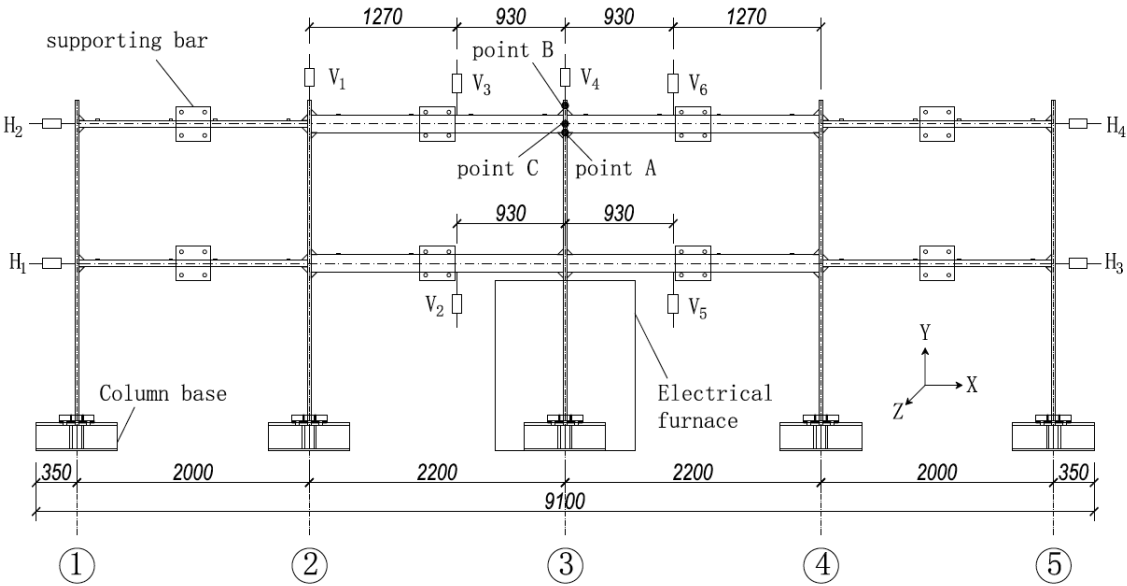


Figure 15 - Displacement gauges, takes from (10)

Vertical displacements are taken from the gauges V 1-6 and horizontal displacements from H 1-4, it is important to underline the fact that the gauges were installed after the load positioning as explained in [3.1], so the measurement does not take into account displacement due to the load set up.

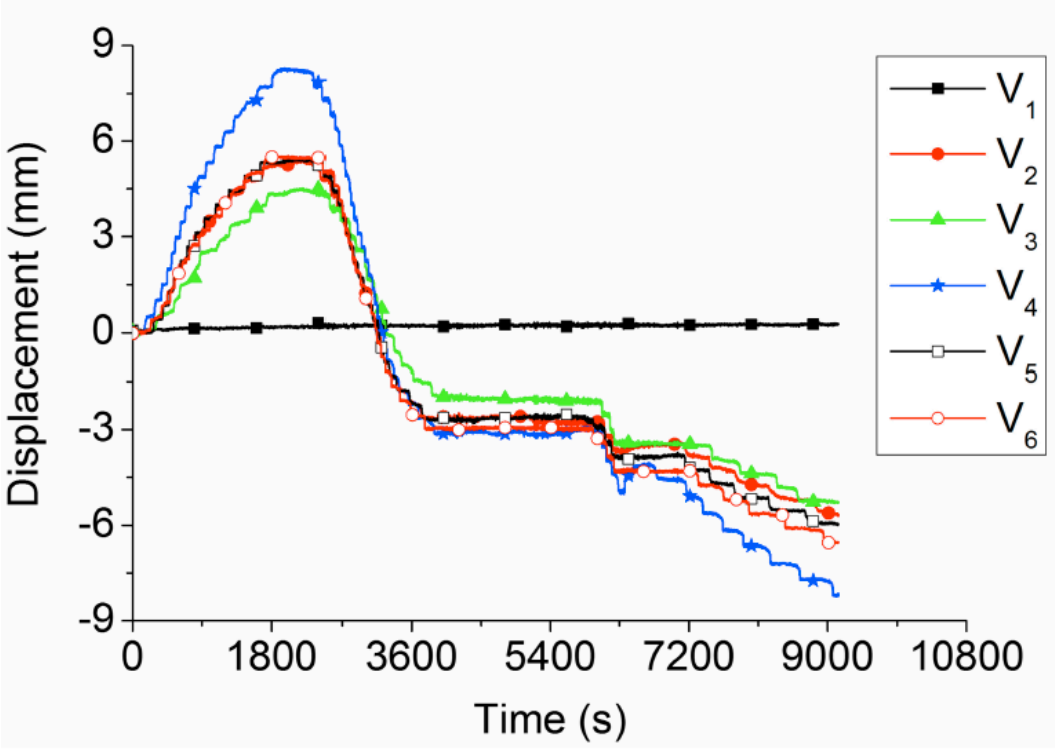


Figure 16 - Vertical Displacement Frame I, from (10)

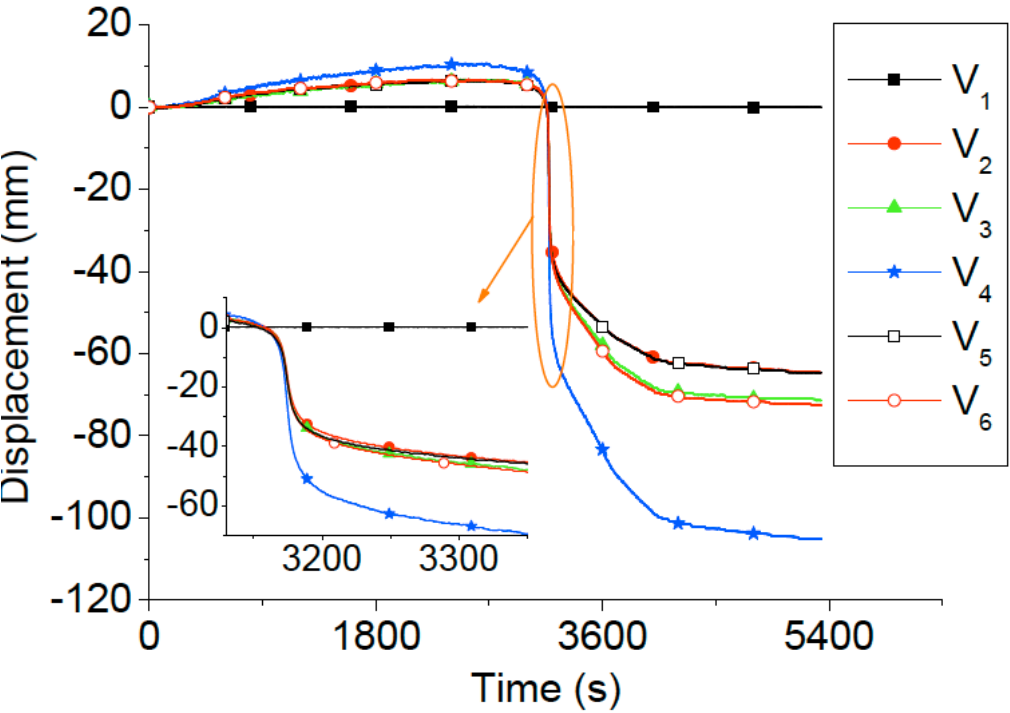


Figure 17 - Vertical Displacement Frame II, takes from (10)

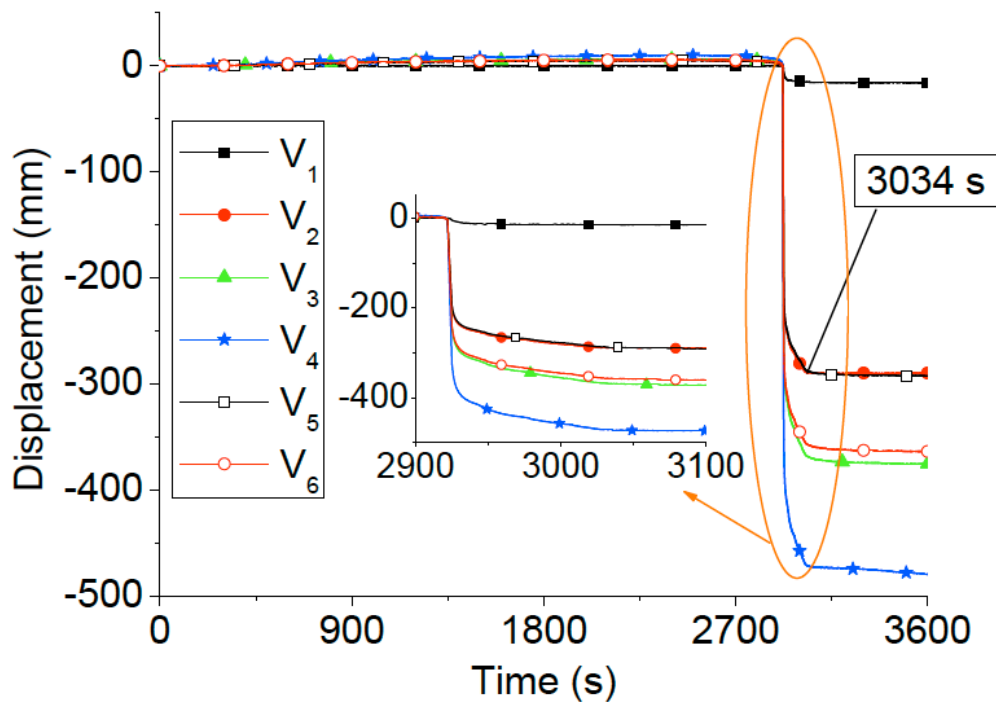


Figure 18 - Vertical displacement Frame III, takes from (10)

The gauge V4 it is placed on the top frame of the central column (fig. 15) and shows the vertical displacement during the whole fire duration. In figures 16,17,18 it is possible to see the vertical displacements of the tests frames during time, and it result clear (from V4), as for all of the three frames the central column ascend gradually because of the thermal expansion then descend due to the column buckling. Furthermore it is possible to notice that the column top descend gradually in frame I but rapidly in frame II and III, indicating a quasi-static failure in the first case and a sudden failure in the others. This can be explained looking at the different load cases of the problem, in which the frame I has the lowest load situation. For what concerning the horizontal displacement it is very small, almost negligible for frames I and II, respectively 1.3 mm and 4 mm and 76.4 mm for the frame III that has experienced a more important instability.

### 3.6.3 Strains

The principal output regarding the strains during the test, is referring to the behavior of the base column number 4 ( $S_{C2}$ ) and the two beams  $B_{I-23}$  ( $S_{B1}$ ) and  $B_{II-23}$  ( $S_{B6}$ ).

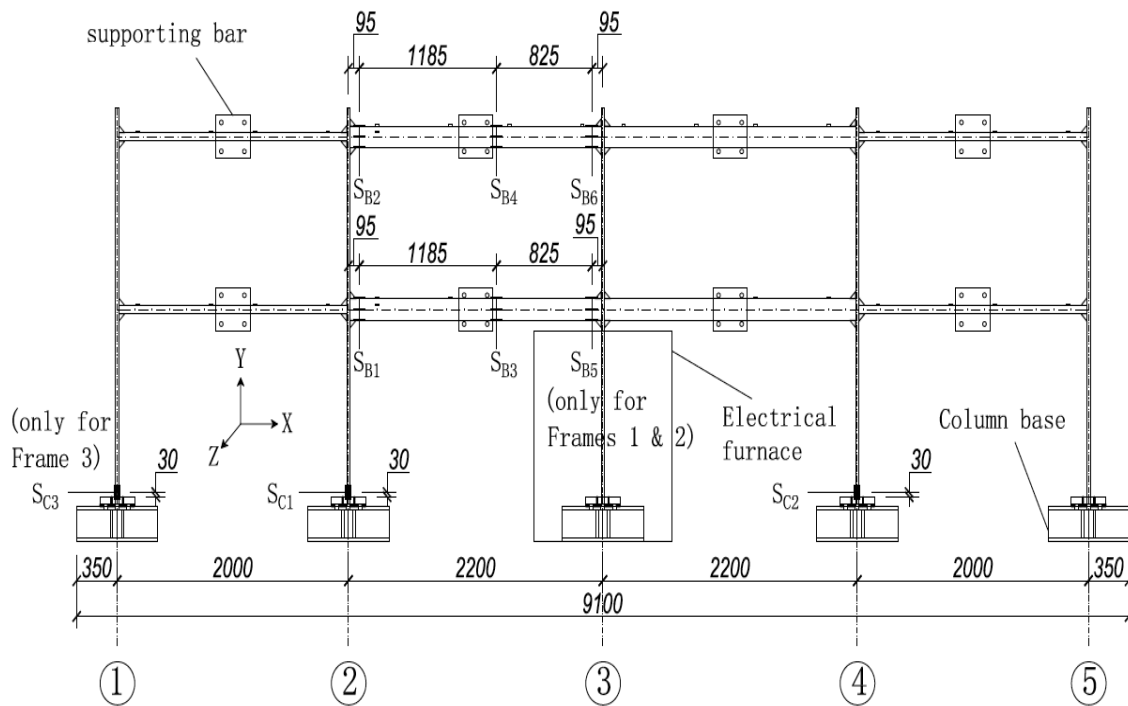


Figure 19 - Strain Gauges, takes from (10)

The most interesting results are related to the strain behavior belonging to the base of column number 4, next to the central one subjected to fire, Figures 20-21-22.

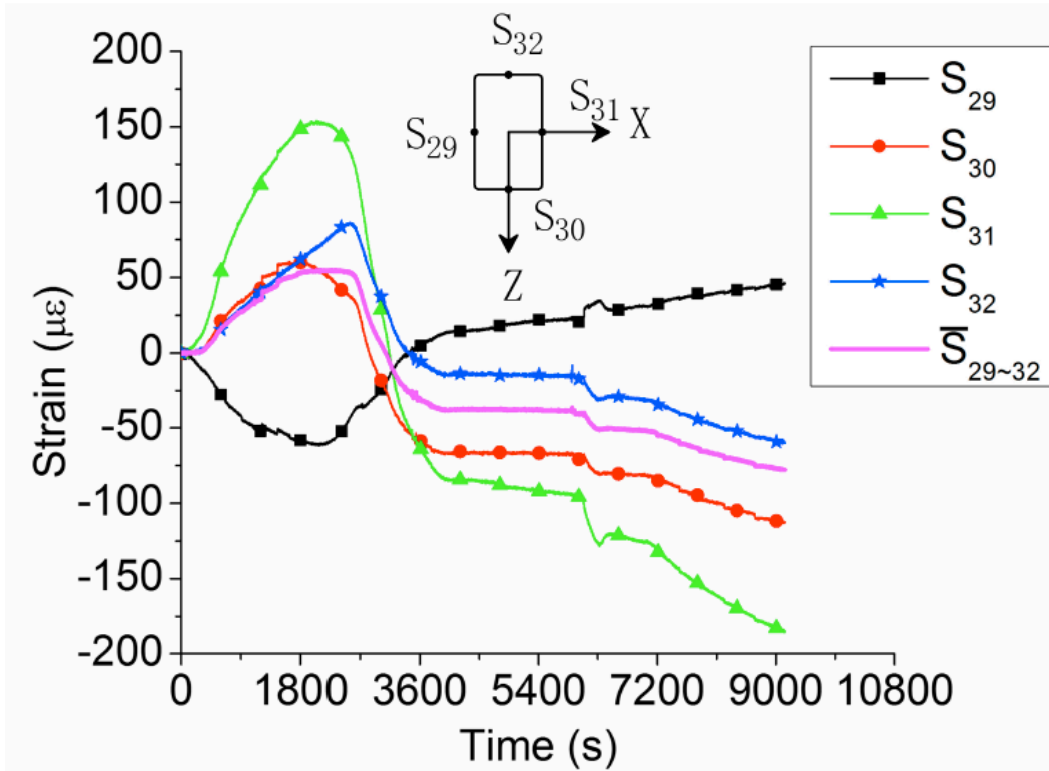


Figure 20 - Strains at foot column  $S_{C2}$ , Frame I, takes from (10)

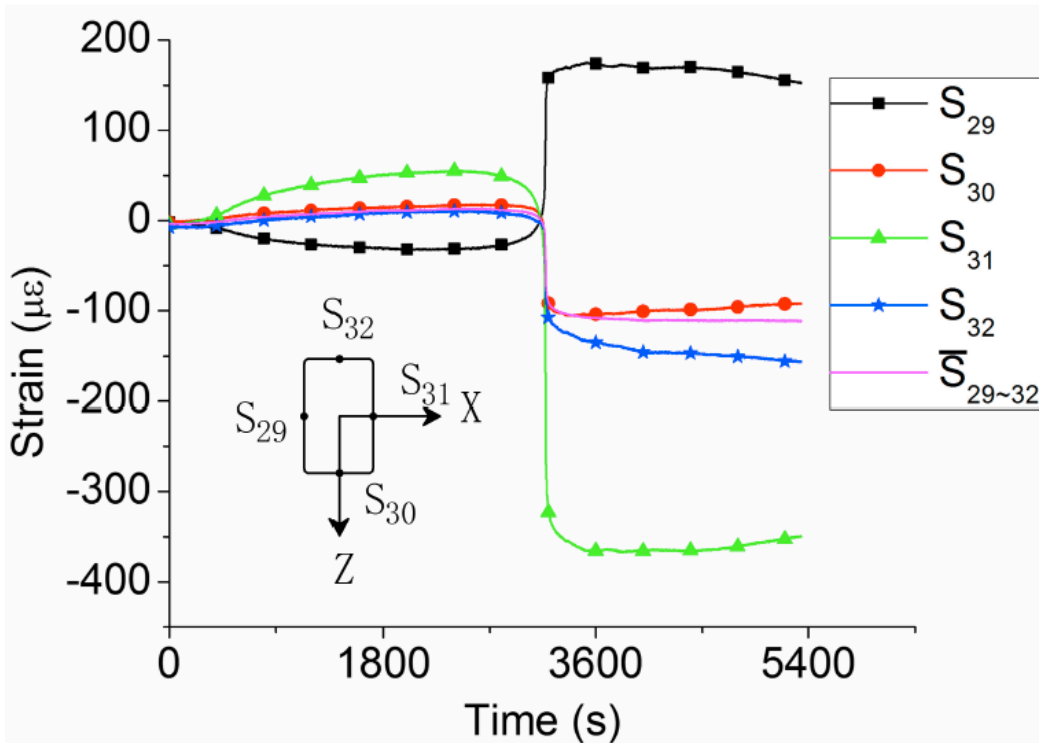


Figure 21 - Strains at foot column  $S_{C2}$ , Frame II, takes from (10)

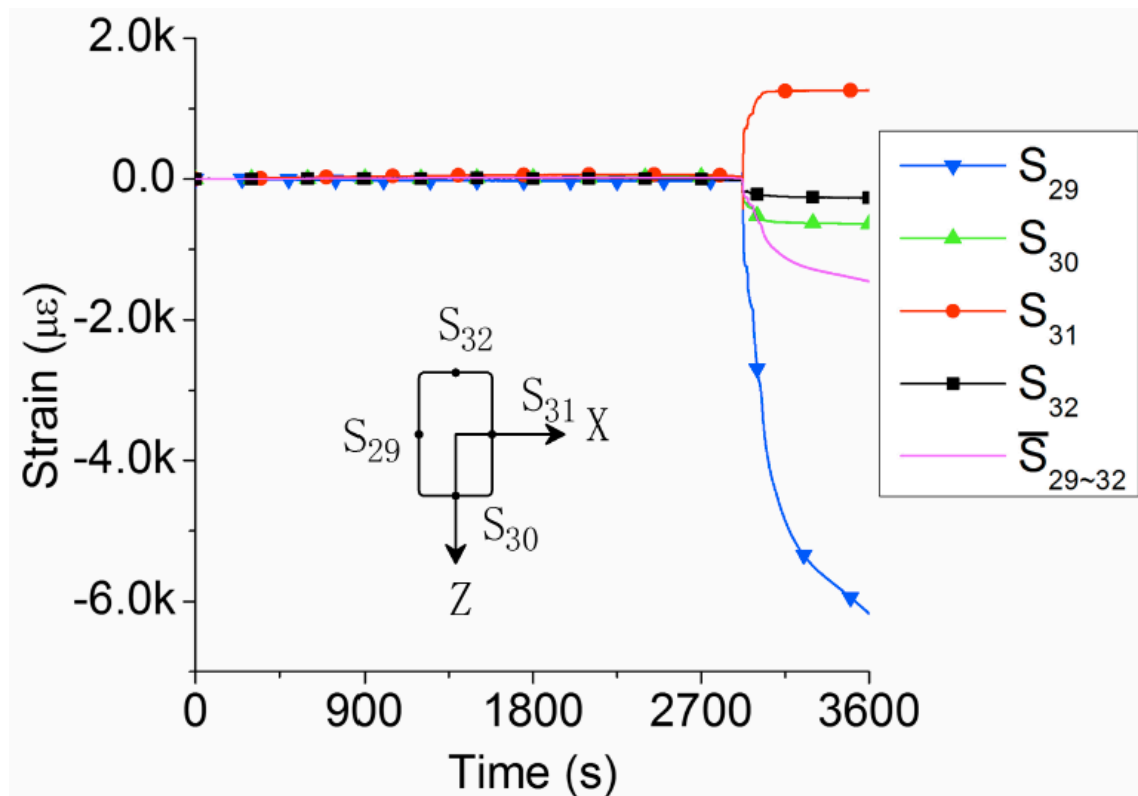


Figure 22 - Strains at foot column  $S_{C2}$ , Frame III, from (10)

Those are the behavior of the strains against time for all the three frames. The pink line named, as  $S_{29-32}$  is the average between all of the values taken from the different point of the section  $S_{29}$  - $S_{30}$  - $S_{31}$  - $S_{32}$ . It reflects the variation of axial force at the measured section. By looking at the different graphs, a common behavior is confirmed both during the heating and cooling phase. In fact during the initial phase of the fire the column experienced a decrease or a release of the carried compressive strength, while the fired column was having a thermal expansion. On the other hand after the buckling of the heated column, 3, it is possible to observe an increase in the carried compression from the column 4 especially in figure 21 for the frame II.

This phenomena, described above, led to chose this research and structural problem as reference model in order to validate the finite element software used for further analysis and also because it can be interesting make a parametric analysis on that frame in order to try to find out important information about the structural behavior of structure under natural fire. Now we have all the necessary information in order to create a numerical model as much as possible similar to the above described.

## **4. DESCRIPTION AND VALIDATION OF THE NUMERICAL MODEL – SAFIR VALIDATION**

In chapter 3 all of the data needed in order to develop a numerical model are given. This chapter is devoted to the creation of the numerical model. Numerical model that should respect as much as possible what was done from the authors in “Experimental Studies on Progressive Collapse Resistance of Steel Moment under Localized Fire” (10). The aim is the one to have a numerical model able to capture the structural behavior experienced from the tested one saw in the previous chapter, especially referred to capture the behavior during the heating and cooling phase.

Before to show how the structure has been modeled an introduction of the finite element software used in order to carry out the numerical model will be given.

### **4.1 SAFIR® - Overview**

From the faculty web page (11): “SAFIR® is a computer program that models the behavior of building structures subjected to fire. The structure can be made of a 3D skeleton of linear elements such as beams and columns, in conjunction with planar elements such as slab and walls. Different materials such as steel, concrete, timber, aluminum, gypsum or thermally insulating products can be used separately or in combination in the model”. The structure of the software is organized as follow:

1. Pre-procession phase, in which the user start to generate his file by creating 2D or 3D geometry, than all of the material, fire and problem propriety should be assigned and the last step is a mesh creation. The most adopted preprocessor program is GID.
2. Procession phase, it is done by running SAFIR, which will achieve the problem convergence based on convergence criteria setting assigned.
3. Post-procession phase, where is possible to have an outlook of the results. The postprocessor program is DIAMOND.

SAFIR® is being developed at University of Liege by Jean-Marc Franssen and Thomas Gernay.

## 4.2 Problem Data

In this chapter, it is explained step by step what are the main phases adopted for the numerical model creation. The purpose is the one to get a model able to capture as much as possible the behavior of the tested structure under natural fire presented in chapter 3. In order to prove that SAFIR® is able to capture complex behavior during different fire phases, as well validate it in such a way to become aware that it can be used for further analysis. Furthermore as a numerical problem, for definition is a model of the reality, we can not expect it to be equals to the real one, for a matter of the software capabilities and test procedure limitation. As a consequence some assumption were done and explained during the chapter.

### 4.2.1 Geometry, Conditions and Material

As it was described in the previous chapter, there will be modeled three distinct frames with the proprieties shown in 3.2 in particular figure 6 and table 1. In order to create a structural model the first step pass troughs the pre-processor software GID where there were created all of the different section needed to build the model.

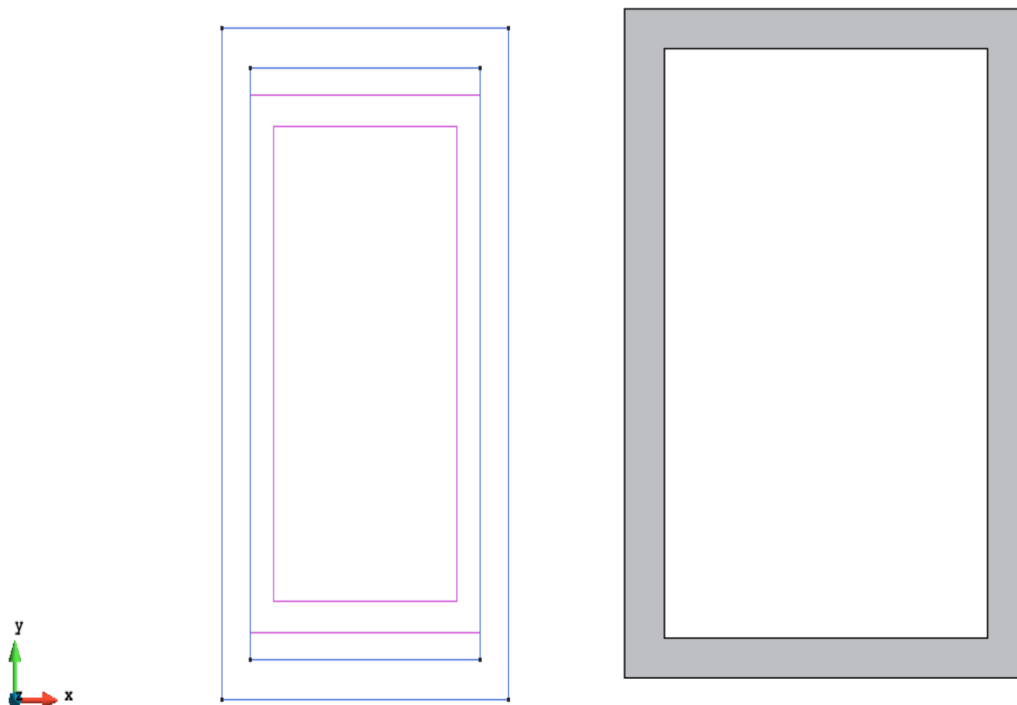
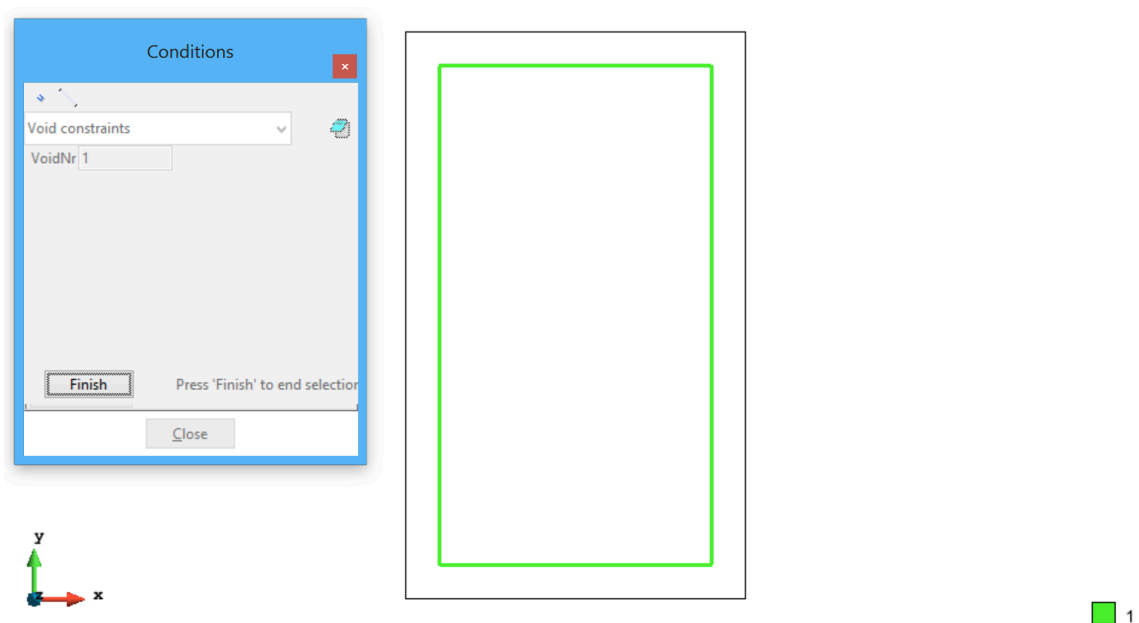


Figure 23 - Rectangular hollow section

In figure 23 two different view of the same section modeled with GID. Each section belonging to the frame structure, was modeled in the  $x$  ,  $y$  axes and based on the orientation given later in the structural model they can work as a column or as a beam. The dimensions of the all member created are in table 1.

Since the sections presents a central cavity an important parameter to set during the model creation is the given by the void. In this case located in the center surface as shown in figure 24.



**Figure 24 - Void condition**

By setting the number of internal voids, in this case only one, the program is now able to understand that in that part of the section there is no material and heat transfers is by convection and essentially by radiation (12).

After that it is necessary to assign frontiers condition in order to establish if there is, the fire applied on the section. In particular for our study case the fire is applied only on the central column as stated in chapter 3, instead for beams and the remain columns since no fire is applied the frontiers will be "F20". It is possible to do that as shown in figures 25-26.

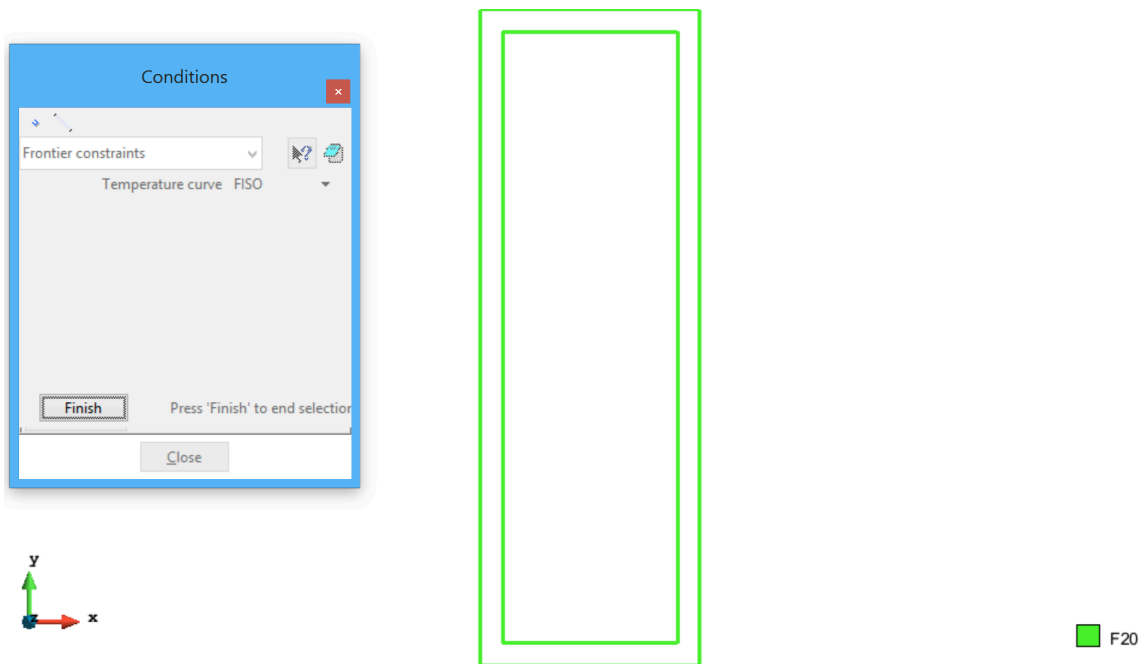


**Figure 25 - Beam cross-section**

For beams and columns not subjected to fire the frontier constraints applied is the temperature curve F20. This imply that the element remain at ambient temperature during the analysis.

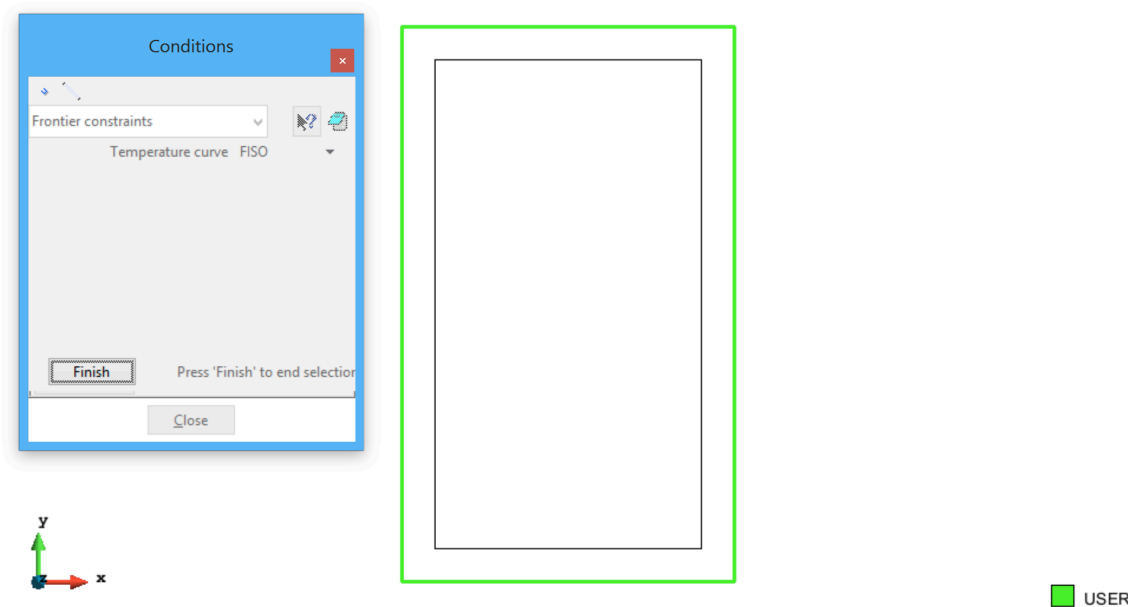


**Figure 26 - Heated Column cross-section**

For as regarding the different heated columns, a temperature fire curve should be applied. In our case there were created three different .txt files representing the different fire curves adopted during the tests (Figures 8-9-10). In fact it is possible to see the denomination of the constraint condition, as “USER” because the fire curve adopted is not an ISO standard fire instead is a natural fire curve created ad hoc.

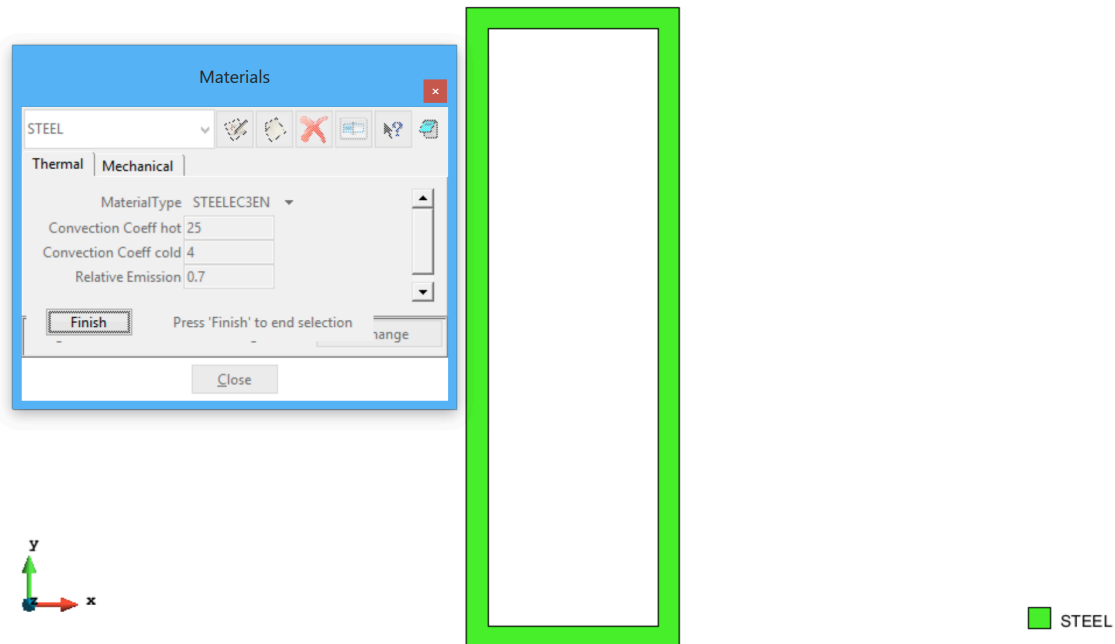


**Figure 27 - E.I. Material proprieties**

In this case it was chosen “STEELEC3EN” material type, the thermal proprieties are left as suggested according to EN1993-1-2, in terms of Convection was selected 25 [W/m<sup>2</sup>K] and relative emission of 0.7. The mechanical proprieties were described in table 2. It was considered the steel with a reversible behavior.

After having assigned all of the proprieties, there is created a structured mesh and solved the thermal problem. At this point it is possible to deal with the structural problem by creating a different model and assigning for each beam element the different section created.

## 4.2.2 Boundary Conditions

After having set all of the sections and made the thermal analysis, it is possible to move at the structural level of the problem. In order to deal with the fact that on the test done there was insert an out of plane restraint (3.3) in such a way to make it behave only in two directions, it is selected a 2D structural model. Where the elements have three degree of freedom, rotation and two-displacement direction. Furthermore at each base column a constraint is applied in order to fix them on the ground.

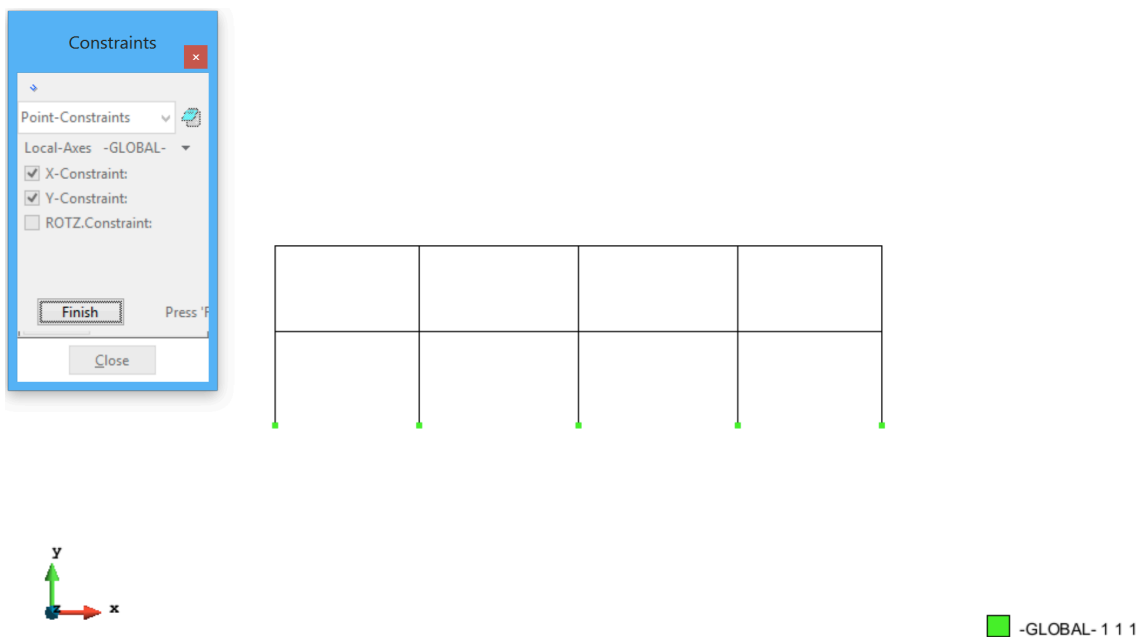


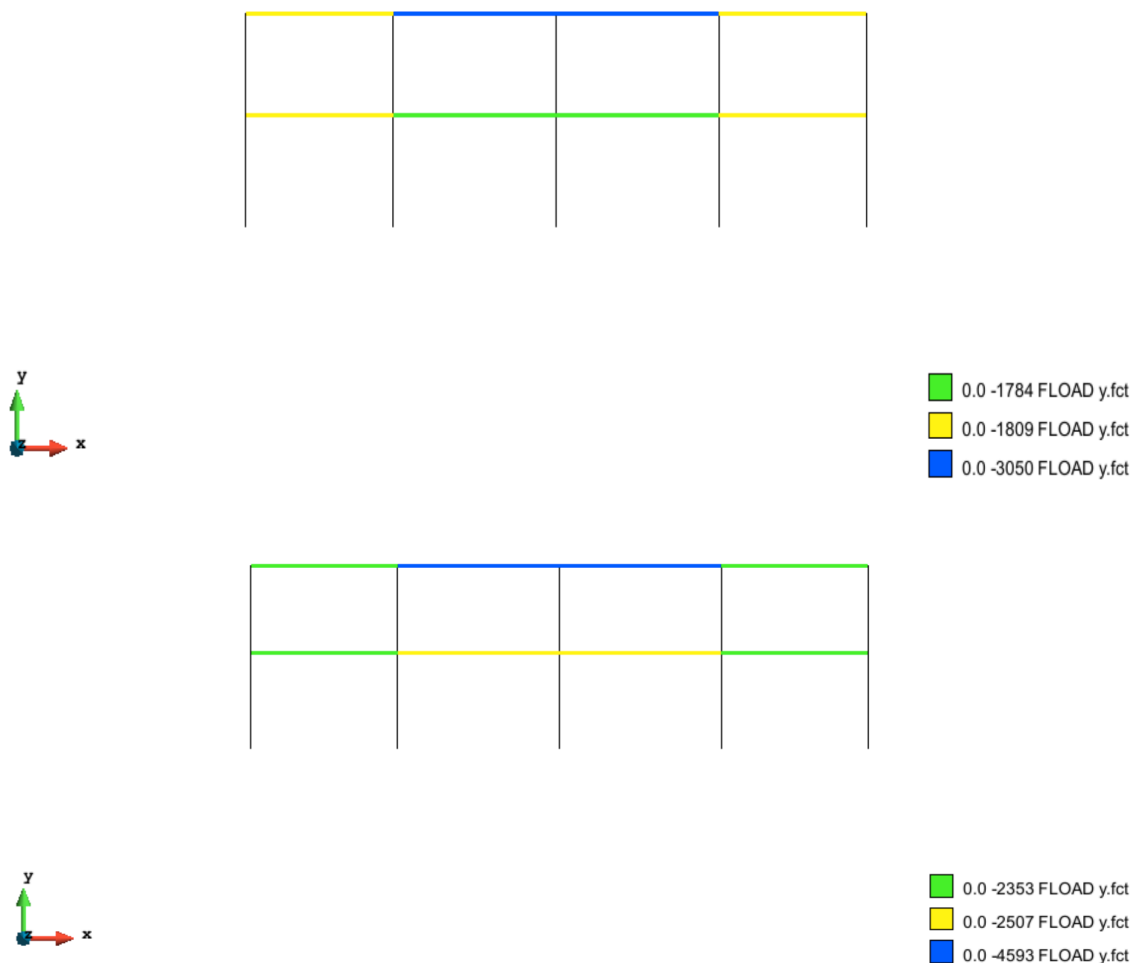
**Figure 28 - Frame Constraints**

Where “GLOBAL - 1 1 1” indicate the fixed degree of freedom in X Y and rotation.

### 4.2.3 Applied Loads

In the real tested frame the load applied were metal lumps contained in steel boxes fixed at the beams, as shown in figure 7. It is possible to know exactly the weight of each steel box for the different test frames from table 3. Should be noticed that applying on the structural model a uniformly distributed load along all of the beam length, it will not reflex exactly the real situation and it might lead to an error in the output result of the numerical model. However after a brief evaluation, where it was compared the finest way to carry the beam (putting the weight exactly where each steel box is fixed on the beam), with the case in which the load were distributed all along the beam length it was noticed that the difference in terms of reaction were small enough (less than 10%) to be able to use the approximate load situation.

Moreover the load function chosen is “FLOAD” this implies a fully applied load after 20 seconds (13). In figure 29 the load values are given in [N/m].



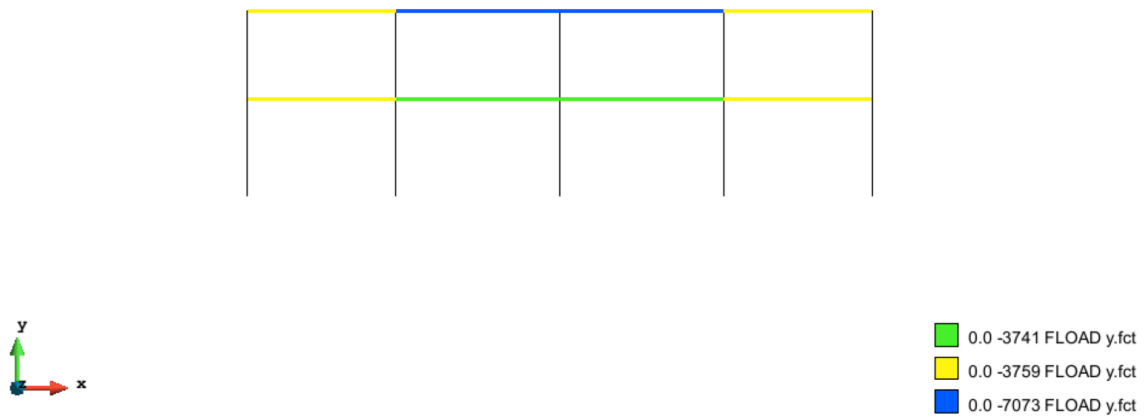


Figure 29 - Load cases for each different test frame

#### 4.2.4 Elements Proprieties

As last step before to run the analysis at each beam element make part of the structure should be assigned the related information got from the thermal analysis, in our specific case it is a .TEM file. In the TEM file there are contained all the information about the evolution of the temperature inside the element.

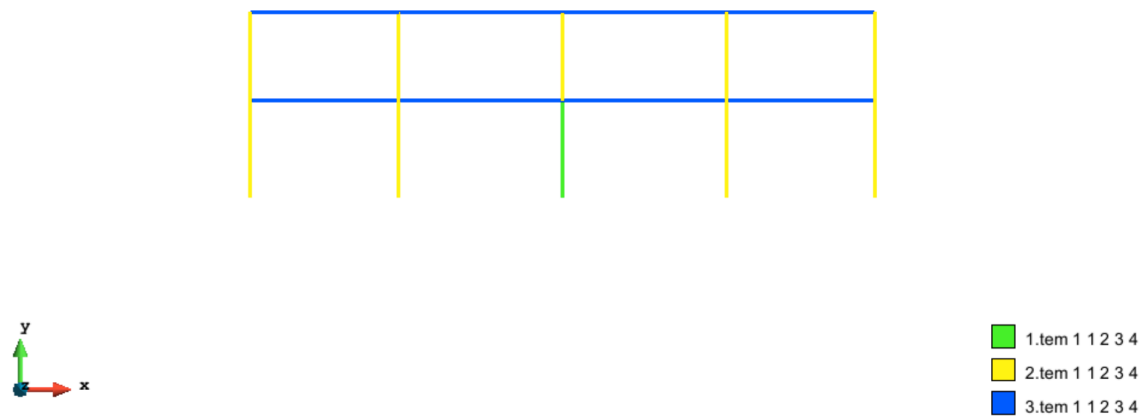


Figure 30 - Assignment of Thermal behavior

The 1.TEM represent the heated column; this is the only heated element in the whole structure. For each frame tested, a new TEM file should be done, because there is a different fire applied and geometry.

## 4.3 Results

How explained before, the numerical model created herein in this chapter has the primary function to validate the finite element software SAFIR®, which will be used later in order to perform parametric analysis on different structures. This is why the aim is to understand which are the parameters able to play a role during the decay phase of a fire for what concern the structural vulnerability. Having said that, the results here presented are compared with the ones shown in chapter 3, derived from the experimental test conducted in (10). The numerical model will be considered validate if it is able to capture the general behavior of the structure in terms of temperature inside the heated element, displacement and load transfer from the heated column to the cold one.

### *4.3.1 Temperature in the heated column*

In chapter 3, figures 12-13-14 showing the temperature during the whole fire duration in the heated column for the different fire curve applied. Since in figure 11 are indicated the thermocouples location all along the column and the temperature behavior in the experimental test is given for each thermocouple, it is necessary to underline the fact that the two thermocouples at the very base and at the top of the heated column are neglected. In fact by looking at fig. 11 it can be seen that T-2-3-4-5 and T-16-17 are located at 5 cm and 2 cm respectively from the column extremities. So it can be assumed that the behavior of the temperature along the column is well represented from the thermocouples T6 until T16. In addition for the steel the temperature in the cross-section is generally uniform. In the figures below a comparison between the temperatures inside the element evaluated with the numerical method and the one from the experimental data is given for the three different frames.

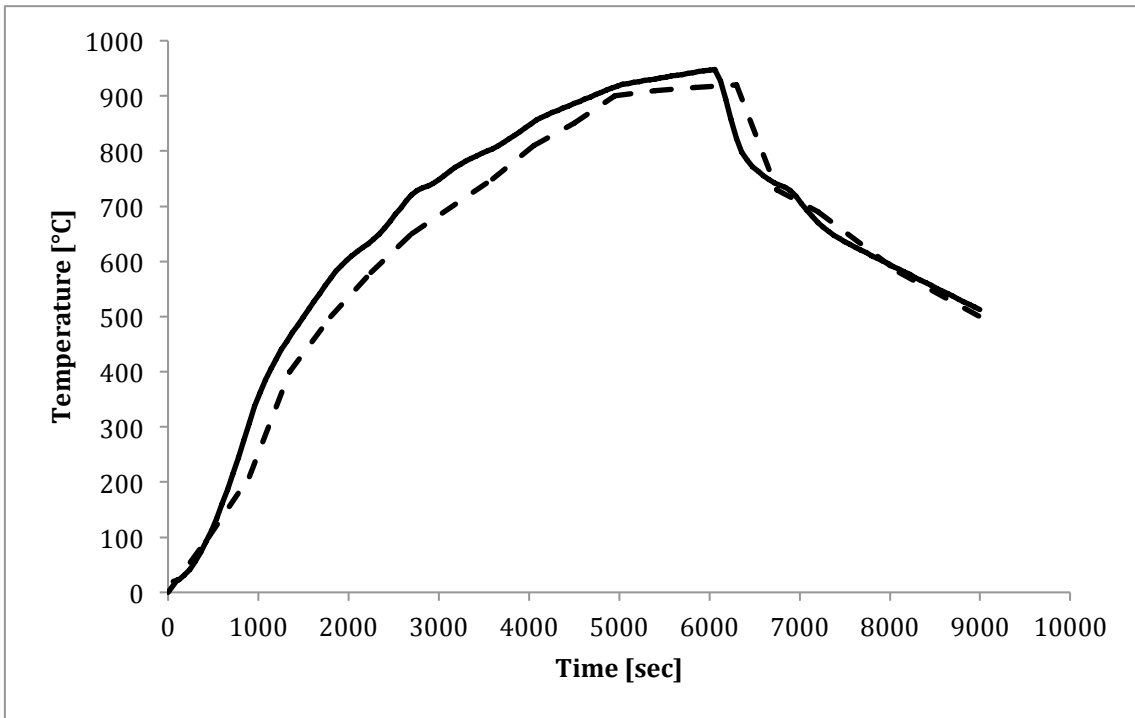


**Figure 31 - Comparison of temperature evolution, heated column Frame I**

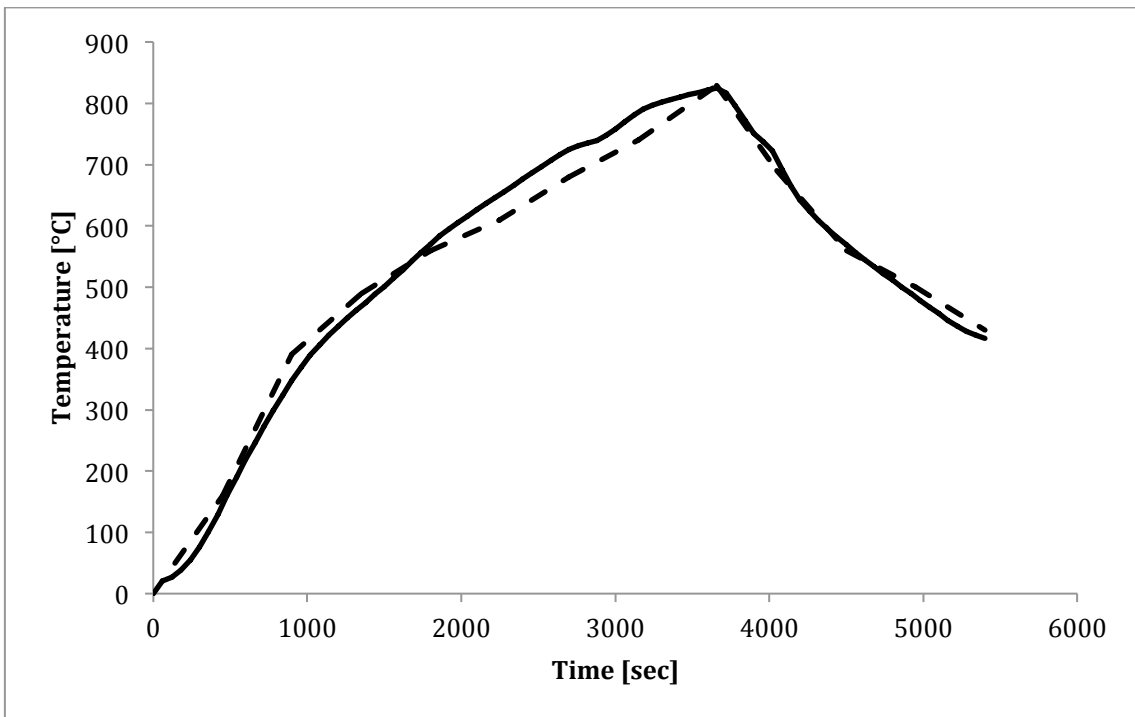


**Figure 32 - Comparison of temperature evolution, heated column Frame II**

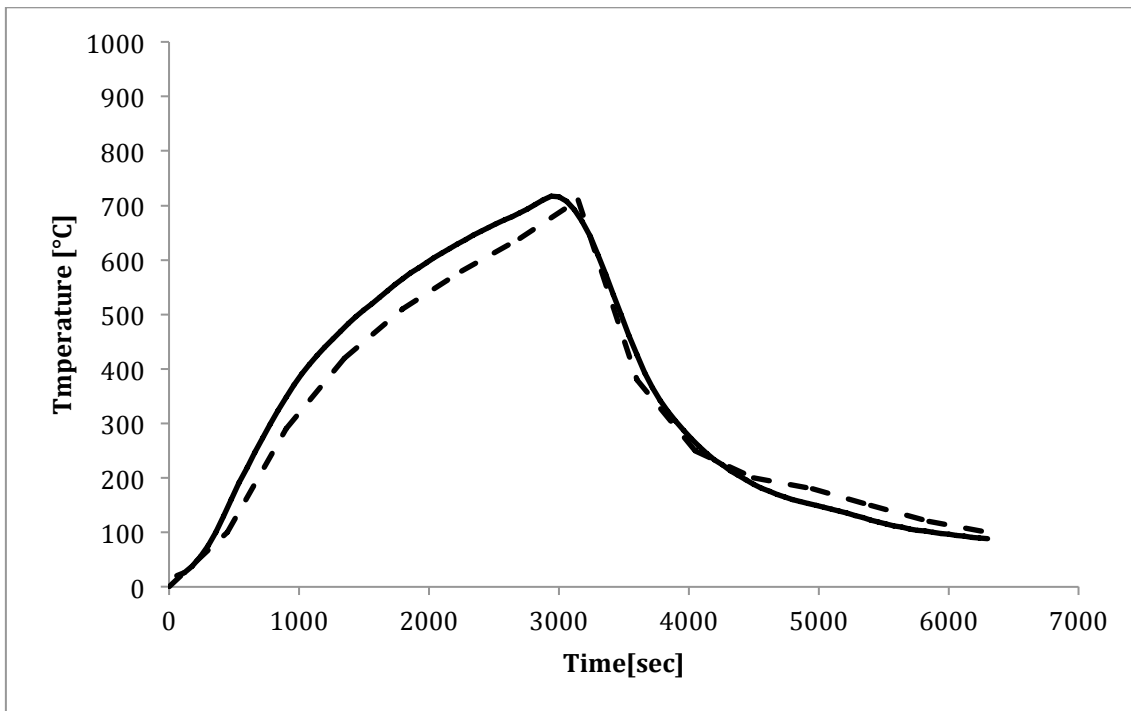


**Figure 33 - Comparison of temperature evolution, heated column Frame III**

Where in the three figures, is shown the temperatures in the section element during the whole fire duration expressed in seconds. The continuous line represents the output given from the numerical model instead the dashed line, stands for the result obtained from the experimental test. It is possible to conclude that SAFIR® captured quite well the temperature behavior inside the column section for the different tested frames.

### 4.3.2 Displacements

Comparing the top displacement registered from the displacement gauge during the experimental test is the adopted procedure for the numerical model validation regarding the displacement results. As it is possible to see from figure 15 the gauge is located above the heated column. This is why it can give us important information about the capability of the software to get the behavior of the heated column during all of the fire phases. In fact it is known how by heating steel, it will react with a thermal expansion and if in a latter stage where buckling or cooling may appear, it might experienced a thermal contraction (10).

The comparison will be done by comparing three different curves: the blue one representing the result given from the experimental test, the red one shows the result of the numerical model with a perfect frame structure and the black line is the result given from the numerical model made by adding an imperfection on the central column according to EN1993-1-1 chapter 5.2.4.5

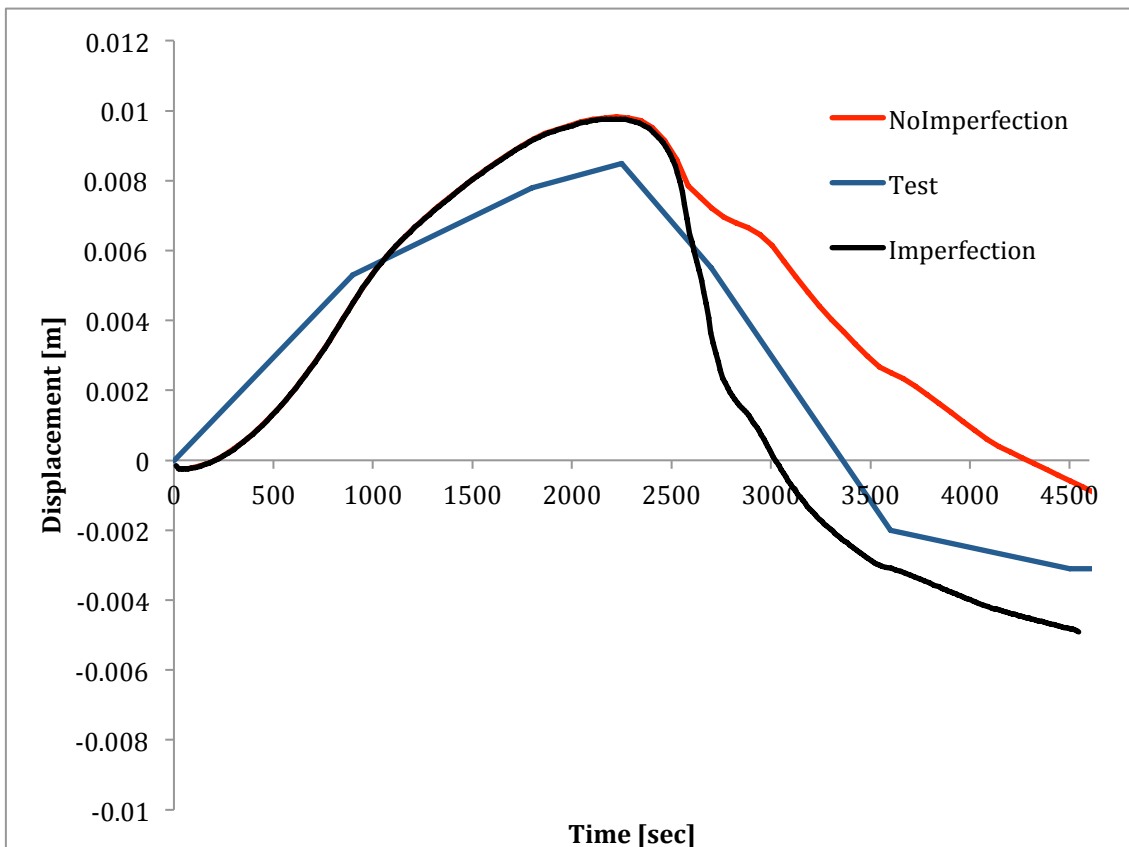


Figure 34 - Comparison of vertical displacement V4 Frame I

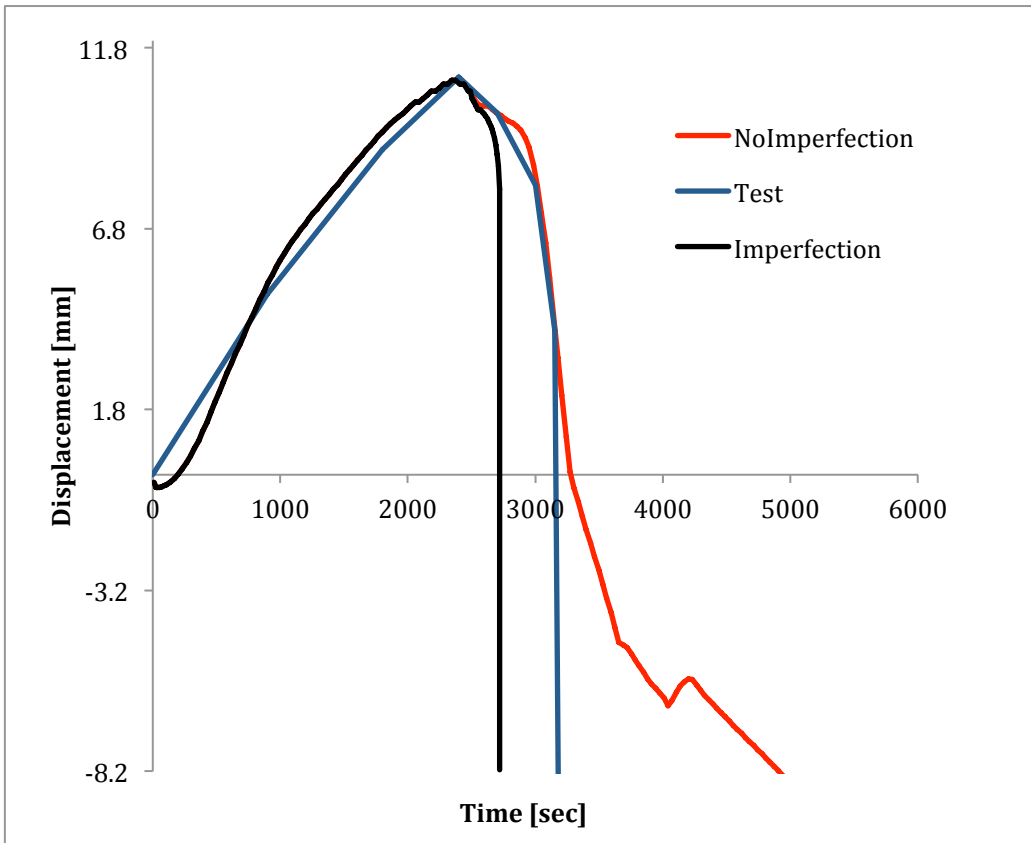


Figure 35 - Comparison of vertical displacement V4 Frame II

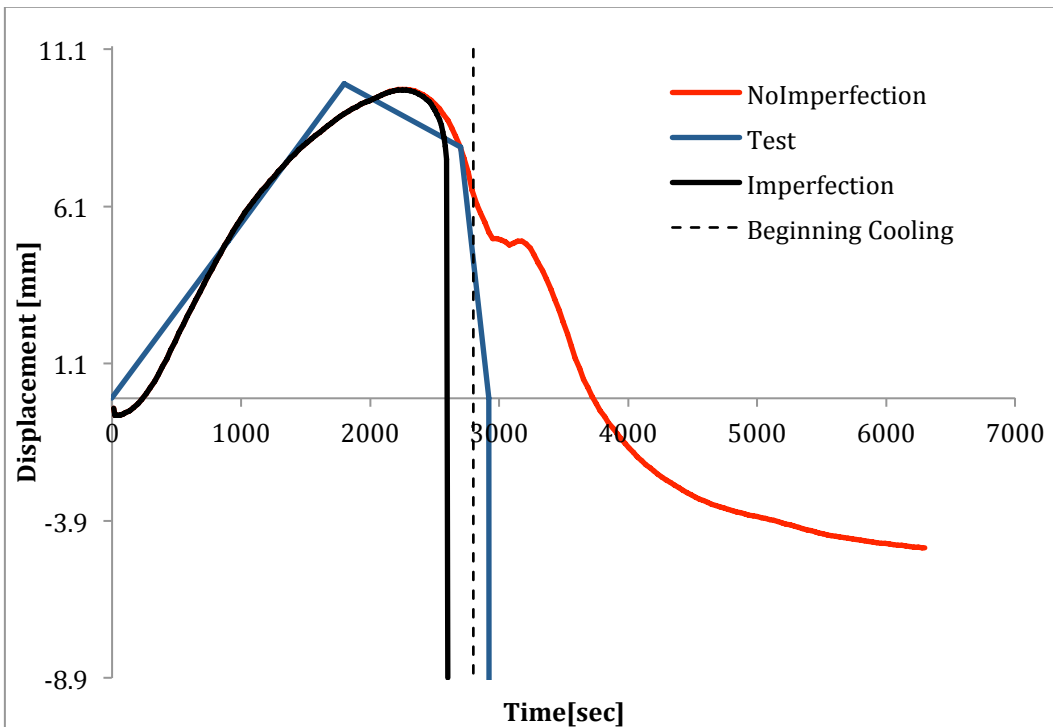


Figure 36 - Comparison of vertical displacement V4 Frame III

In figures 34-35-36 is plotted the comparison between the tested results (supposed to be correct), and the results obtained from the simulations performed. From here some consideration can be done. For all of the simulations done, the one performed with the imperfection better represent the “real” behavior, so regarding further studies, the geometry of the heated column will be made by adding an imperfection. Furthermore it is clear how during heating the column experienced a thermal elongation and then when it started to buckle a contraction appear, gently in the first frame (fail in a quasi-static way) and suddenly for frame II and III as argued in (10). Moreover it is possible to see also how the simulations show an initial descending branch, in the first initial seconds; on the other hand the tested one does not present this feature. This is simple explained because the tested frames are loaded first and then the displacement gauges are applied (see 3.1), so the initial deflection due to the load application is not considered. Instead the numerical model simulation started to have a fully load applied on the structure after 20 seconds and obviously the immediate deflection caused from the application of the load is not neglected in this way.

### 4.3.3 Load Transfer

As described in 3.3.6, the authors of the study were able to identify a load transfer during the fire's phases between the central column Nr.3 and the side column Nr.4 (figure 6) in which the strain gauge  $S_{C2}$  was located. This kind of behavior is also captured from SAFIR in the numerical analysis, here below are proposed the different pictures, in which it is possible to see the evolution of the vertical reactions during the main phases of the fire. It is very clear how the load is transferred from a column to the other.

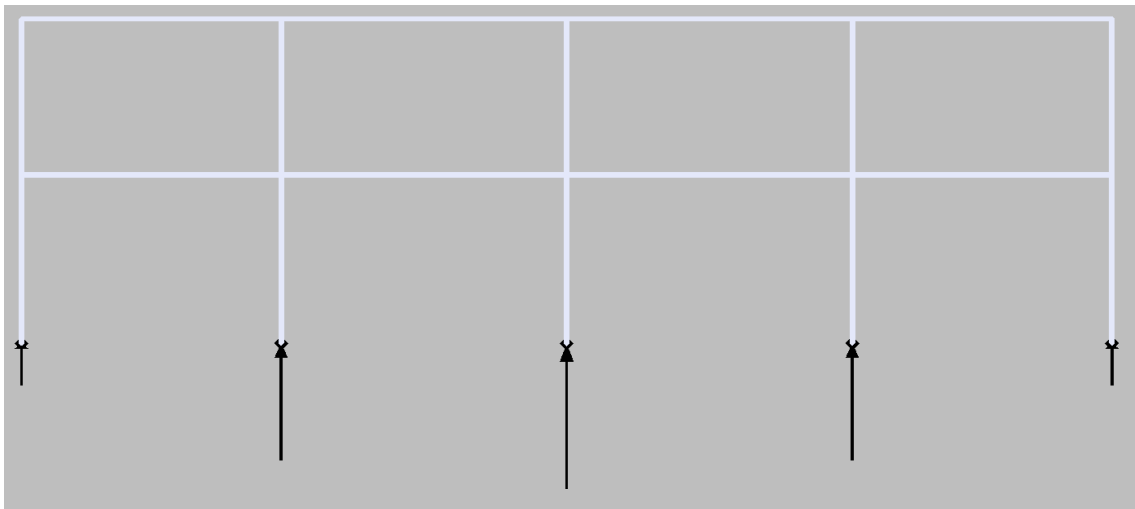


Figure 37 - Vertical reaction, Frame I, Time 20 seconds

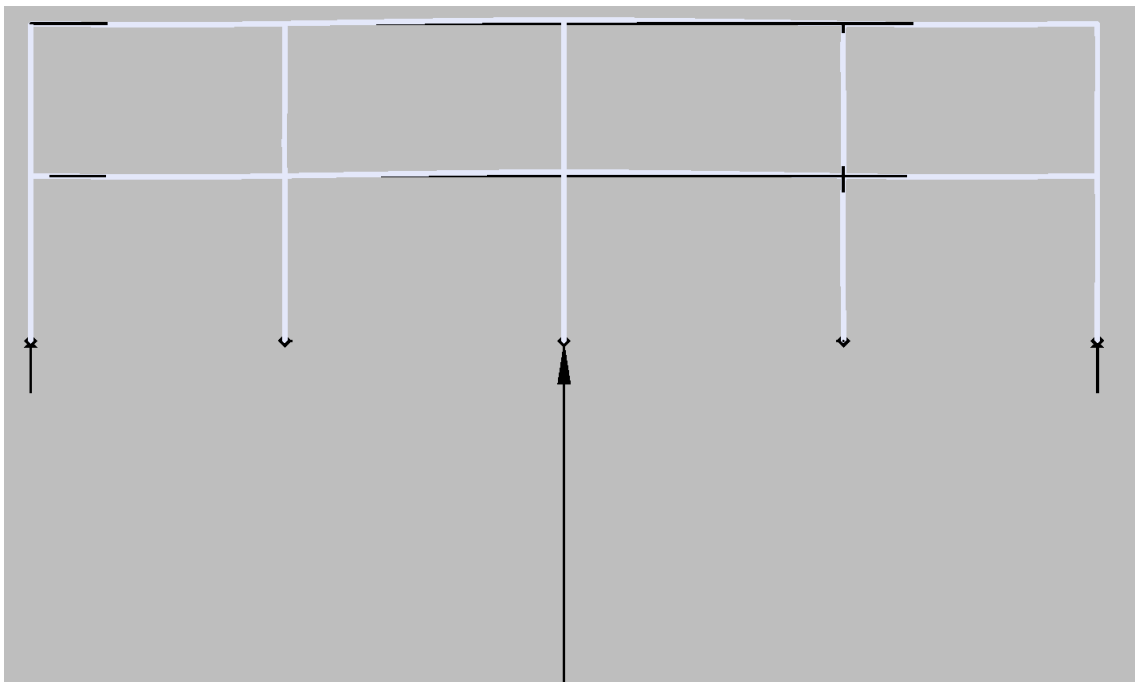
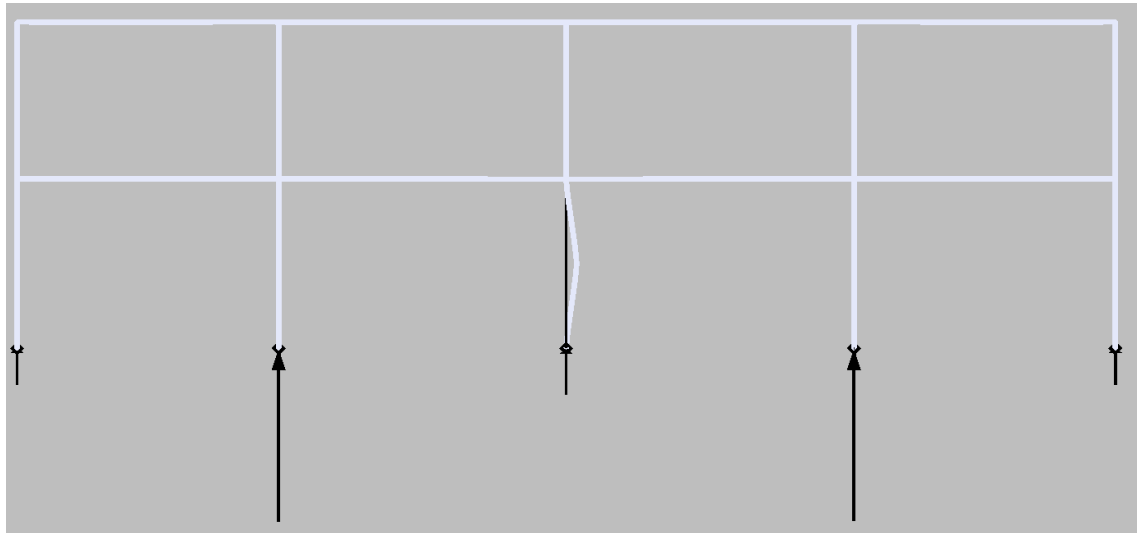


Figure 38 - Vertical reactions, Frame I, Time 2100 seconds

The 2100 seconds time shot represent the moment in which frame I is next to the buckling of the central column and it has experienced the maximum thermal elongation.



**Figure 39 - Vertical reactions, Frame II,**

Figure 39 shows the end of the simulation in which the central heated column is buckled and the load is almost completely transferred from the central column to the sides. So it is possible to conclude that the numerical model is able to capture the behavior of the tested structure during all of the fire phases at which was subjected and it is possible to proceed with further study cases.

From the validation of the numerical model it is possible to see how the software captured the structural behavior under fire quite well. Furthermore it gave important information about how to model for further studies. In figures 34-35-36 it is clear how the result is more accurate by adding an imperfection, for this reason all of the further analysis presented will be created by adding an imperfection.

## 5. VULNERABILITY OF STEEL STRUCTURE UNDER NATURAL FIRE.

The analysis performed here are linked with the results obtained from the study used for the validation of the numerical model (see chapter 3), where we noticed a load transfer from the heated column to the cold one. Since this kind of behavior might be linked with the vulnerability of structures under natural fire, several analyses will be performed in order to study this particular effect. The chapter starts explaining briefly, which is the reference model adopted and which parameters will be used for the study purpose. A general overview of all the performed analysis is given, and then the results obtained from the different parameter adopted are presented in terms of DHP indicators. After that for all of them, the most representative cases are studied. The representative cases give an idea regarding how the structure behaves during the performed simulation, since it was possible to find different way to behave depending on the parameter adopted, the conclusion will be given by gathering all of the main result classified based on the structural response under each parametric natural fire adopted.

### 5.1 Reference model

As a logical consequence for what said herein above, the reference model adopted is made with the same geometry of the one used for the validation model.

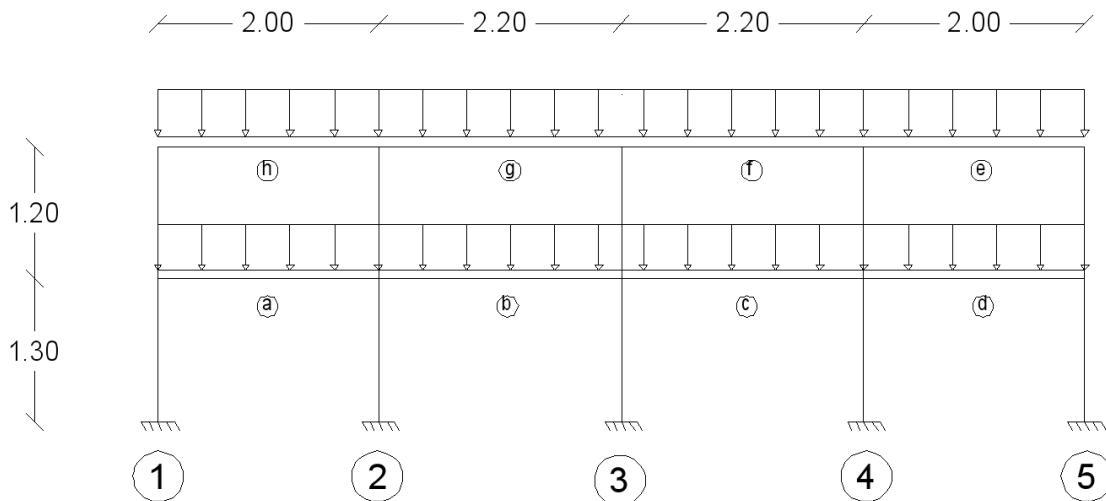


Figure 40 - Reference Model - Geometry

Figure 40 is the reference model, meant as general load case situation (only distributed load) and structure, in particular test frame of four bays and two stories, the span length of the two middle bays is 2.2 m each and the two side bays 2.0 m each, the heights of the

columns are 1.3 m and 1.2 m for the first and second storey respectively. Different simulations are performed by changing beams section, load applied and fire severity.

### 5.1.1 Materials

The material is steel for all the columns and beams; more specifically it was assigned the “STEELEC3EN” material with a reversible strength behavior.

	$E_s$ (Pa)	$\sigma_y$ (Pa)	Poisson Rate	Convection (W/m <sup>2</sup> K)	Emissivity
STEELEC3EN	2.1e+11	3.55e+08	0.3	25	0.7

**Table 4 Thermal and mechanical proprieties**

In table 4 are summarized the mechanical and thermal proprieties adopted for all the simulations presented in this chapter, unless something different is stated during the output results description they should be considered the material proprieties adopted.

## 5.2 Parametric analysis

A parametric study implies a changing in some input data in order to see how the outputs will change. After some physical consideration and observation made upon the experimental test studied, the key parameters that may play an important role during a natural fire are: Fire Curves adopted, the load ratio and the beams cross-section dimension. For this reason the parametric study is conducted by varying them case-by-case.

### 5.2.1 Beams Cross-section

As we have seen from chapter 3, the load transfer phenomena from the central heated column to the side one, is amplified when the beams section is bigger, it can be interesting understand how this particular phenomena can affect the structural vulnerability.

For this reasons by taking the geometry proposed in figure 41, there were created 3 different models or test frames :

FRAME No.	Column	Middle beam	Side Beam
1	50x30x3	60x400x3,5	60x40x3,5
2	50x30x3	150x100x5	150x100x5
3	50x30x3	250x100x5	250x100x5

**Table 5 - Beams section (mm)**

It is possible to see in table 5 the different beams section adopted in order to carry the parametric study. In particular The frame number 1 represent the frame III seen in chapter 3, it was decided to take it as a first frame and then make a parametric study upon the beams geometry by increasing them of two times in frame 2 and almost 4 times in frame 3. I'm perfectly conscious that it may be questioned the fact that the case number 3 might be not realistic at all, for this reasons I searched some steel structures that can be comparable with the frame 3.



**Figure 41 - Example similar to Frame 2, pictures takes from (18)**

Here in figure 41 an example of steel beams section  $\frac{2}{3}$  times bigger than the column, this structure can be associated at the frame 2.



**Figure 42 - Example similar to frame 3, a picture takes from (19)**

Figure 42 is an example of frame 3, in which the beams section is almost four times the column size.

### ***5.2.2 Load Ratio***

The load ratio in this study is meant as the ratio between the applied loads on the column element over its ultimate load at ambient temperature. In order to find the ultimate load at ambient temperature for column 3, several analyses are performed for all of the geometry studied (see 8.3).

It is also important to underline that during the whole fire duration, the applied load is kept constant. Therefore, since the load on this structure (see. Figure 40) is given by an uniformly distributed load along all of the beams and the load ratio is referred to the column 3, the distributed load upon the beams is evaluated in such a way to give a desired load ratio for the column studied.

This is an important parameter for two reasons, the first one, is because being able to find the smallest load ratio for which an element in the structure will fail under a certain parametric fire curve gives us the DHP indicator. Secondly by looking at the load ratio related to the DHP indicator it is possible to understand at first sight, if our study case is a mere academic result or it may have practical implementation. As a reference, under fire condition a realistic load ratio goes from 0.2 to 0.7 of the maximum bearing capacity at ambient temperature.

### 5.2.3 Fire Curves

See how the behavior of the structure changes by changing fire severity is important because changing the adopted fire curve allow us to see how the structure will react of a less or more severe fire conditions. Therefore by increasing the duration of the fire, not only is increasing the heating phase but also the cooling phase.

The adopted fire is the parametric fire curve proposed from EN1991-1-2 Appendix A (3), the construction is explained in 8.1. Each parametric fire curve in figure 43 has a different duration of heating phase, those fire curves will be all used to test the different models, in particular only the column 3 (see figure 40) is subjected to fire.

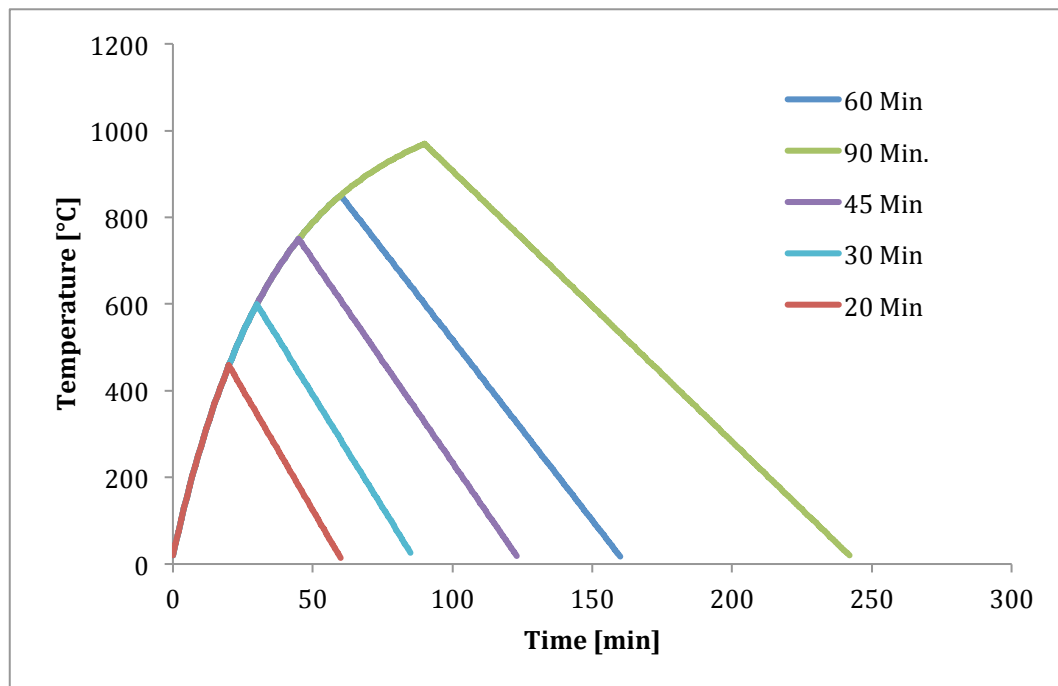


Figure 43 - Parametric Fire curves adopted

### 5.2.4 Conclusion

To summarize, at the end we have 3 different test frame, each one with the same columns but different beams dimension (table 5). They are tested under different parametric natural fire (figure 43) applied on the central column, applying a load ratio kept constant for the whole fire duration.

## 5.3 Results

The results are given following a certain order, first there is proposed a general overview of all the simulations conducted with the main results obtained for each of them. After that the most meaningful are gathered and proposed in terms of DHP indicator and described step by step. At the end a general overview is given in order to better understand the behavior, specially regarding the different kind of failure, in such a way to capture the vulnerability associated at each different study case.

### 5.3.1 General Overview

TEST FRAME	DHP [min]	LOAD RATIO [%]
1	15	/
1	20	0,9
1	30	0,23
1	45	0,23
1	60	0,093
1	90	0,04
2	15	0,69
2	20	0,58
2	30	0,22
2	45	0,18
2	60	0,06
2	90	0,05
3	15	0,76
3	20	0,69
3	30	0,1
3	45	0,08
3	60	0,019
3	90	0,003

Table 6 – Test Results, general overview

Table 6 gives a general outlook of the obtained results in terms of DHP indicators, ordered by test frame number, duration of heating phase of the associated parametric fire curve and load ratio applied. Behind those final output regarding the DHP indicators in function of the load ratio and the duration of heating phase of the parametric fire curve adopted, there is an iterative process repeated many times in order to find the minimum load ratio corresponding to a first element failure for a given parametric curve. The procedure is explained in Annex section 8.2, and essentially is the way to find the DHP indicator.

It is important underline the fact that for failure, in particular local failure of the heated column is meant when the element is not anymore able to carry vertical loads ( $N \leq 0$ ). Instead it is possible to have a global failure when more than one column fail and the structure is not anymore able to withstand the load. This important distinction is useful because it will be shown how by increasing the beams section size there will be a better redistribution of the carried load between the columns, and although the heated column is failed the structure is still in equilibrium thanks to its robustness.

Therefore some consideration can be done about the load ratio applied, in fact when the load ratio is not present it means that for that kind of model it was necessary, in order to have a first failure, a load ratio higher than 0.9. So practically the structure should be loaded as almost its load bearing capacity at ambient temperature in order to reach a first failure. It is also possible to notice that the most severe fire curve, with an high DHP have an associated load ratio really small, practically this is meaning that the fire is too much severe for the structure geometry and in order to have a first failure (local or global) only the proper structure self-weight is enough.

For what stated above, even if the model and the related result are correct not all the results should be taken in consideration because for instance the load ratio in order to be considerate as realistic case should be in between 0.2 and 0.7.

In the next paragraphs each frame modeled will be studied more in detail by providing the results obtained in terms of DHP indicators. Furthermore for each frame number it is possible to observe different way to behave under fire conditions. Those ways to behave will be studied as a “relevant case” and are treated more in detail. At the end it will be possible to collect and organize all the “relevant cases” founded, and by classifying them it will be possible to deliver general results in terms of structural behavior under fire condition depending on load ratio adopted and fire severity. The most important thing is that this general classification gives an idea on how the structure behave depending on fire severity and load ratio applied and by knowing that it gives us important information about the vulnerability under a certain fire and load condition.

### 5.3.2 Frame 1

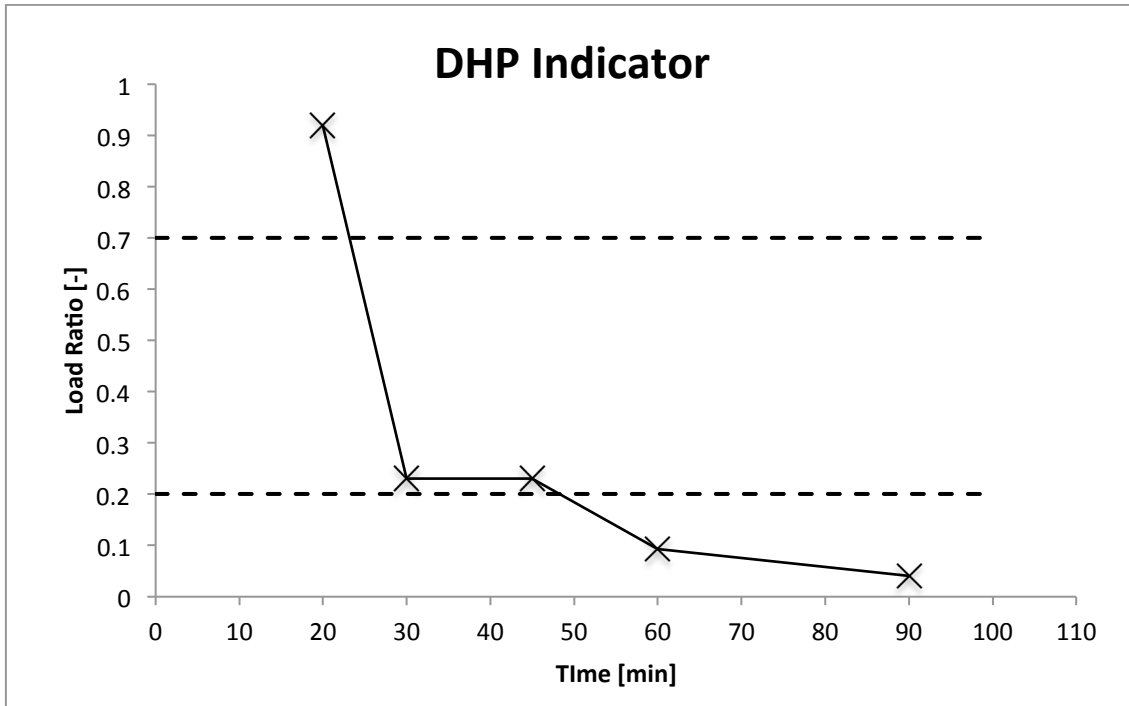


Figure 44 - DHP indicators, Frame 1

In figure 44 are represented the results obtained from the frame 1. The vertical axis represents the ratio between the applied load and the load capacity at ambient temperature; the horizontal axis is referred to time in minutes. The two-dashed lines are the range of load ratio for which the study case can be assumed realistic as explained above. The black line is the DHP indicator, this means that each point found to construct this line is representing the minimum load ratio able to trigger at least a local failure under a certain duration of heating phase (considering the parametric fire adopted). This means that for this kind of geometry, every couple made of load applied ratio and established duration of heating phase above this line will bring at least to a local failure of the hated column.

It is possible to see how duration of heating phase of 60 and 90 minutes are too severe for the tested structure, in fact in this specific case a small load ratio is required to reach the failure of the first structural element. It is possible to say that practically the structure will fail under its self-weight for duration of heating phase of 90 minutes. On the contrary by taking duration of heating phase of 20 minutes it would be necessary a big load ratio applied in order to get failure, quantified as almost the entire load capacity at ambient temperature.

In conclusion the most realistic duration of heating phase range is in between 30 and 45 minutes that see as a maximum load ratio to keep the structure safe 0,23.

### 5.3.2.1 Relevant case 1, Frame 1

Here is shown how the structure behave during the fire, by taking as reference the study case with duration of heating phase of 45 minutes and load ratio equal to 0,23.

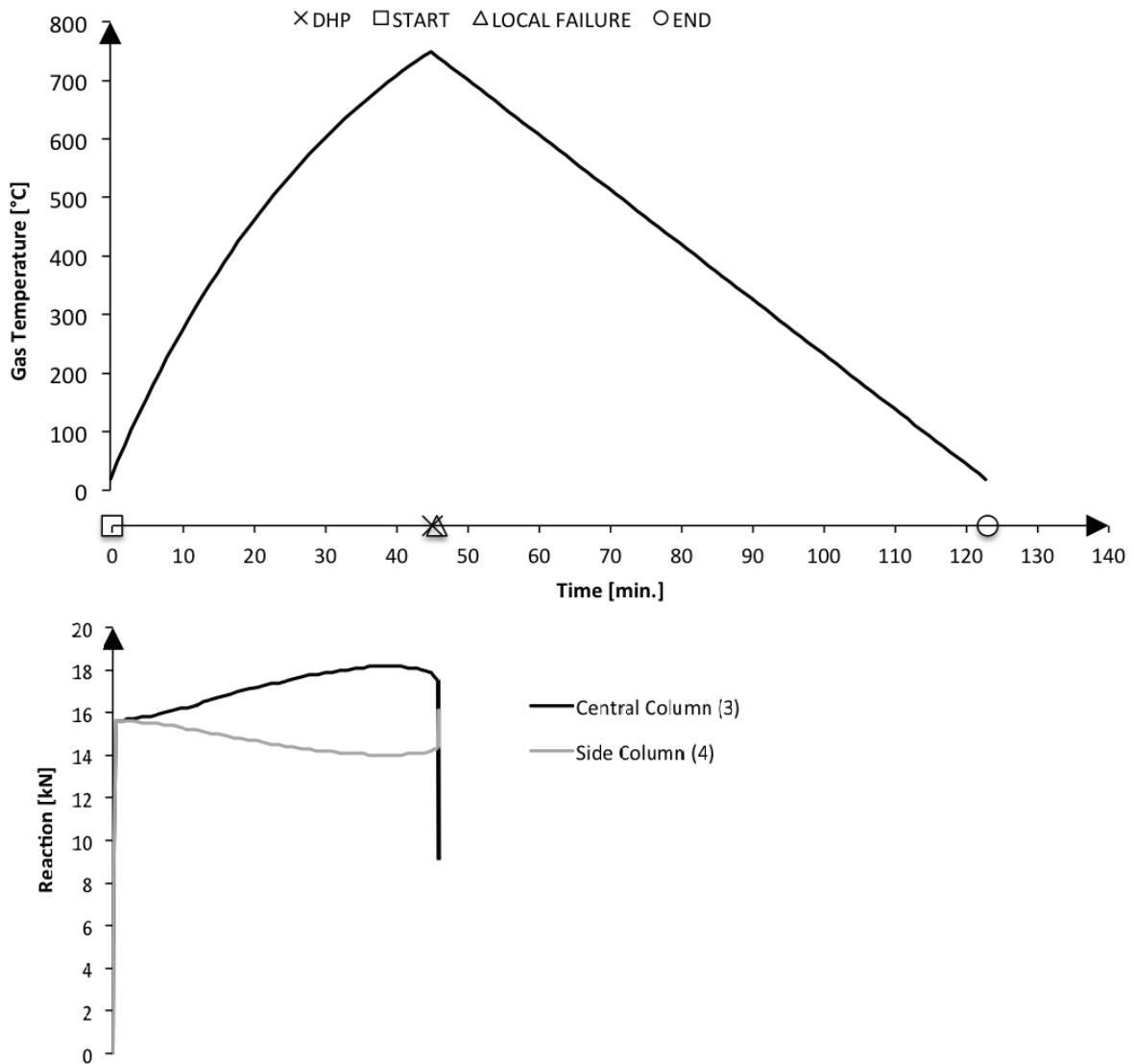


Figure 45 - Behavior during the test, relevant case 1, frame 1

Figure 45 shows the behavior of the relevant case from different point of view. Starting from the top, it is possible to see a curve representing the gas temperature during the supposed whole fire duration. The horizontal axe, indicates the time duration of the test and at the same time gives important information such as the fire starting time, the duration of the heating phase of the fire (45 minutes), the moment in which the failure happen and with the circle, the supposed end of the parametric fire curve. In this case when the failure occurred the simulation stopped before its natural ending point. On the bottom it is possible to observe how the reaction at the column base behave during the fire. In

particular the two lines are referred to the central column and the side column (see figure 40).

From this picture it is also possible to see an ascending curve regarding the base reaction of the heated column during the whole heating phase, this fact is related to thermal expansion of the column that going to create additional internal stress. After 1 minute to the end of the heating phase the column failed suddenly without any load redistribution toward the side one. For this reason, is possible to conclude only that the failure is referring for sure the central column and it was a sudden failure. Nothing can be stated about the global behavior of the structure because of a premature interruption of the analysis.

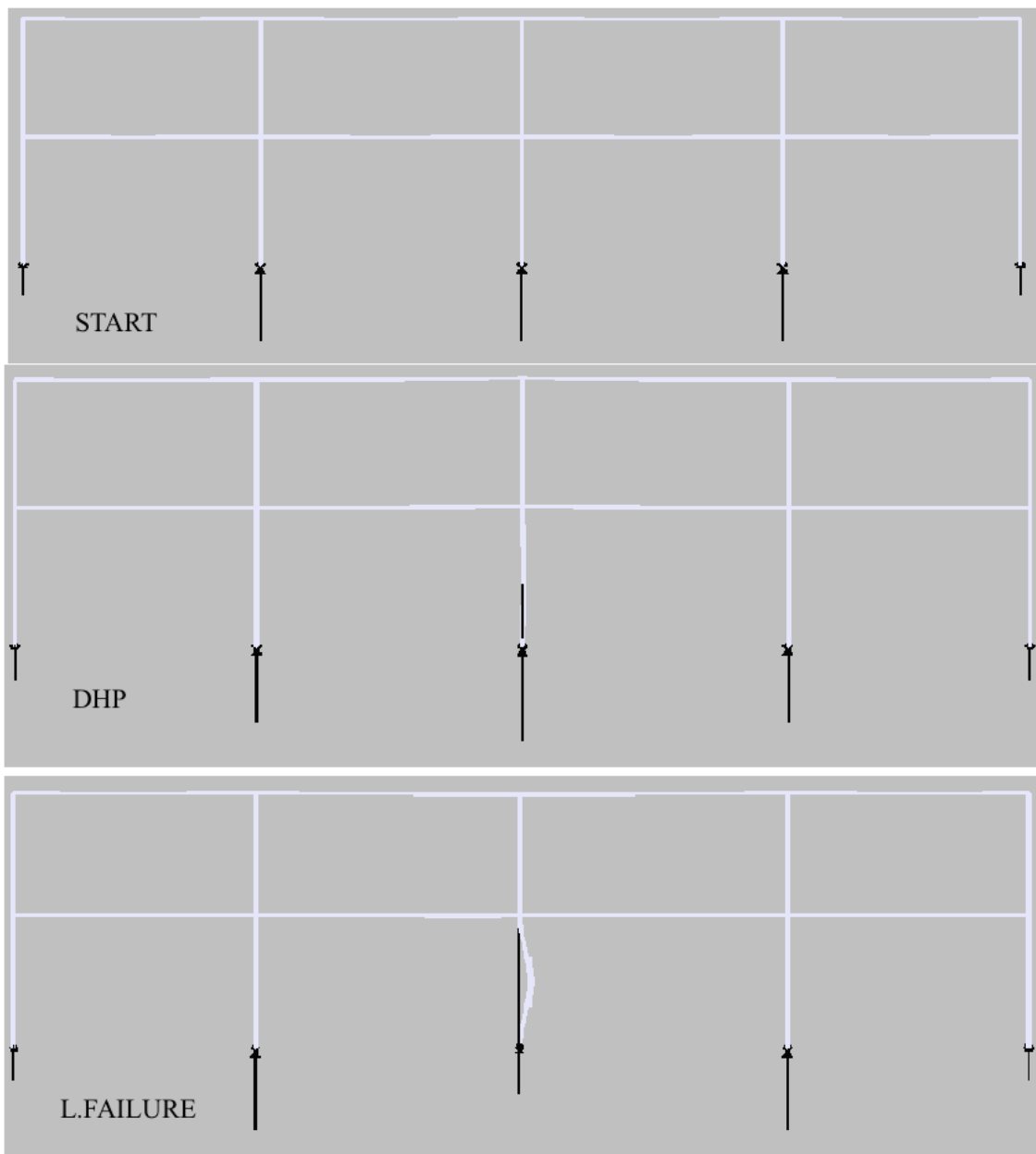
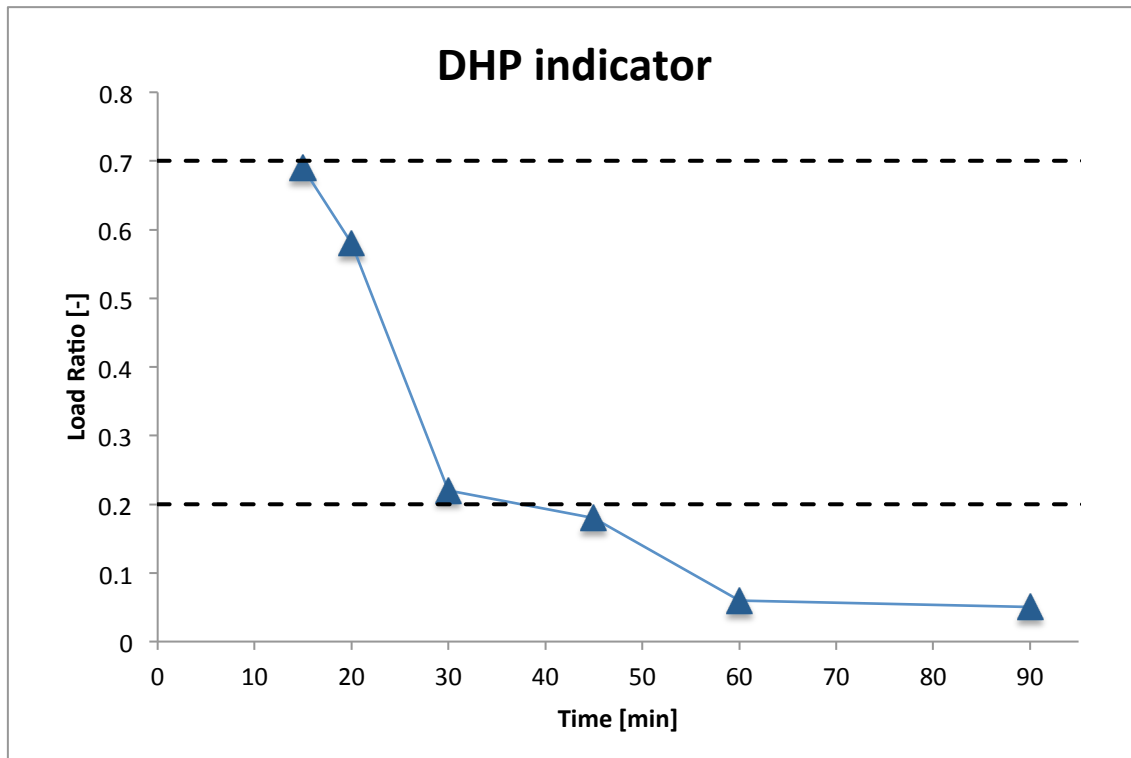


Figure 46 - Reactions-Displaced Configuration

Figure 46 shows the main phases during the fire, the starting point is referred to time 0 minute, the DHP is referred to 45 minutes and the Local Failure represent the situation at 46 minutes. From here it is clearly visible the thermal elongation experienced from the central column at the end of the heating phase, followed with a relevant increase in the base reaction. At the end, local failure appears at 46 minutes due to the column instability.

### 5.3.3 Frame 2



**Figure 47 – DHP indicators frame 2**

In figure 47 are represented the results obtained from the frame 2. The vertical axe represents the ratio between the applied load and the load capacity at ambient temperature; the horizontal axe is referred to time in minutes. The two-dashed lines are the range of load ratio for which the study case can be considerate realistic as explained above. The blue line is the DHP indicator, this means that each point found in order to construct this line is representing the minimum load ratio able to trigger at least a local failure under a certain duration of heating phase (considering the parametric fire adopted). As a consequence for this kind of frame every couple load applied ratio and established duration of heating phase above this line will bring to at least to a local failure of the hated column.

Even for this geometry, it is possible to see how duration of heating phase of 60 and 90 minutes are too severe for the tested structure, in fact in a small load ratio is required to

reach the failure of the first structural element. It is possible to say that practically the structure will fail under its self-weight for duration of heating phase of 90 minutes.

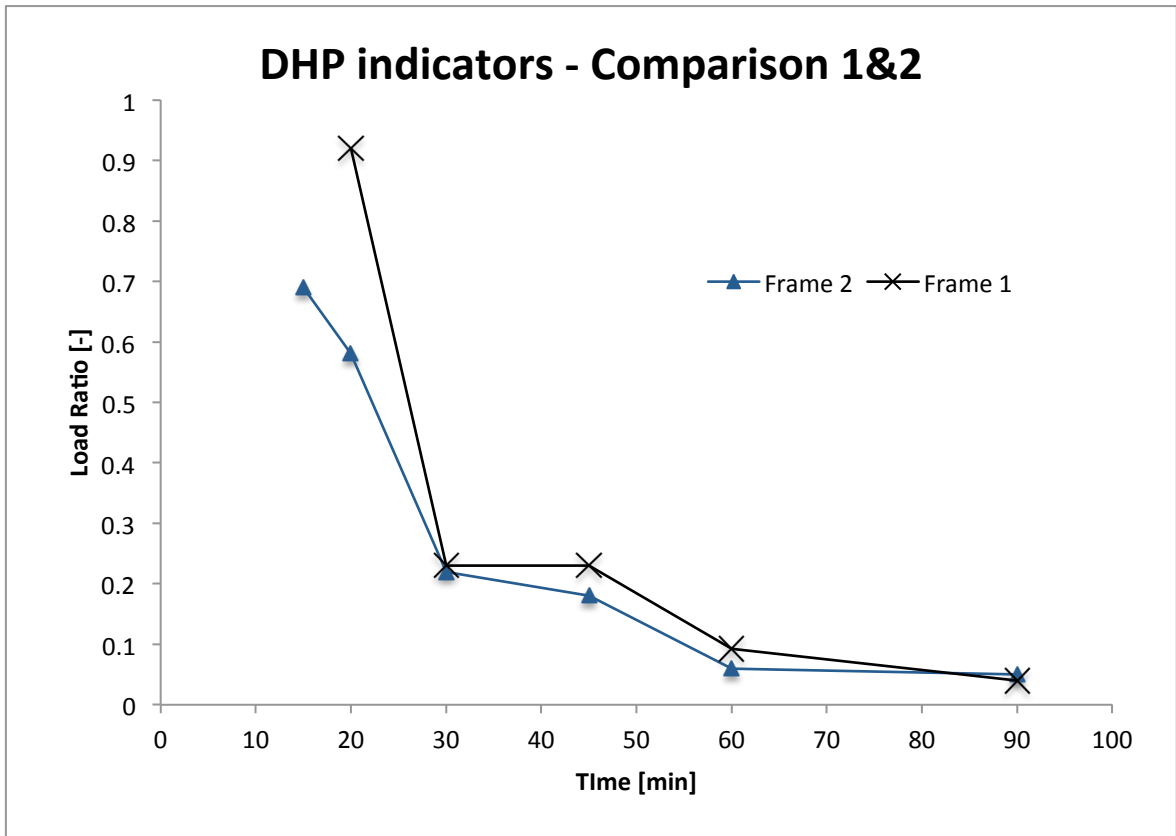


**Figure 48 - Comparison DHP indicators, Frame 1 & 2**

Figure 48 has the purpose to show how an increasing in beams section (Frame 2) does not seem to bring relevant benefits for the structure in terms of DHP indicators. In fact by comparing the DHP indicators obtained from frame 2 (with a bigger beams cross-section) with the others obtained from frame 1, seems clear how a bigger beams sections leads to a slightly decrease in the load ratio required to have the first failure for every parametric fire curve studied. But even if the DHP related to frame 2 as a smaller load ratio respect to the one obtained in frame 1, the gain associated to a structure with bigger beams cross-section is clearly visible by looking at its behavior during the fire.

### 5.3.3.1 Relevant Case 2, Frame 2

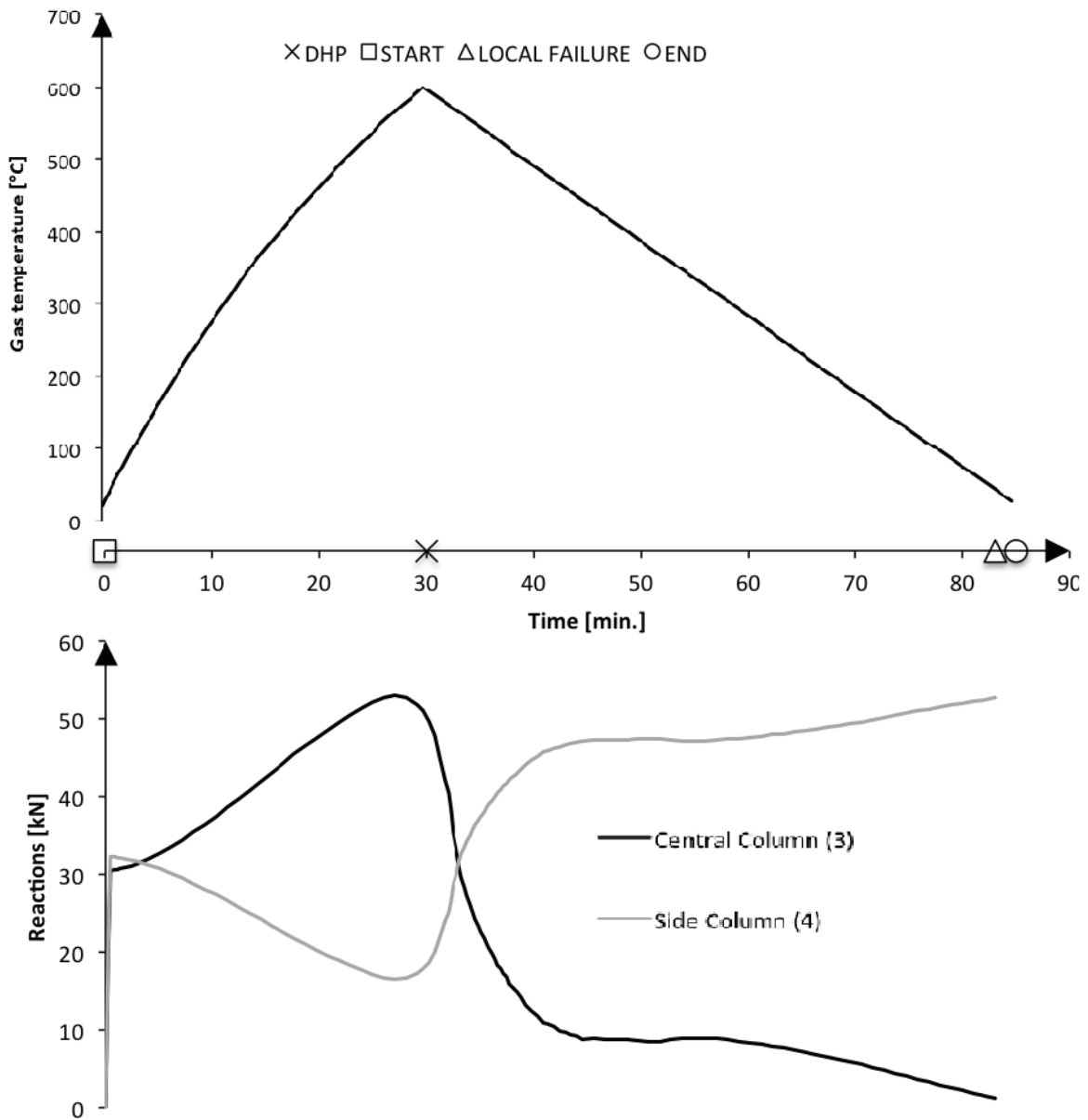


Figure 49 - General Behavior, Relevant case 2 Frame 2

Figure 49 shows the general behavior of the frame 2, in particular referred to the case DHP 30 minutes and load ratio 0.23. At the top the graph, there is indicated the gas temperature during the whole supposed duration of the fire curve applied to the element. The time axe gives information about the fire start, the duration of heating phase and the moment in which the failure happen. In this case the failure comes more than 50 minutes after the heating phase, almost at the end of the fire curve adopted. Then by looking at the base columns reaction in function of the time it is possible to see how the different beams cross-section facilitate the load transfer phenomena. It is clear a first phase in which the central

column during the heating increasing in its reaction due to a thermal elongation, then when buckling coming and starts to reduce its length the base reaction begin to decrease, and at the same time the reaction at the side column increase until when, almost at the end of the whole fire duration the central column is not anymore able to withstands vertical load, so it is considered failed. In this particular case is very clear how the load transfer phenomena develop during the whole fire duration and tell us that increasing in beams cross – section it may bring a slightly less load ratio to failure but the global structural behavior during fire became very different.

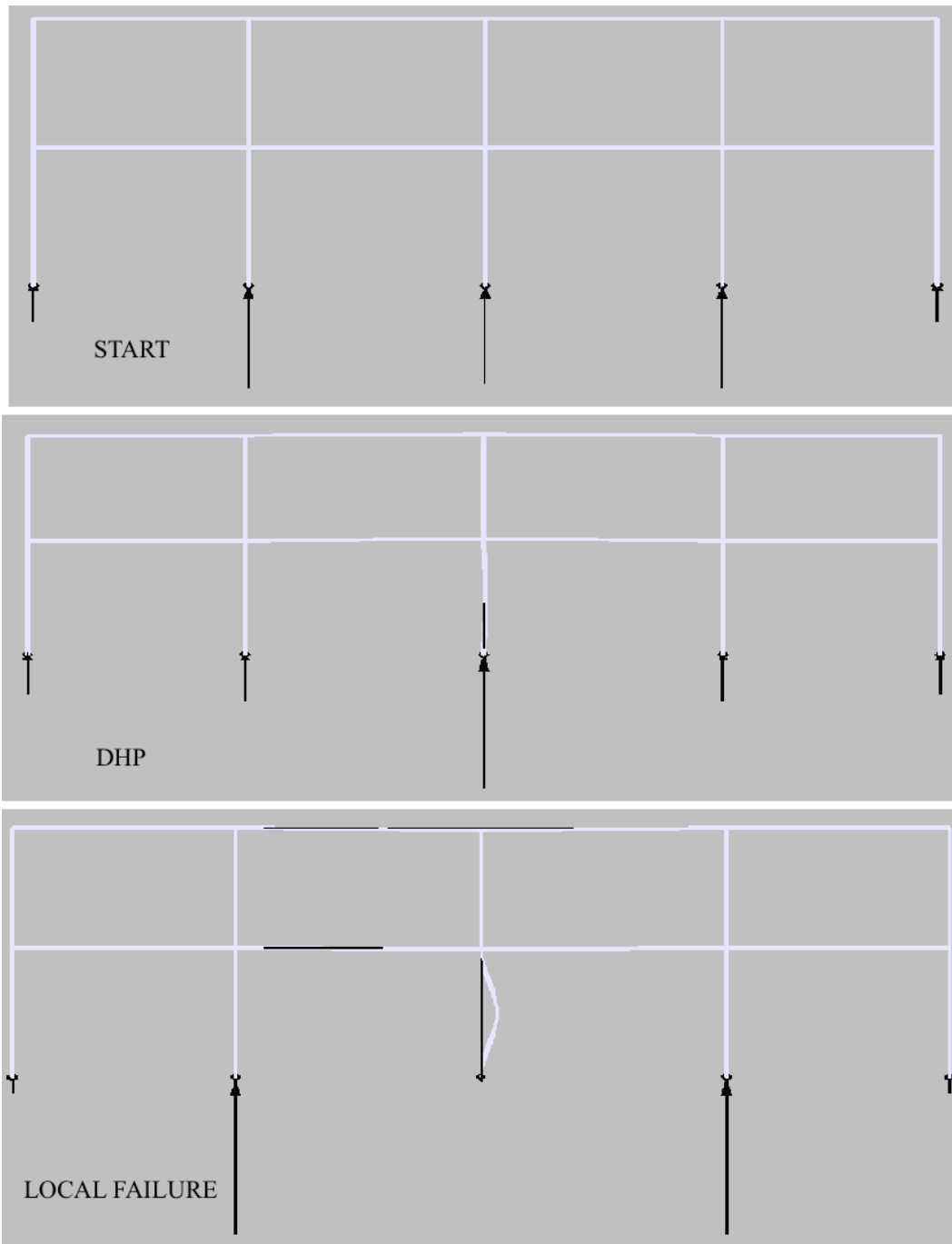


Figure 50 - Reactions-Displaced configuration

In figure 50 it is possible to see the entire structural behavior in terms of reactions and displaced scale during the whole fire. At the beginning for time 0 minute the load reaction among the column 2-3-4 is the same, when it is reached the DHP 30 minutes the reaction in column 3 increased significantly respect to the column 2-4. At the end 83 minutes a local failure of the central column happened ( $N=0$ ) and the column 2-3 has increased their carried load.

### 5.3.4 Frame 3

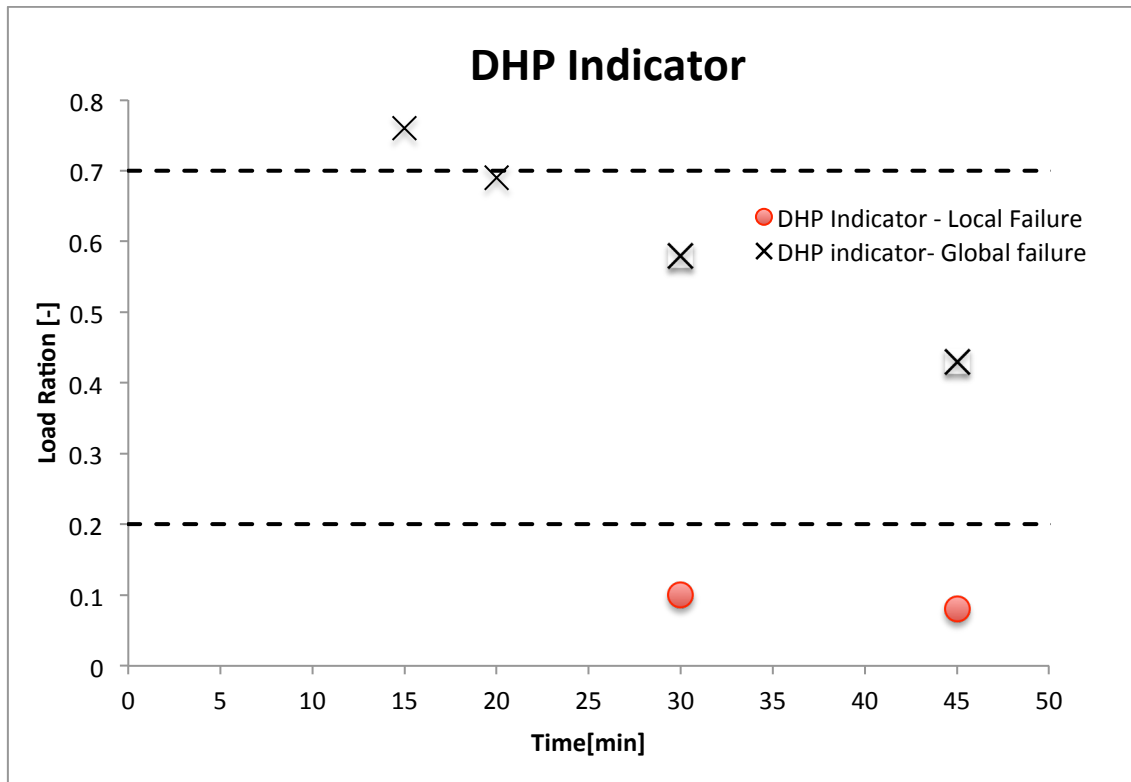


Figure 51 - DHP Indicators, frame 3

Until now the DHP indicator was used to individuate a couple of points (Load applied, Duration heating phase of selected fire curve) that were able to give us the minimum configuration leading at the first failure. In frames 1 and 2 there were found only failure at local level, in particular regarding the heated column. By performing the analysis for frame 3 with the biggest beams sections, it is found that even in this case increasing the beams section has decreased the minimum load ratio necessary to get the first failure. On the other hand, although the minimum load ratio for the first failure decreased it was possible to notice that the structure even after a column loss was robust enough to withstand the whole fire duration. At that point, other analyses with higher load ratio were performed until when the structure experienced a global failure. This is the reason why in figure 51 it is possible to look at 2 different DHP indicators, one referred to the heated element failure (local) and the other one referred to the global level. In particular if we look at the parametric fire with a duration of heating phase of 30 minutes, by applying a load ratio in between 0.1 and 0.58 the heated column will experienced a local failure. Instead starting from a load ratio more than 0.58 the structures will loss also a side column. The singularity is that there were found two different ways experienced from the structure that leads to a global failure. The first one is mentioned above, local failure of the heated column and then failure of the side column. The second one can be found for the parametric fire curve of duration 20 minutes with a load ratio of 0.69. In this case the frame for a 20 minutes fire curve below a load ratio of 0.69 is able to withstand the whole fire duration. Otherwise, if

the load applied is bigger than 0.69 it fails globally due to a failure of the side column that for instance is not even heated. This kind of behavior was got also for 15 minutes DHP parametric curve and it can be considered as the most detrimental for the entire structure.

From here we have seen how by increasing the section geometry it is possible to obtain different structural behavior during the fire phases, since the vulnerability of the structure is related to all of that, those particular cases will be analyzed in the specific.

### 5.3.4.1 Relevant case 3, frame 3

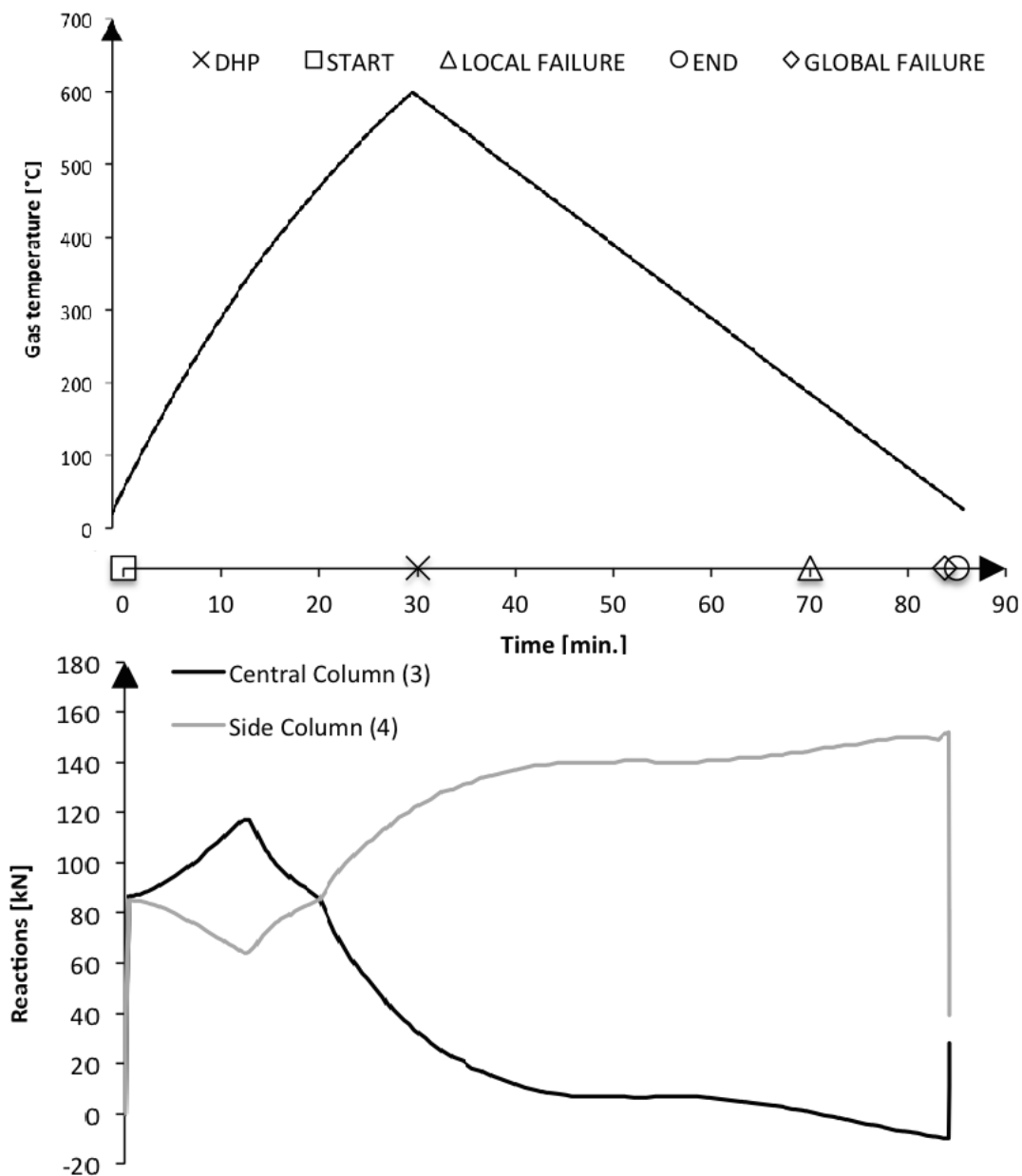
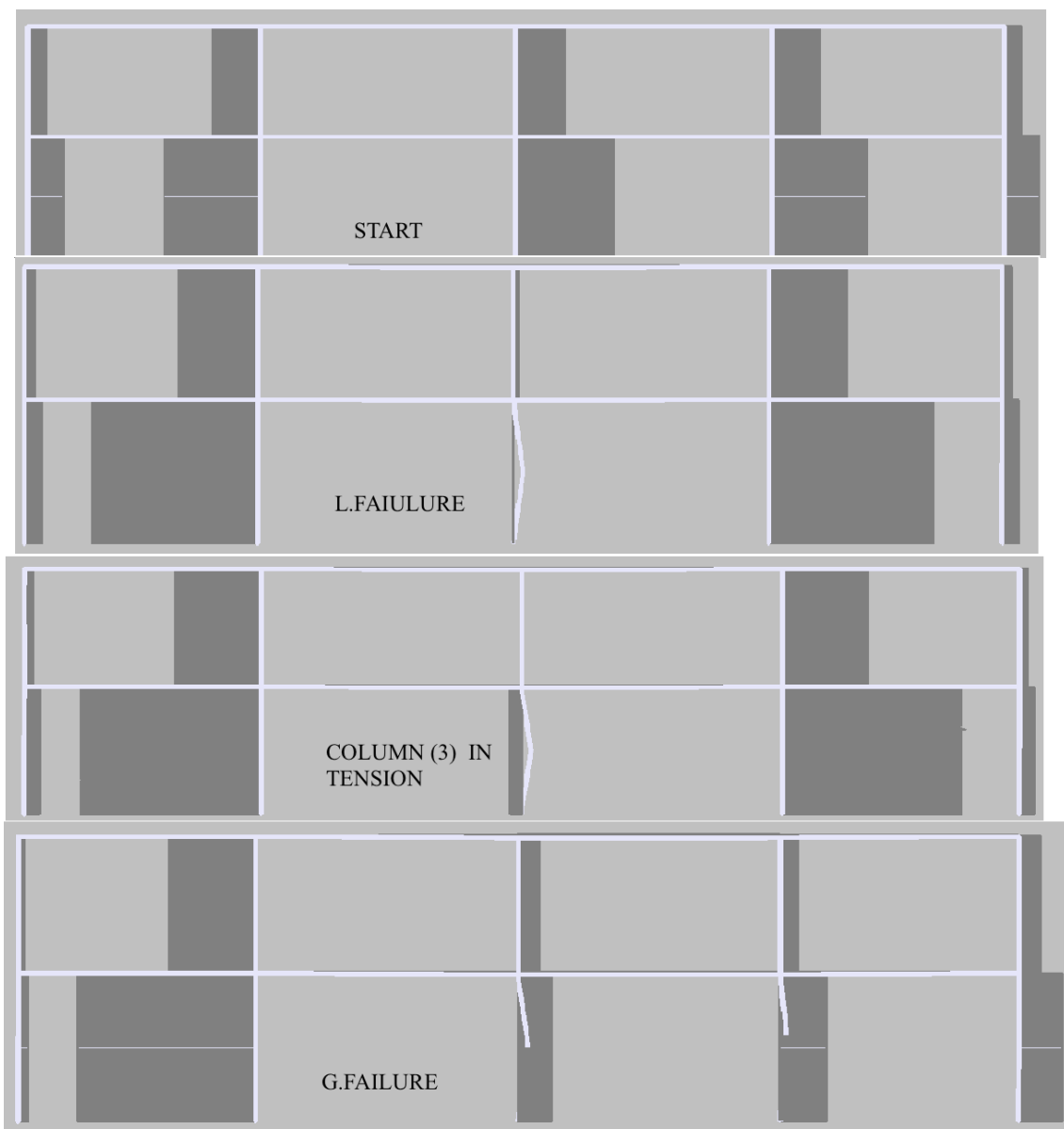


Figure 52 - General Behavior, Relevant case 3, Frame 3

Figure 52 is referring to the load ratio 0.6 for a DHP of 30 minutes. In this case the structure under fire, shows the first local failure in the heated column at 70 minutes, then almost at the end of the supposed fire duration the side column number 4 reached its maximum capacity generating a global structural failure. This way to behave is quite interesting, after the local failure of the central column at 70 minutes, it is possible to appreciate the fact that the central column is not anymore compressed but instead it is in tension. As a consequence after its failure it is possible to say that the column is pulling down the two beams, and at the same time, the structure is using its robustness being still in equilibrium. Only after some minutes in which the pulling action of the column was increasing gradually, the side column reached its maximum capacity and failed, leading to the global failure of the entire structure.



**Figure 53 - Evolution of the Axial force during the fire, Relevant case 3 , Frame 3**

In figure 53, where all of the main fire phases are shown in function of the axial force in the elements and displaced scale it is clear how from a starting situation in which the axial load was distributed on all of the frame column, step by step with the passing of time goes to 0 for the central column (Local Failure) then starting to pull the beams down (Column 3 in tension) and after a while also the side column failed generating the global failure of the structure.

Since this particular way to behave from the structure is interesting, and at the same time the initial assumption made upon the steel behavior under fire was to have a reversible strength. It is decided for this case only, DHP 30 minutes with load ratio of 0.6 to adopt a more refined steel behavior. In particular a loss of yield strength is assumed  $0.3 \text{ [MPa/}^\circ\text{C]}$  when the element has been heated beyond a temperature value of  $600^\circ\text{C}$ .

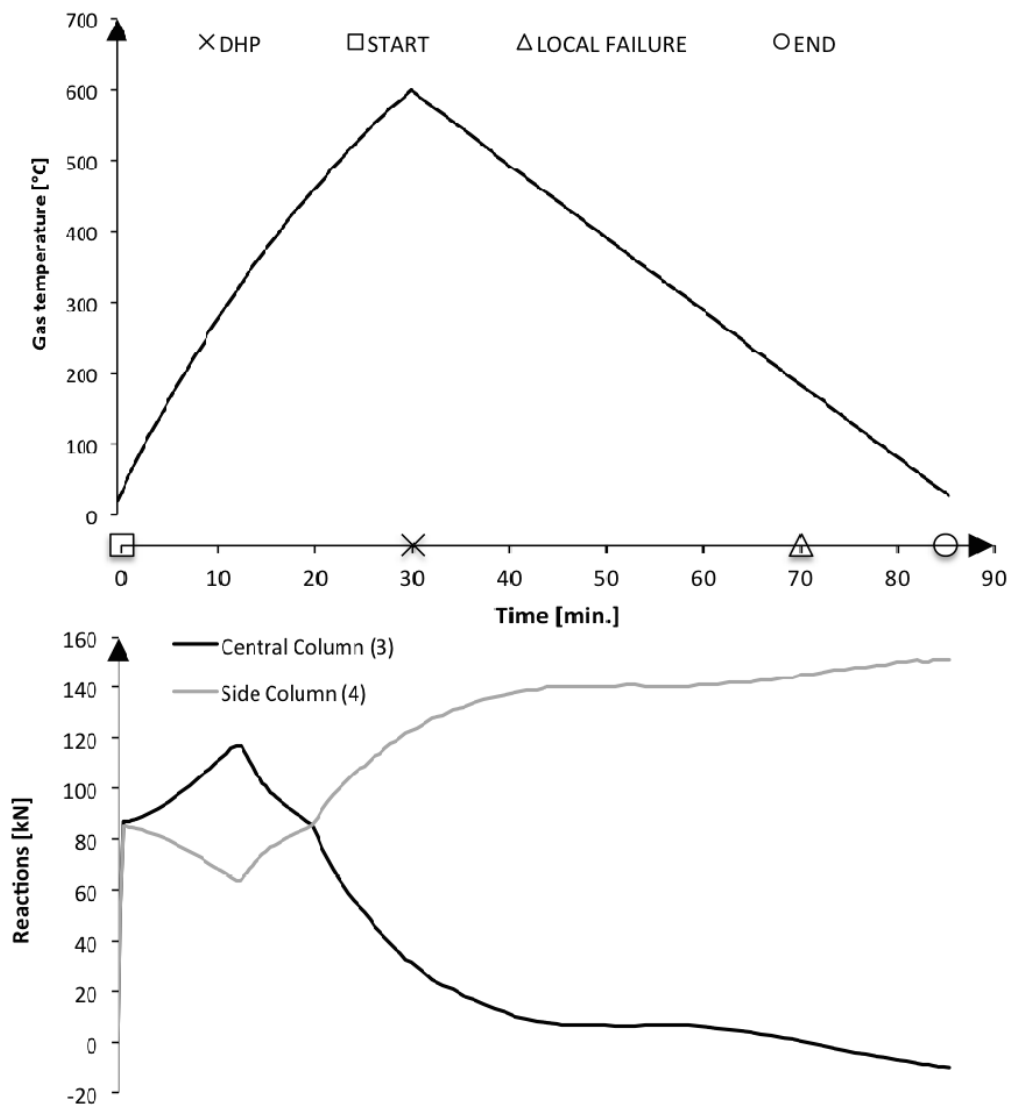
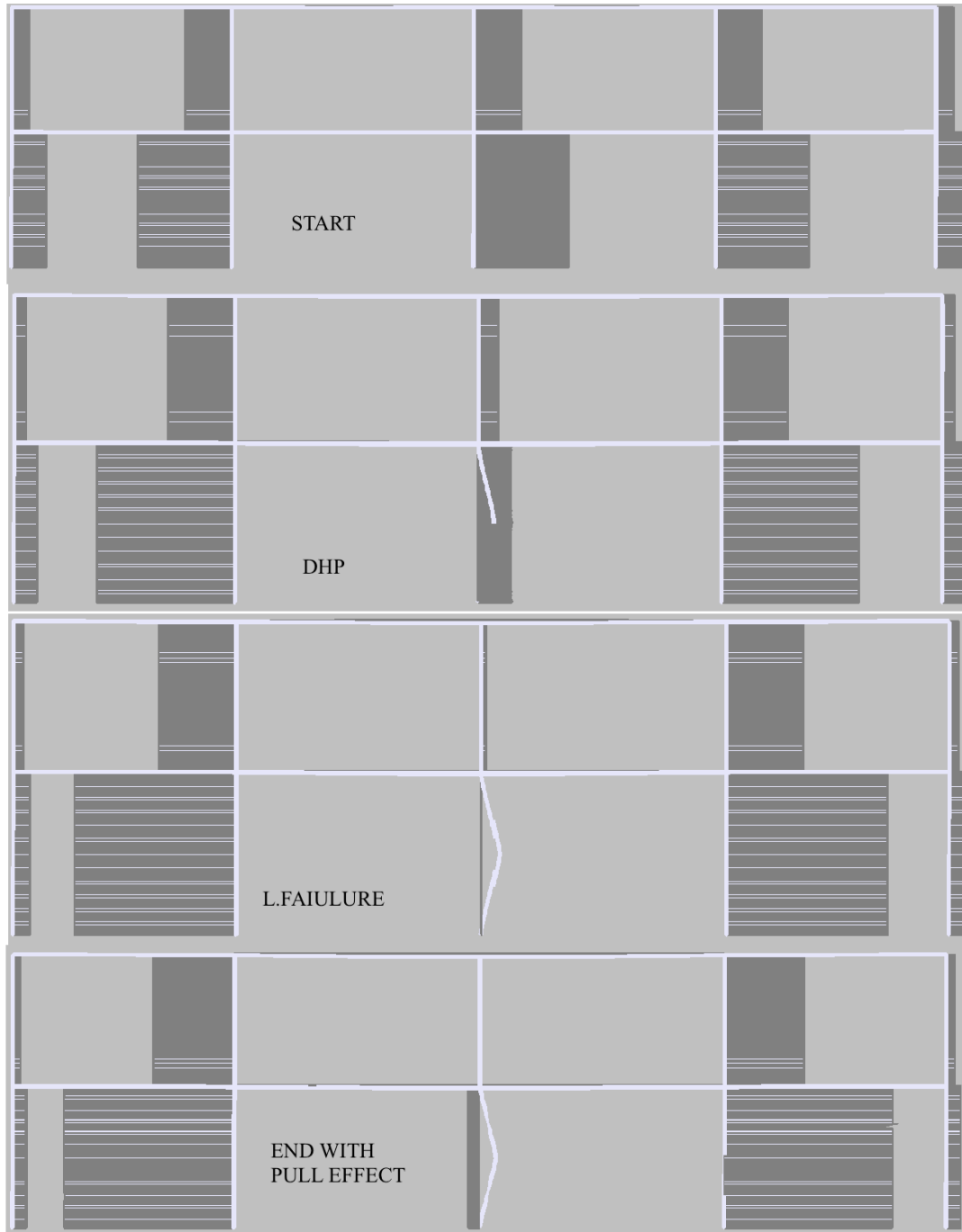


Figure 54 - General Behavior, Relevant case 3, Frame 3 , non-reversible tensile strength behavior

Figure 54 is the result obtained by making the numerical analysis of the relevant case 3 upon the frame 3 but with a non-reversible tensile strength behavior for the steel. The output is very similar, in this case the structure does not reach a global failure, but it is possible to see how the local failure point for the heated column is the same (70 minutes) and the side column 4 is next to his maximum capacity (153kN). Furthermore, also for this simulation the central heated column after its local failure starting to pull down the above beams.



**Figure 55 - Evolution of the Axial force during the fire, Relevant case 3 , Frame 3 Non Reversible behavior.**

### 5.3.4.2 Relevant Case 4, Frame 3

As mentioned before there were found two different ways in which the structure under natural fire can reach the global failure. This is the second one and it is the most dangerous. The presented results are related for a 15 minutes DHP of the parametric fire curve and a load ratio of 0.76

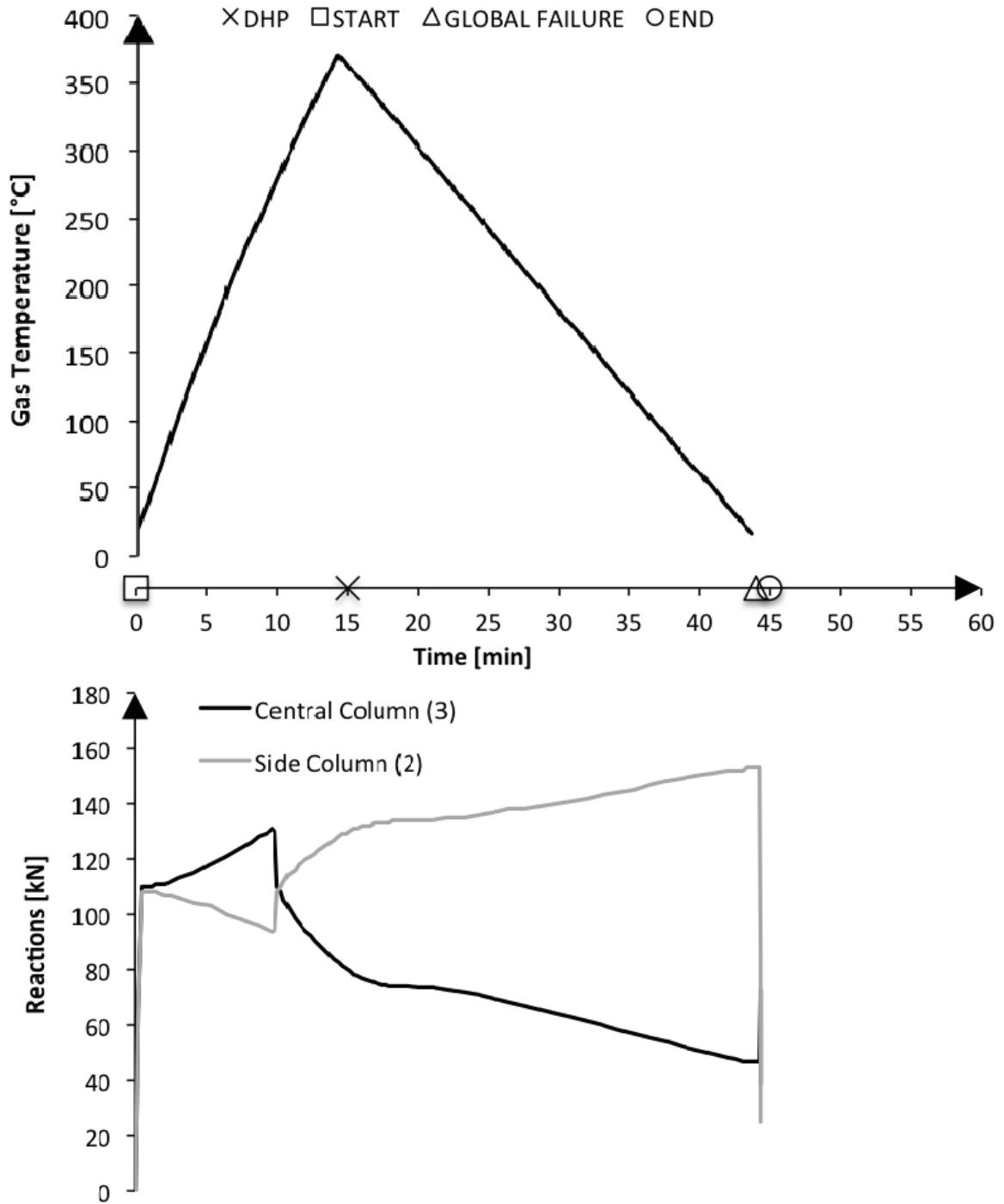
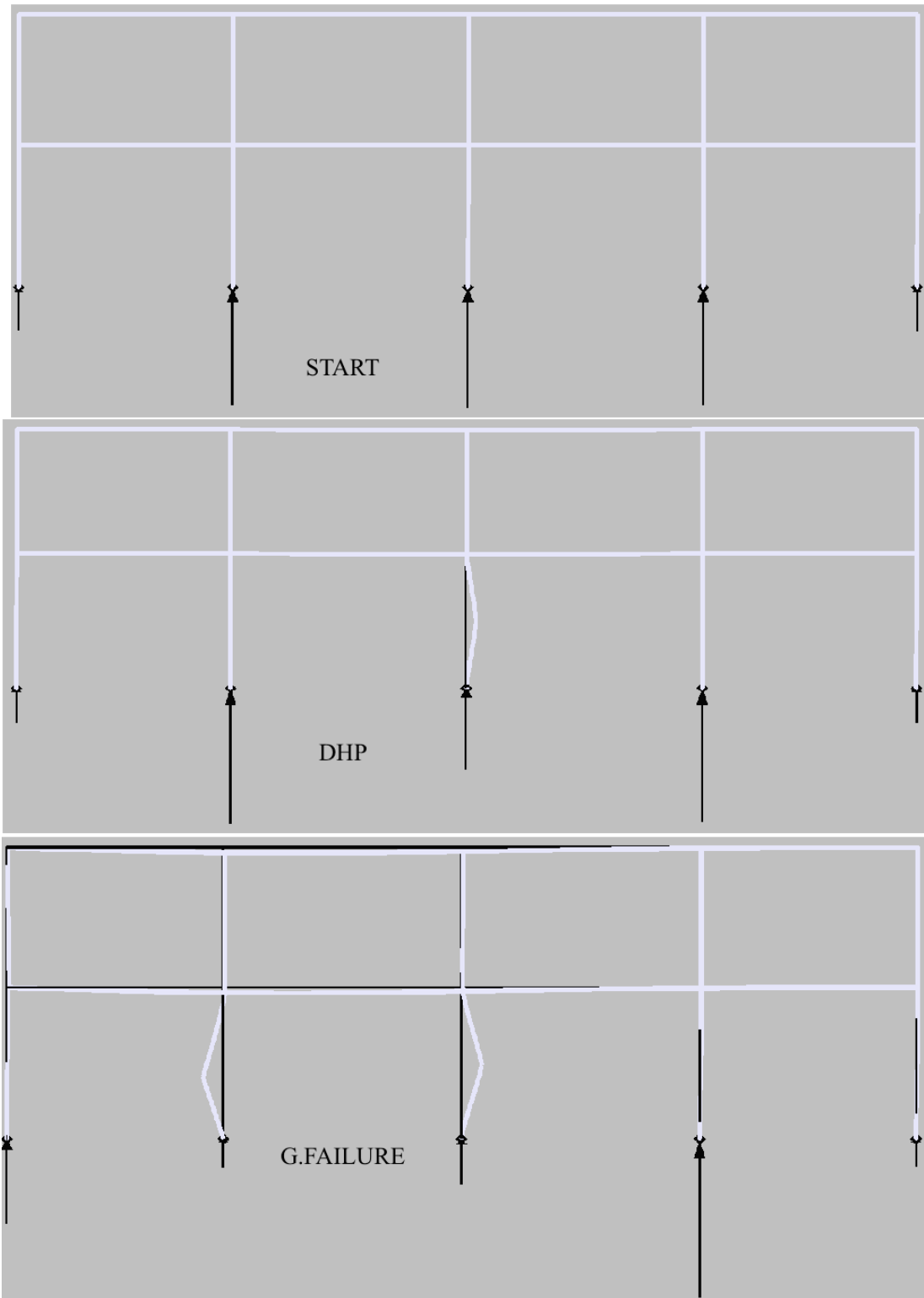


Figure 56 – General Behavior, Relevant case 4, Frame 3

From figure 56 it is possible to see the gas temperature evolution in function of the time. The horizontal axe has some reference point, the fire starting, the DHP and the time to failure. This case is particular because shows another different response of the structure under a natural fire. Until now we have seen from case 1 to case 3, local failure of the column due to buckling, then local failure followed by a load transmission and just above local failure of the heated element followed from the failure of the non-heated one. In this situation the column buckle some minutes before the ending of the heating phase (might be for the high initial load ratio), then the reaction to the base column 3 (central one) is continuously decreasing. In the meanwhile the column to the side, for instance the one at ambient temperature, due to the load transfer phenomena reached its maximum capacity by failing first. It is possible to see how in the same moment in which the side column failed, the central column experienced firstly an increase and then suddenly a decrease of axial compressive strength. This means that in the exact moment in which the side column failed the central one tried to carry loads, but since it was already buckle it could not carry anymore loads and failed too. This kind of behavior is very dangerous because trigger a sudden failure of the whole structure even though the heated element was potentially able to survives to the whole fire.

In figure 57 it is visible the base reaction for each column and the displaced scale. If we look at the bottom part of the image, it is stated global failure even if there is a reaction at the column base. The residual reaction at the column base worth nothing, this is why the analysis suddenly stopped by showing how the reaction in column 2 decreased in less than one second from more than 140kN to 20kN (figure 56). Furthermore it is possible to see how when the side column failed, the load was redistributed to the central one (figure 56) that experienced an increase in the base reaction followed from a sudden decrease that lead to think that it is failed almost in the same moment.



**Figure 57 – Reactions – Displaced configuration**

## 5.4 Conclusions

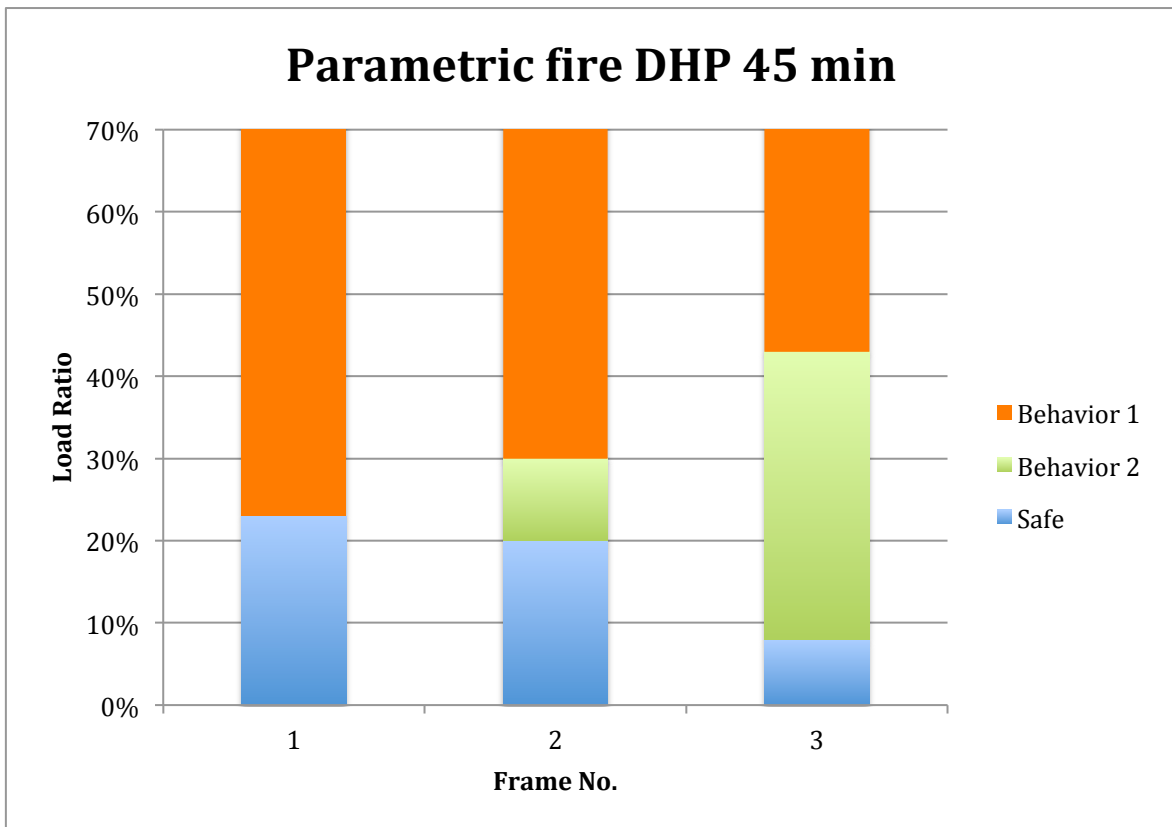
After having discussed some of the most relevant analysis performed, it is clear how a structure under a natural fire can fail during the cooling phase of a fire. In this study were performed different analyses by adopting different geometry of the study frame under different parametric fire curve and load ratio. It was possible to see that based on the beam section size, the behavior of the frame changed in terms of DHP indicators (minimum load ratio required in order to experienced a first element failure under a certain parametric fire curve) and in terms of structural response. Summarizing what we have seen until know, it is possible to say that mainly 4 different structural responses have been found among all of the performed analysis. Since the vulnerability of structures under natural fire is related to the way to behave under the fire itself, the following table is used to classify the different way to behave of the structure under the different simulation performed.

1	Local failure heated column	Relevant case 1 (see 5.3.2.1)
2	L. Failure heated column → load transfer	Relevant case 2 (see 5.3.3.1)
3	L. Failure heated column → load transfer → G. Failure	Relevant case 3 (see 5.3.4.1)
4	L. Failure side column → G. Failure	Relevant case 4 (see 5.3.4.2)

**Table 7 – Relevant case classification**

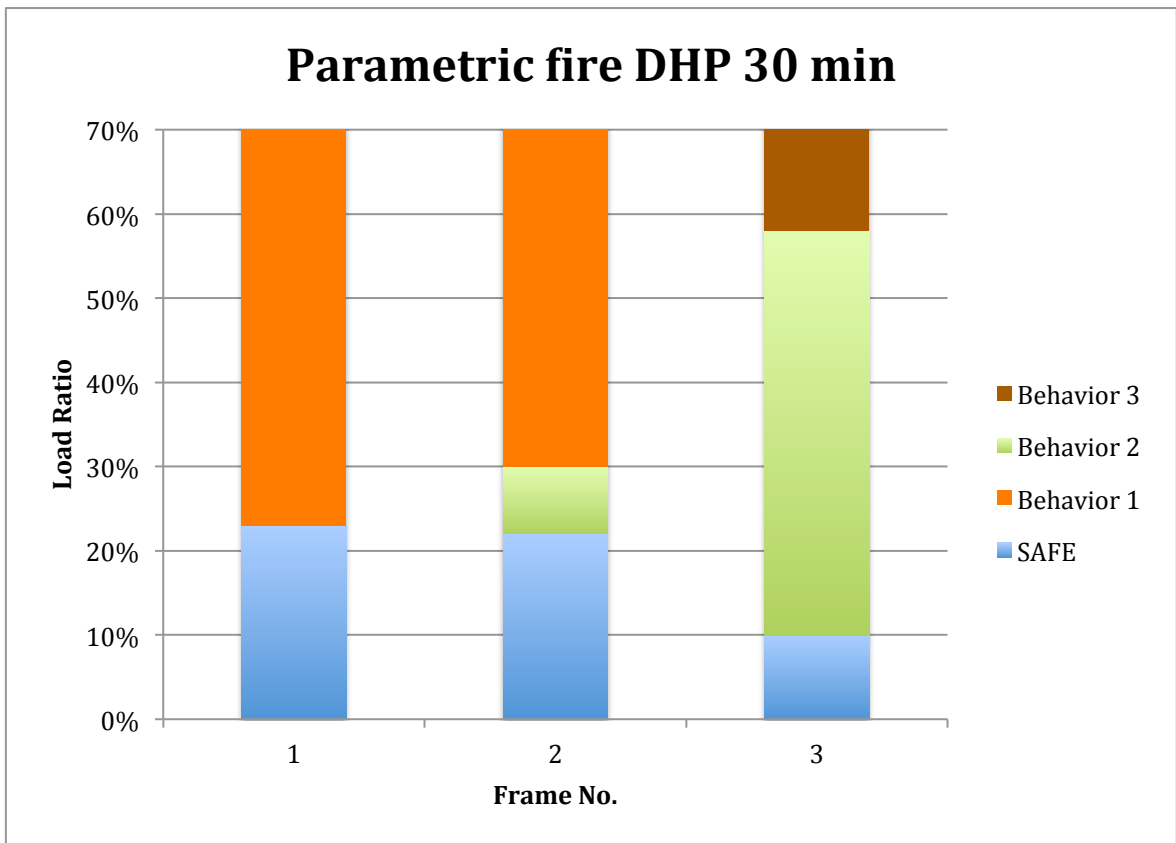
Table 6 summarizes the different behavior obtained from the structure under the different analysis, all of the obtained result are gathered and classified according to this table. In particular:

- **1**, the structure under fire has a sudden local failure of the heated column and the analysis does not give further information because it is stop there.
- **2** a failure of the heated column appear, but the simulation continuing until the end of the fire showing the ability to redistribute the load between the columns
- **3** Is very similar to the number 2 but the simulation does not come to the end because a global failure appear when the side column fail after a load redistribution
- **4** Is the most dangerous situation, during the cooling phase a side column (not heated) fail, and at the same time global failure is trigged



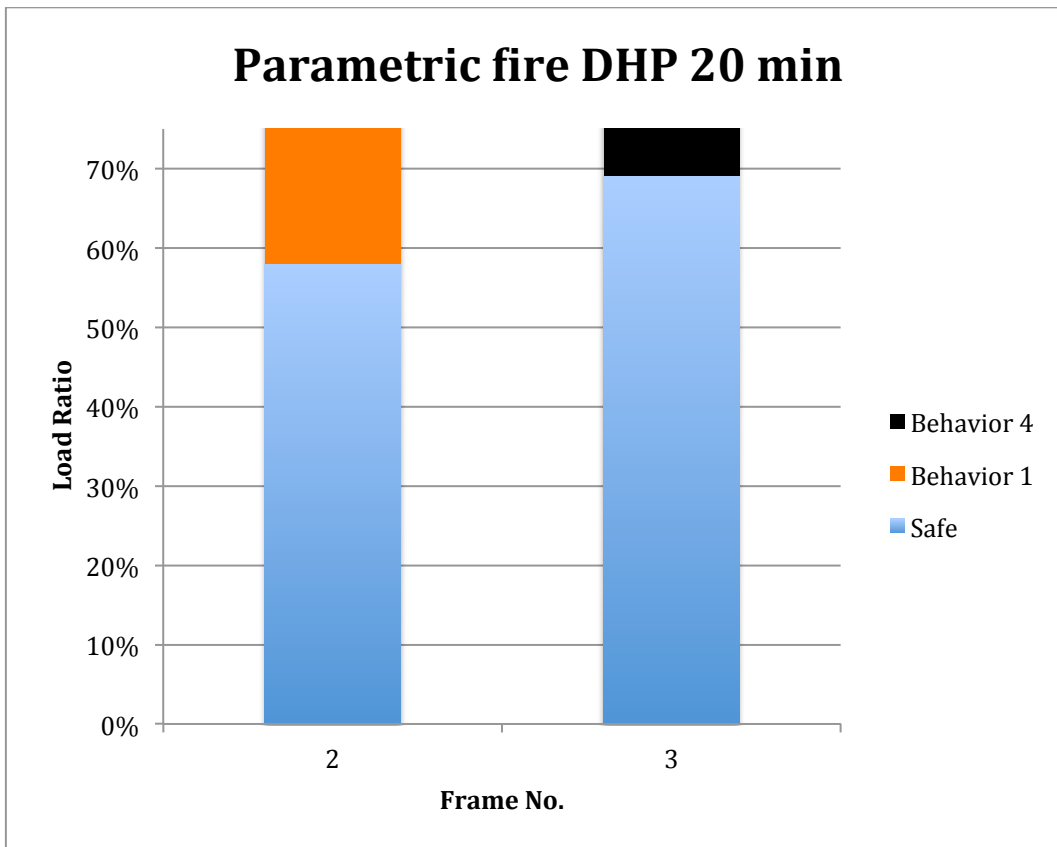
**Figure 58 - Frame response overview**

Figure 58 represents the frame response for a parametric fire curve with DHP 45 minutes respect to the different frames studied, where frame 1 has the smallest beam section and frame 3 the biggest. In the legend the safe color shows the maximum load ratio for which the structure is able to withstand the whole fire duration. Behavior 1 as stated in table 7 represents a sudden failure of the heated element without load redistribution. The behavior 2 represents the behavior observed in 5.3.3.1 where after a local failure the structure shows the ability to redistribute the load between the columns. Having said that, from this figure it is possible to notice how the structure with the smaller beam section remains safe (able to withstand the whole fire without any failure) for a bigger load ratio respect to the others. It can be observed that the more the beams section is increased the more the load ratio necessary to a first failure is decreased. On the other hand it is possible to see which is the real gain to have a bigger beam section, in fact frames 2 and 3 develop the ability after the local failure of the heated column to withstand the fire thanks to a load redistribution among the columns (behavior 2), instead frame 1 does not behave in this way, it is possible to see that after load ratio 0.22 it fail suddenly according to behavior 1.



**Figure 59 – Frame response overview**

The same is done for all of the geometry tested under a parametric fire with duration of heating phase of 30 minutes. In figure 59 it is possible to appreciate the same pattern that show how increasing the beams section size the load ratio in which the structure is considered safe is decreasing, but at the same time the general stability of the whole structure is increasing. For this specific parametric fire the tested geometry with the biggest beam section (frame 3) at high value of load ratio 0.58, experienced a global failure (as described for behavior 3) after having kept its global stability without a column.



**Figure 60 – Frame response overview**

Figure 60 is referring only to frames type 2 and 3, because for a parametric fire with duration of heating phase of 20 minutes the frame 1 until 0.7 is safe. It is obvious respect to the previous cases that the load ratio necessary to have the first failure is increased, because the fire is less severe. Something important comes up from the frame case 3 behavior, in fact it is safe until a load ratio of 0.69 then a global failure according to the behavior 4 appears. Instead for frame 2, even if the load ratio necessary to have the first failure is 0.58, when this value it is over helmed the failure comes according behavior 1, meaning that for sure there is a sudden local failure of the heated column but from the output results it is not possible to say something else, so in theory a global failure might be avoided.

## 6. VULNERABILITY OF REINFORCED CONCRETE STRUCTURE UNDER NATURAL FIRE

As mentioned in chapter 1, less effort is put to the concrete if compared with what has been done for the steel. The main goal of this chapter will be try to understand if it is possible observe for a reinforced concrete structure the same behavior obtained for the steel cases. Particular focus is put on the likelihood to obtain a failure during cooling and about the possibility to see load transfer behavior from one column to another that might lead to collapse.

### 6.1 General design

One of the reasons why less effort is put on the reinforced concrete structure is because in this case there was not a starting experimental study as we had for the steel, so logically more attention was dedicated more upon steel. In this paragraph it is explained how the model is designed from the general geometry to the sectional and material level.

#### 6.1.1 Geometry

The structure's geometry was assigned simply by scaling the steel structure previously studied by multiplying the length of each element by two.

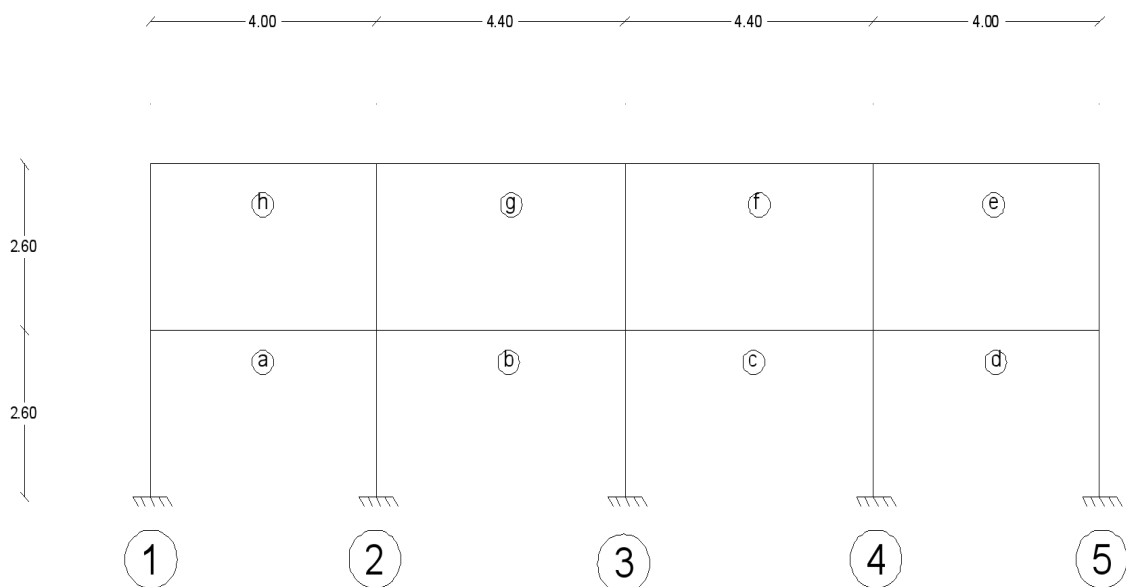


Figure 61 - Reinforced concrete geometry

Figure 61 describe the global frame geometry, it is made of four bays and two stories, the span length of the two middle bays is 4.4 m each and the two side bays 4.0 m each, the heights of the columns are 2.4 m for the first and second storey.

### 6.1.2 Columns & Beams

For as regarding the constituting elements, in particular columns and beams they were designed by following the general rules proposed from EN1992-1-1 (14). Regarding the column design, according to EN1992-1-1 the minimum amount of longitudinal steel bars allowed are 4, the minimum steel reinforcement area goes from 0.02  $A_c$  to a maximum of 0.04  $A_c$ , where  $A_c$  is the concrete area. The frame's columns 1-2-3-4-5 are equals between each others as described in table 8.

Section [cm]	N. of Rebar	Rebar Diameter [cm]	Cover [cm]
30x30	4	1.6	3

Table 8 - Columns sectional proprieties

For the beams according to EN1992-1-1 the longitudinal reinforcement should not exceed a certain area, in particular  $A_{s,max} = 0.04A_c$  where  $A_c$  is the concrete area. Three different beams section are designed as it was made for the steel.

Beam Type	Dimension [cm]	Upper Reinforcement [mm]	Lower Reinforcement [mm]	Cover [cm]
A	30x40	2 $\phi$ 10	3 $\phi$ 18	3
B	30x50	2 $\phi$ 14	3 $\phi$ 24	3
C	30x60	2 $\phi$ 16	4 $\phi$ 28	3

Table 9 - Beams Proprieties

With this kind of conception, at the end it is possible to have three different frames:

FRAME No.	Column [cm]	Beam Type
1	30x30	A
2	30x30	B
3	30x30	C

Table 10 – Frame models

### 6.1.3 Material properties

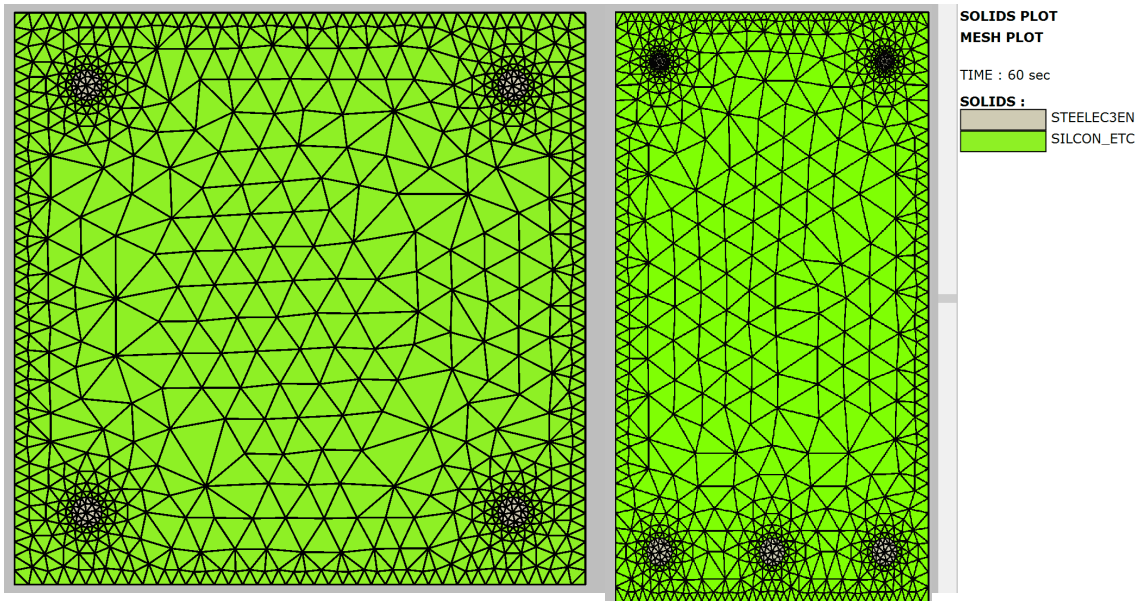


Figure 62 – Column & Beam model

Figure 62 it is a picture used to represent how the different elements were modeled, it is possible to see the kind of material associated at the different surfaces. For the sake of simplicity the figures are not scaled, in fact the beam's height is bigger than the column one (table 8 and 9) because with this figure the purpose is making understandable which kind of material were associated for concrete and steel.

Two different materials are used, "SILCON\_ETC" it means siliceous concrete adopting the explicit transient creep model and "STEELEC3EN". The material used for the steel, has the properties according to EN1993-1-2 (15). The model adopted for the concrete how explained in the SAFIR manual-Material properties (16), is based on Explicit transient Creep, the concrete model is the one present in EN1992-1-2, except that in the ETC model the transient creep strain is treated by an explicit term in the strain decomposition, whereas in the EC2 model the effect of transient creep strain are incorporated implicitly in the mechanical strain term. It is preferred to adopt the ETC model for the concrete because many authors shown how the use of the Implicit Transient Creep model even if can bring acceptable results for element heated with an ISO standard fire curve, will lead to unsafe or erroneous results regarding the natural fire. This is why the transient creep strain considered in the implicit model is recovered during cooling (17).

For as regarding the mechanical and thermal properties of the two materials there are summarized in the table below:

Material	E (Pa)	$\sigma_y$ (Pa)	Emissivity	Convection (W/m <sup>2</sup> K)
<b>Steel</b>	<b>2.1e+11</b>	<b>3.55e+08</b>	<b>0.7</b>	<b>25</b>
Material	Conductivity (W/mK)	fck (Pa)	Emissivity	Convection
<b>Concrete</b>	<b>0.5</b>	<b>3.0e+7</b>	<b>0.7</b>	<b>25</b>

**Table 11 - Material proprieties**

## 6.2 Parametric analysis

A parametric analysis is done in order to address the study's aim, the three different frame described in table 10 are analyzed by changing time by time relevant parameters such as fire curve, applied load and convergence criteria settings.

### 6.2.1 Applied Load

The load applied on the structure, is given from an uniformly distributed load spread all among the beams made of the beams self weight plus an additional load derived from an accidental load, depending on the structure's destination. Since the beam's self weight change case-by-case depending from the geometry, the distributed loads are summarized in the table below. Where the concrete self weight is taken as  $25\text{kN/m}^3$  and the accidental load  $5\text{kN/m}^2$ .

<b>Distributed Load [kN/m]</b>	
<b>Geometry 1</b>	8
<b>Geometry 2</b>	8.75
<b>Geometry 3</b>	9.5

Table 12 - Distributed loads on the beams

In addition a punctual load is applied on each column as described in figure 63.

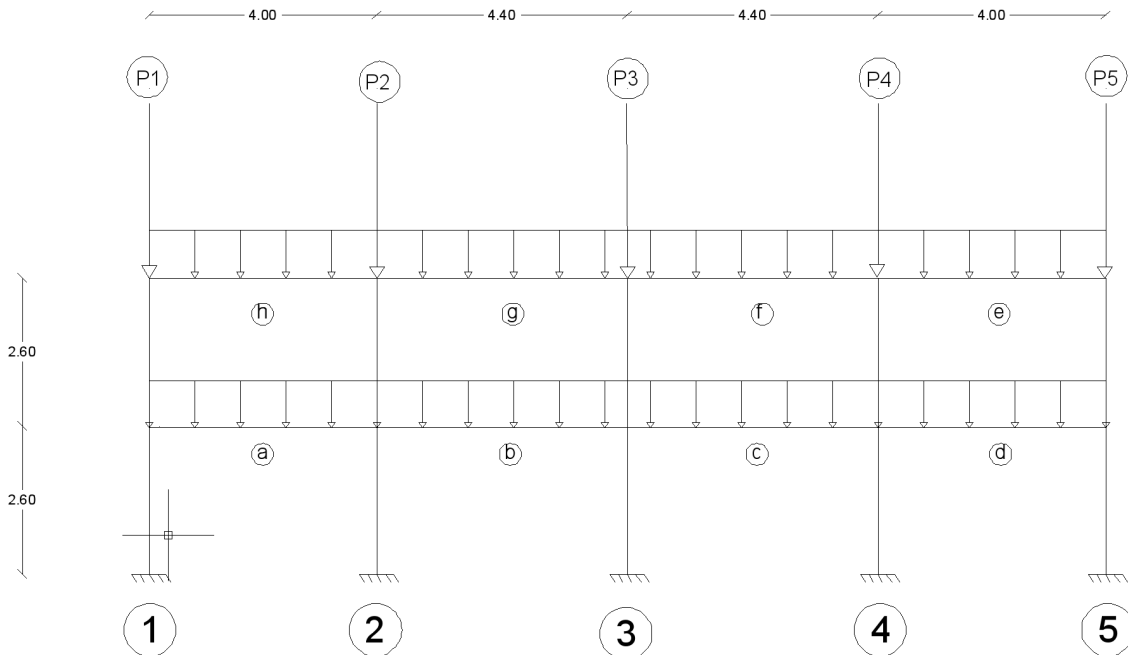
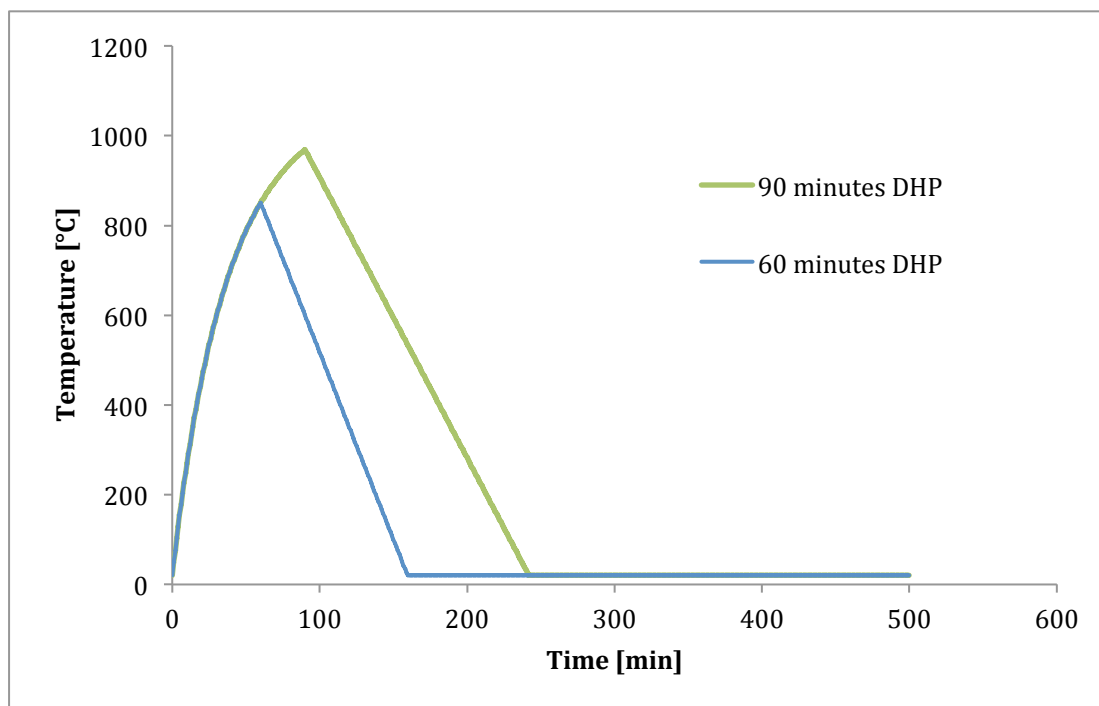


Figure 63 - Load Applied

It is chosen this kind of load configuration with a uniform distributed load on the beams and a punctual load applied on each column (P1-P2-P3-P4-P5) for two main reasons. The first one, because it is the best way to represent a multy storey concrete building in which the punctual load stands for the upper floor column's weight. The second was for a matter of assignment of the load ratio desired for each column. It is simpler take constant the distributed load and increases the punctual load on each column. In the appendix 8.3 it is shown witch is the load maximum capacity at ambient temperature for the columns.

### 6.2.2 Fire curves

The fire curves adopted in order to test the concrete structure are principally two:



**Figure 64 - Adopted fire curves**

Those fire curves are created according to the suggestion in EN1991-1-2 Annex A (3) for the parametric time temperature fire curves. The ascending branch is the heating phase of the fire and the descending branch is the cooling phase. When it is referring to those curves, will be done by indicating the heating phase duration that for instance is the same of the ISO standard fire ( $\Gamma = 1$ ). As it is possible to see an horizontal plateau is present after the descending branch, in which the temperature is kept constant at 20 °C until 500 minutes (almost 8 hours). This is why the elevated thermal inertia in the concrete is able to keep the temperature on the central zone in the section and release it after the fire burnout, making the concrete elements more prone to delayed failure (17). So it may be interesting

monitoring the frame for more time after the fire burnout. The heated section will be the central column one.

### 6.2.3 Convergence criteria and settings

“In order to converge to a solution, a tolerance value has to be specified in the program. SAFIR® use an iterative procedure to converge on the correct solution for each increments; a good precision value is dependent on the type of structure that is being analyzed. Suggested value for dynamic analysis is 0.0005 and the convergence procedure for beam type element is the “PURE\_NR” Newton Raphson” (13). Since the reinforced concrete is composed from two materials and generally the resistance to fire is bigger than steel (imply longer fire curves in terms of time) usually the duration time for each analysis is longer than steel. For this reason for all the analysis performed in order to find the DHP indicator there were used a reversible tensile strength behavior for the steel and ETC model for the concrete, as a precision a value of 1e-2 and as a come back a value of 1e-3. The convergence procedure adopted was the suggested one, Newton Raphson.

Since this kind of settings are not the finest choice, but at the same time useful to speed up the various analysis performed, once has been found the DHP indicators for each geometry and fire adopted, a parametrical analysis will be done upon only the DHP indicators couple of value (load ratio and Fire severity) with a more refined model.

In particular it will be adopted a non-reversible tensile steel behavior with a decrease in yield strength of 0.3 MPa/°C when the temperature exceed a value of 600°C, then as precision a value of 1e-04 and as a comeback a value of 1e-04.

Settings	Precision	Comeback	Tensile Steel Behavior
<b>Less Refined</b>	1e-02	1e-03	Reversible
<b>More Refined</b>	1e-04	1e-04	Non Reversible

**Table 13 - Convergence criteria settings, material proprieties**

In table 13 is summarized what stated above, practically in order to find the DHP indicators there was used a less refined model and after that only on the DHP indicators a new analysis is run with a more refined data settings in terms of convergence criteria and material behavior.

## 6.3 Results

The results obtained are given presenting first a general outlook and then through DHP indicator frame by frame.

### 6.3.1 General Overview

TEST FRAME	DHP [min]	LOAD RATIO [-]
1	60	0,68
1	90	0,54
2	60	0,7
2	90	0,56
3	60	0,74
3	90	0,6

Table 14 – Test Results, general overview

In table 14 are gathered the simulation done upon the three different frames studied under the two different fire curve selected. DHP stands for the duration of the heating phase for the selected parametric fire curve created with  $\Gamma=1$  as showed in the appendix 8.2, the load ratio associated indicate the minimum applied load in order to have the first failure. The load ratio represents the applied loads on the column element over its ultimate load at ambient temperature. In order to find the ultimate load at ambient temperature for column 3, several analyses are performed for all of the geometry studied (see 8.3).

It is also important to underline that during the whole fire duration, the applied load is kept constant. Therefore, since the load on this structure (see. Figure 63) is given by an uniformly distributed load along all of the beams plus a punctual load above each column in order to have the desired load ratio only the punctual load is increased. This is why it can be more realistic having an uniformly distributed load upon the beams left constant, representing the self weight and accidental loads. In fact by increasing the vertical load upon the column to get the load ratio desired it could be seen as an additional floor upon the structure.

Generally it can be observed that the load ratio to get the first failure is decreasing by the increase of the DHP of the parametric fire curve and for the same fire curve's severity the load ratio increase with the increasing in the beams cross-section. It is remembered that frame 1 has the smallest beams cross-section and frame 3 the biggest, both in terms of section size and steel area.

### 6.3.2 Frame 1

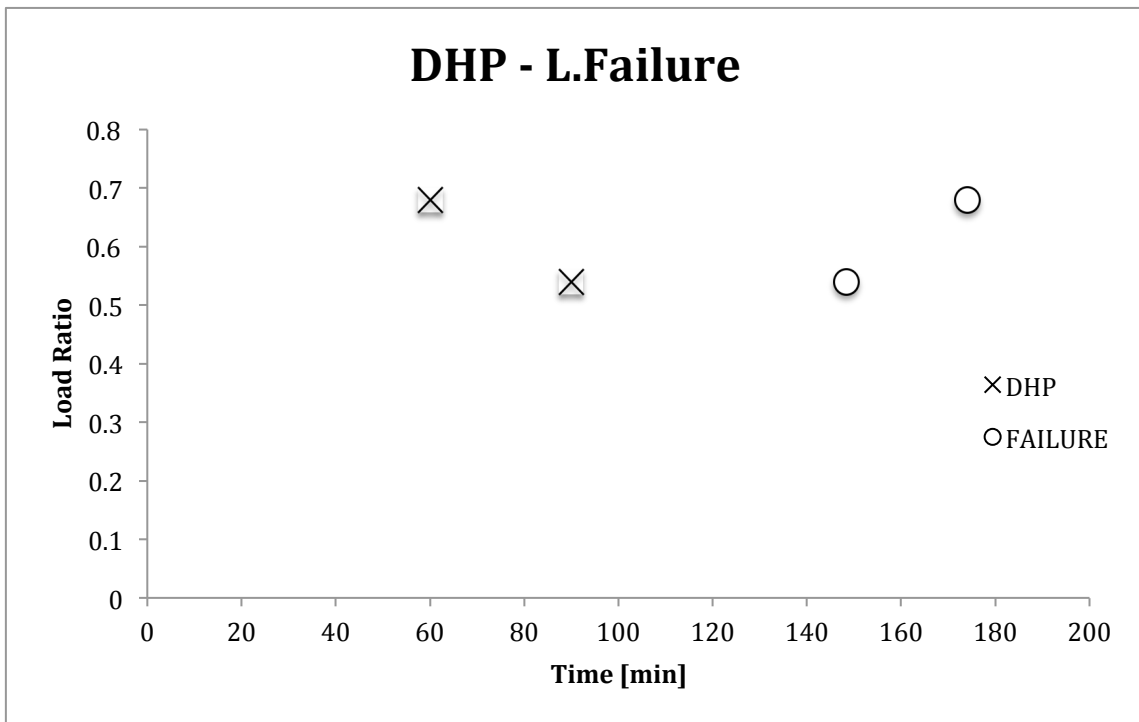
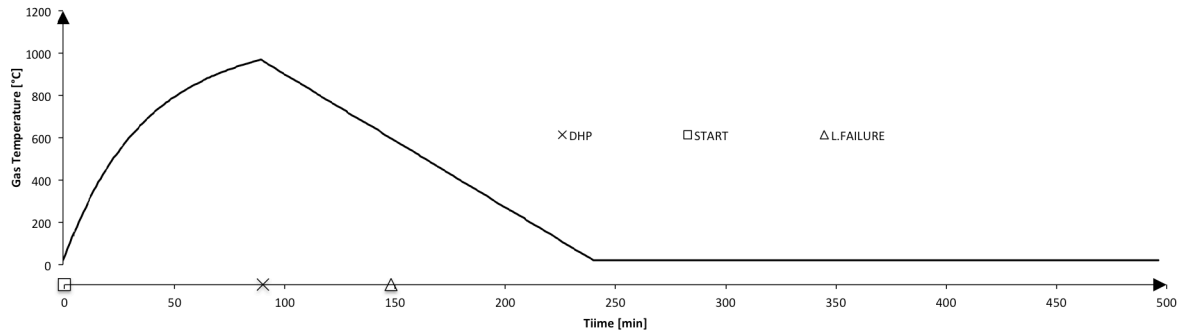


Figure 65 - DHP Indicator, time of local failure, Frame1

In figure 65 the results obtained from the simulations performed upon the frame 1, in terms of DHP indicators (cross shape) and failure time (circle shape). Where the time axe should be read as the duration of heating phase for the DHP indicators related to the selected parametric fire curve. Instead for the time in which the failure appear during the fire for the circle shape. To clarify, if we take the parametric fire curve with a duration of heating phase of 60 minutes and, as a load applied upon the heated column 0.68, not only this is the minimum load ratio needed to see the first failure for the related parametric fire, but also by looking at the circle it is possible to see that the failure appears at 175 minutes.

Therefore it is possible to notice how the failure appears one hour after the heating for the 90 minutes fire curve and two hours after the heating phase for the 60 minutes parametric fire curve. It seems that for a shorter heating phase the failure is more prone to come in a latter stage.

It is here presented the results obtained from the case with the parametric fire of 90 minutes duration heating phase and load ratio applied 0.54.



**Figure 66 - Gas temperature over time**

Figure 66 describe the gas temperature behavior for the parametric fire selected over the times in minutes. In the vertical axe the temperature in °C is indicated, instead in the horizontal axe the time in minutes. On the horizontal axe it is also possible to see the main phases represented with a cross for the duration of heating phase and the moment when the structure has experienced the column's failure is indicated with the triangle.

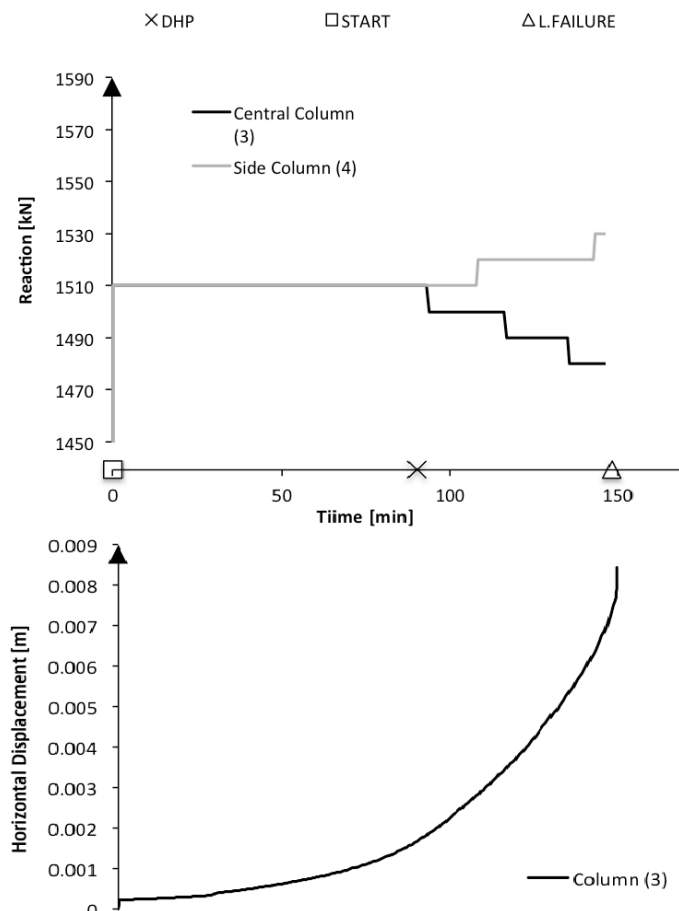


**Figure 67 – General behavior, Base reaction – Horizontal displacement.**

Figure 67 help to understand how the frame behaves in terms of column base reactions and horizontal displacement, measured at half of the height of the central column. In the time axe are also indicated the main phases of the performed simulation, start, DHP and failure. Frame 1 has the smallest beam section, so a sudden interruption of the analysis as happen in this case it can be reasonable, as it has been seen for the steel. It is possible to say that the column failure is not due to the reaching of his maximum capacity in compression under fire, because looking at the horizontal displacement of the central column is clearly visible a sort of vertical asymptote in correspondence of the analysis stopping time. It is also possible to observe from the base reactions graph how after the duration of the heating phase the two columns starting to transfer load from the central to the side one. So it is possible to see this behavior also for concrete. The same kind of behavior is obtained for the parametric fire curve with duration of heating phase of 60 minutes.

By repeating the analysis with the finer convergence settings and different steel behavior, as mentioned in 6.2.3, it was found basically the same result, a local failure of the central column with a sudden interruption of the analysis that does not allow getting more information on the global structural response under cooling.

Frame No.	DHP	Failure time	Load Ratio	Capacity 20°C	Max.Base Reaction	Max Horizontal Displacement
	[min]	[min]	[-]	[kN]	[kN]	[cm]
<b>1</b>	60	174	0,68	2790	1920	0,5
<b>1</b>	90	148	0,54	2790	1530	0,8
<b>1*</b>	60	173	0,68	2790	1920	0,59
<b>1*</b>	90	147	0,54	2790	1530	0,8

**Table 15 - Comparison between different data settings**

In table 15 it is possible to compare the main output from the analysis made with the “less refined settings” and the others obtained with the more refined settings indicated with \*. Where the failure time referring to the time in minutes when the heated column experienced a local failure, the maximum base reaction is given for the side column and the maximum horizontal displacement for the central heated column. Basically the maximum base reaction and horizontal displacement values are almost the same although the precision and the time step adopted were finer. Furthermore no significant variation are registered regarding the time of failure for the heated column, the difference by adopting the non reversible tensile strength behavior is confined in 1 minute.

### 6.3.3 Frame 2 & 3

The results obtained from the other frames, in this case 2 and 3 show basically the same behavior in terms of base reactions and horizontal displacement in the central column. All of the performed simulation stopped prematurely as we have seen in the previous case. For this reason the results will be presented in terms of DHP indicators for both the two frames. With the purpose of does not present the same behavior of the structure under different fire many times, some cases will be shown as seen before, and the other results are given in table by indicating the base reactions and the maximum horizontal displacement at the moment in which the analysis stopped.

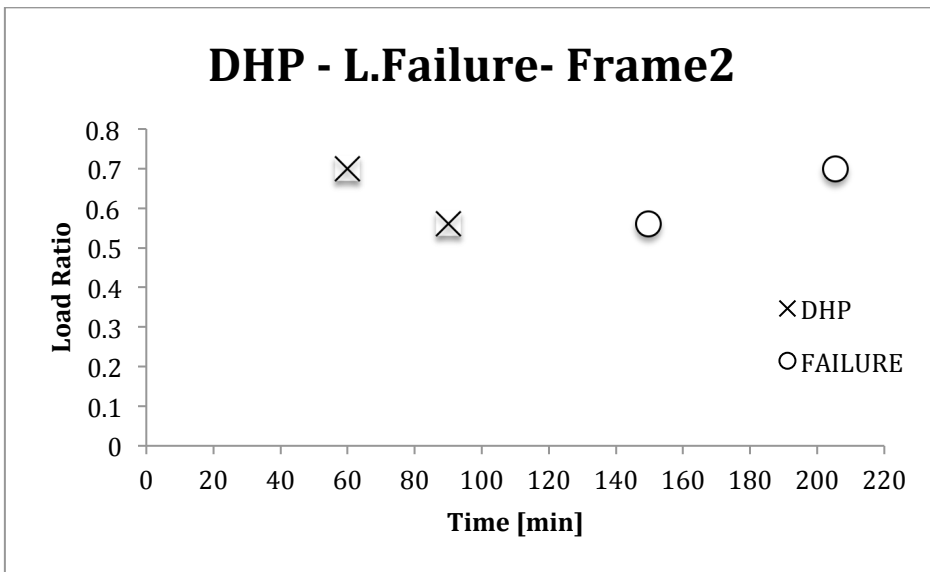


Figure 68 - DHP indicators and Failure time, Frame

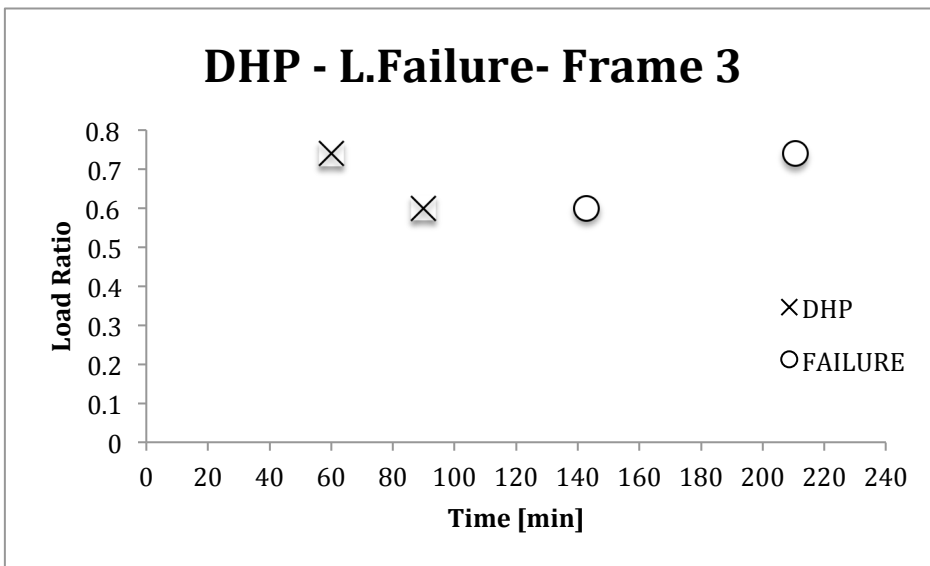
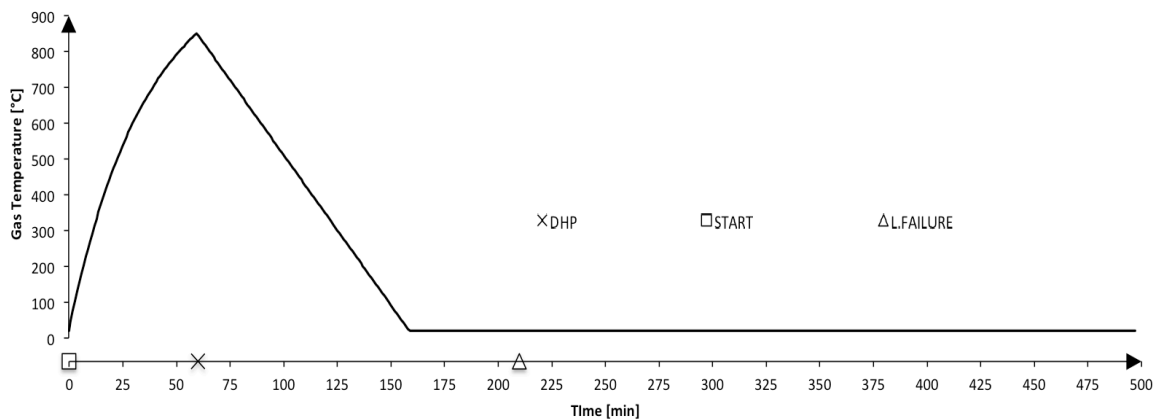


Figure 69 - DHP indicators and Failure time for frame 3

From figure 68-69 it is possible to see the results obtained from the performed simulations upon the frames 2 & 3, in terms of DHP indicators (cross shape) and failure time (circle shape). Where the time axe should be read as the duration of heating phase for the DHP indicator, instead for the time in which the failure appear during the fire for the circle. To clarify, if we take in frame 3, the parametric fire curve with a duration of heating phase of 60 minutes and, as a load applied upon the heated column 0.74, not only this is the minimum load ratio needed to see the first failure for the related parametric fire, but also by looking at the circle it is possible to see that the failure appears at 210 minutes.

Furthermore it is possible to notice as done for frame 1, how the failure appears also for frame 2 and 3 in a latter stage for the less severe fire curve adopted. In particular both frame 2 and 3 show failure after 2 hours the end of the heating phases for a fire curve with DHP 60 minutes. Instead for a fire curve with DHP of 90 minutes in less than 1 hour after the heating phase for both the frames.

The results obtained from frame 3 with a load ratio applied of 0.74 and a parametric fire with 60 minutes of duration of heating phase is shown.



**Figure 70 - Gas Temperature over the time – main phases**

In figure 70 it is plotted the parametric fire curve adopted to test the frame 3 for a load ratio of 0.74. In the horizontal axe the main phases of the simulation are delivered, in particular the starting point, the duration of heating phase and the local failure of the column that appear in a very latter stage, when the gas temperature is at ambient temperature from almost one hour.

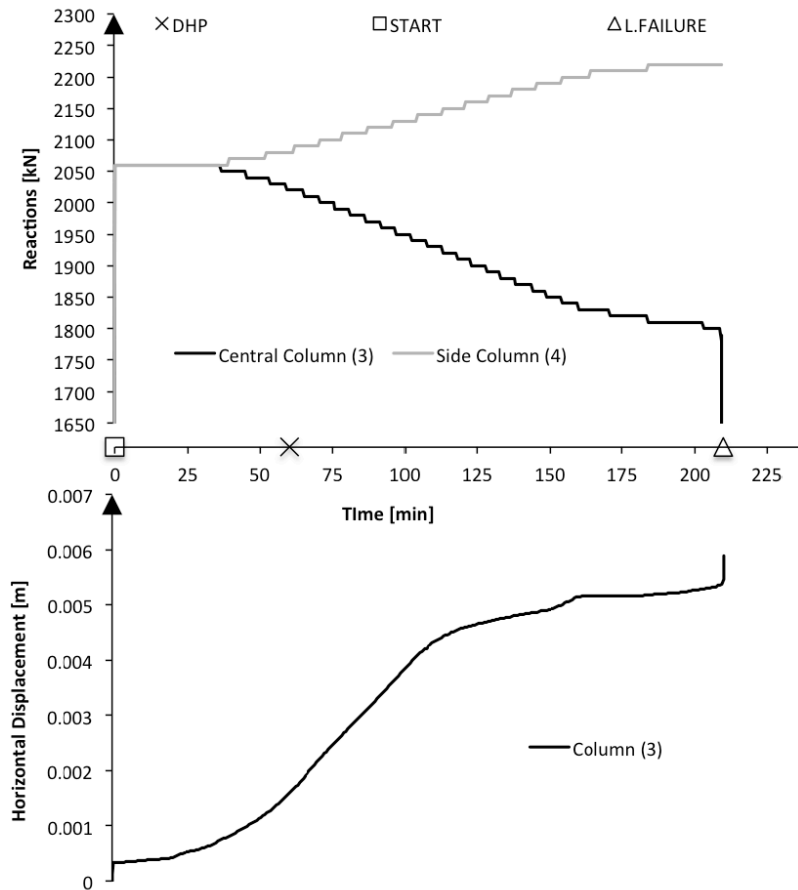


**Figure 71 - General overview**

Figure 71 provides a general overview in terms of column base reactions and horizontal displacement, measured at half of the height of the central column. In the time axis are also indicated the main phases of the performed simulation, start, DHP and failure. If we compare this scenario with the one got from frame 1 (with the smallest beams section) in figure 69, it is possible to see how the different frames have more or less the same behavior. In fact although the base reaction is  $> 0$  it is possible to say that in both cases there is a local failure of the column, for frame 1 due to a large horizontal displacement, and for frame 3 seems due to the reaching of the maximum capacity for the central column under fire. In fact the displacement behavior seems to be quite linear until when a sudden drop of the base reaction appears. In this case with a bigger beams section it is possible to see how the load transfer is more pronounced. In both cases the analysis stopped at the local failure of the heated column, without leaving further information upon the frame behavior as happened for steel.

Frame No.	DHP	Failure time	Load Ratio	Capacity 20°C	Max.Base Reaction	Max Horizontal Displacement
	[min]	[min]	[-]	[kN]	[kN]	[cm]
2	60	205	0,7	2790	2030	0,56
2	90	150	0,56	2790	1620	0,85
2*	60	198	0,7	2790	2030	0,55
2*	90	148	0,56	2790	1620	0,82
3	60	210	0,74	2790	2220	0,58
3	90	143	0,6	2790	1780	0,8
3*	60	197	0,74	2790	2220	0,57
3*	90	132	0,6	2790	1780	0,84

**Table 16 - Comparison between different data settings**

In table 16 are delivered the main results obtained from the different convergence and material setting used (6.2.3). The symbol \* stands for the more refined model. Where the the failure time referring to the time in minutes when the heated column experienced a local failure, the maximum base reaction is given for the side column and the maximum horizontal displacement for the central heated column. As regarding the base reaction and the horizontal displacement, even here as seen for frame 1, are practically identical between the two analyses. The failure time for frame 2 and 3 respect to frame 1 is increased but does not seems to have a considerable delta.

For reinforced concrete structure it was not possible to see the structural response after the heated column's local failure, this fact does not exclude a priori the possibility also for concrete to get different responses as we have seen for steel. As a consequence the conclusion upon concrete should be careful it is not possible to state for sure that the structural response seen here is the only one possible, instead this fact leave open further research and perspectives. This is why more detailed analysis can be done, in terms of different design, convergence criteria and fire severity.

## 7. CONCLUSION

The aim of this study is primarily referred to the investigation of structures behavior when subjected to the full course of the natural fire. The researches made upon this topic are very scares in literature, and having seen recent structural collapse some hours after the fire burnout was an additional stimulus to focus on this kind of works, in particular investigating on the structural response during the fire.

After having found a research upon a real tested steel frame under natural fire, it is noticed a particular force redistribution between the frame's columns that could probably interest the structural vulnerability and its response during the decay phase of the fire. This was the starting point of the work done, in fact by means of numerical analysis it has tried to address the study's aim above mentioned. But before starting to run multiple numerical analyses it has been done the validation of the non-linear finite element software adopted in order to conduct the principal part of the study. The validation was performed on the real steel tested frame and it has been established the software reliability in one hand, and on the other, by confirming the capability of the software to capture the main structural behavior under fire condition it is confirmed also the reliability of the results presented.

A steel frame with the central column subjected to natural fire was modeled and studied by varying fire severity, beams section and load applied. It is addressed the structural response during the whole course of the natural fire in particular referred to the decay phase. From the work done it is possible to list the main founding:

- Structural steel frame under natural fire can fail during the fire decay phase
- The failure can be local (column instability) or Global, principally depending on the geometry of the structure
- The global failure is triggered from load redistribution phenomena during the decay phase of the fire
- In some cases generally for big beams sections after the local failure of the heated column the structure shows global stability for the whole fire duration.
- It has been seen how increasing beams section is not always a gain for the global stability of the structure. In some cases with the biggest beams section the load redistribution phenomena upon the unheated column became more pronounced, make it fail provoking a sudden collapse of the entire structure.

A reinforced concrete frame was modeled and studied as it was done for the steel. From the results obtained it is possible to conclude:

- Reinforced concrete frame can experienced a failure at least local (regarding the heated element) during the decay phase of a fire
- Less severe fire curves in terms of duration of heating phase, with the same load condition lead to a latter stage failure also after the complete fire burnout.

### **PERSPECTIVES**

Improving the actual knowledge about the structural response of structures under natural fire condition, in particular during the decay phase of a fire, is an urgent need to be satisfied. A better knowledge on the structural and material behavior can reduce drastically the risk put on the fire brigades each time they make an intervention. Furthermore having clear which are the parameters that playing a role and the different structural response will help to have a risk reduction from the design stage. The study carried on the steel gives an outlook on which can be the possible structural responses of a frame subjected to natural fire and the main parameter that are able to play a role. The same result was not found for the concrete structure, which shows only local failure due to the fact that probably convergence has not been reached during the simulation. Obviously further studies about concrete structure should be done in order to find something more starting from the observed phenomena.

## 8. APPENDIX

### 8.1 PARAMETRIC TEMPERATURE-FIRE CURVES

The fire curves applied for all the parametric studies are the parametric fire suggested from EN1991-1-2 (3) , Annex A.

The temperature-time curves in the heating phase are given by:

$$\theta_g = 20 + 1325(1 - 0,324e^{-0,2t^*} - 0,204e^{-1,7t^*} - 0,472e^{-19t^*})$$

**Equation 1 - Gas Temperature during heating**

where:

$\theta_g$  is the gas temperature in the fire compartment [°C]

$t^* = t \cdot \Gamma$  in [h] with t time in [h]

NOTE in case of  $\Gamma = 1$ , equation (1) approximates the standard temperature-time curve.  
The temperature – time curves in the cooling phase are given by:

$$\theta_g = \theta_{MAX} - 625(t^* - t_{MAX}^* \cdot x) \quad \text{for } t_{MAX}^* \leq 0,5$$

$$\theta_g = \theta_{MAX} - 250(3 - t_{max}^*)(t^* - t_{MAX}^* \cdot x) \quad \text{for } 0,5 < t_{MAX}^* < 2$$

$$\theta_g = \theta_{MAX} - 250(t^* - t_{MAX}^* \cdot x) \quad \text{for } t_{MAX}^* \geq 2$$

**Equation 2 - Gas temperature during cooling**

## 8.2 DURATION OF HEATING PHASE (DHP)

The DHP indicator is a key point for this research, it allows classifying and comparing the structural elements analyzed under natural fire curves. Here, it is my intention to show which is the process that leads to obtain the DHP, and at the same time try to clarify as much as possible what this indicator represents, since it is largely used in the output results.

For a certain structural elements there is a natural fire for which the element will fail, in this particular case (referred to DHP) the natural fire is defined from the parametric fire in EN1991-1-2 Annex A (Chapter 8.1) by choosing  $\Gamma = 1$ . With this kind of assumption it is possible to have a well defined time temperature fire curve in heating and cooling phase for a given  $t_{max}$  (duration of heating phase). Furthermore by having  $\Gamma = 1$  in the parametric fire model, makes the heating phase of the fire model approximately equal to the standard ISO curve with obviously a proper decay phase. As previously said the DHP represent the shortest heating phase duration time ( $t_{max}$ ) according to the parametric fire curve used under a certain load ratio, for which it is possible to have the failure of the structural component under fire.

It is important also to underline that the DHP does not give information about the time of collapse that can happen in the different fire phases.

The process behind the acquisition of the DHP for a structural component under a certain load ratio is complex and time demanding. This is why it is an iterative procedure consisting in several analysis done under a fixed  $t_{max}$  by varying in each step the load ratio applied in order to obtain the minimum one that leads to failure. Obviously, because of the iterative procedure, making experimental tests is not possible, so numerical or analytical models should be done.

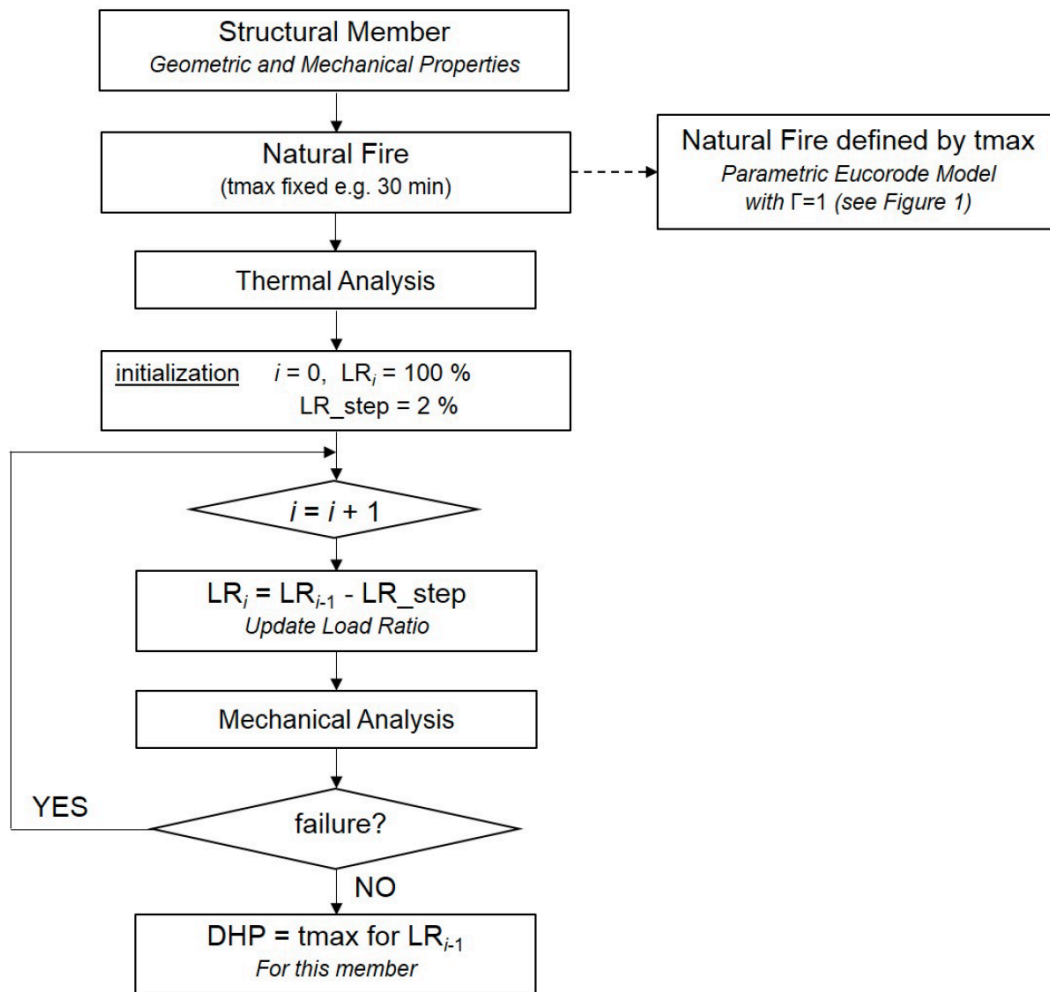


Figure 72 – Fixed Fire curve iterative method to obtain DHP, picture takes from (20)

In figure 72 is well explained the iterative procedure behind the DHP indicators, it has been followed for all the numerical simulation conducted.

### 8.3 Maximum load capacity at ambient temperature

The load ratio used in this study is meant as the ratio of the load applied on the element subjected to fire over its maximum capacity at ambient temperature. In order to evaluate the maximum capacity at ambient temperature for the column studied, a specific analysis is performed. In particular the simulation was done by considering the structure at ambient temperature. Then as load condition a function called “F1PS” that allows having each second an increment of the load applied. In this way when the simulations arrive to the end it is possible to get the maximum capacity at ambient temperature.

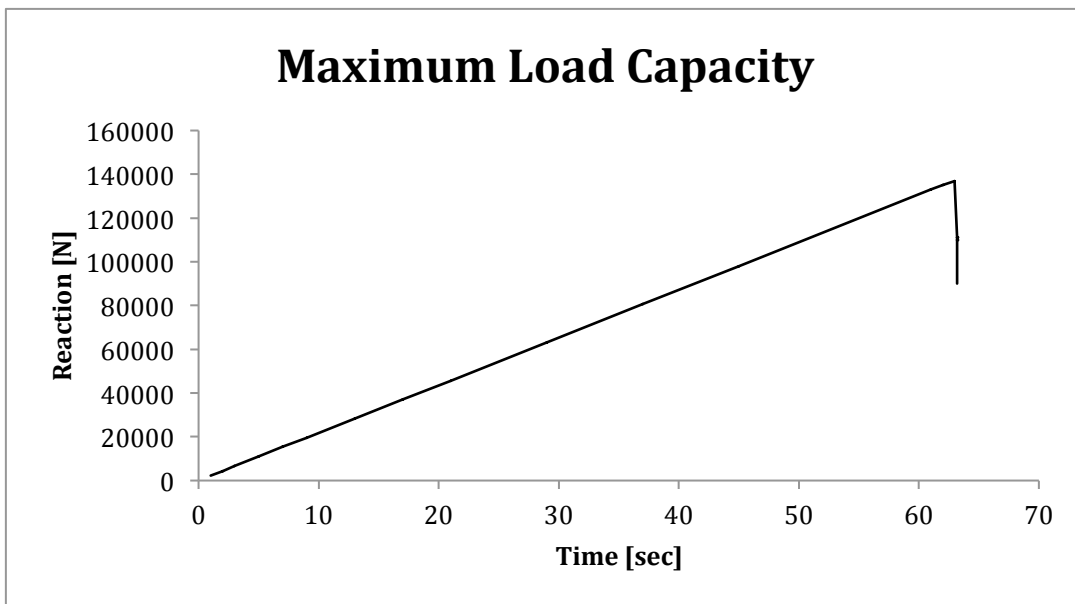


Figure 73 - Output example maximum load capacity

In figure 73 it is shown an output example of the simulation, in particular the vertical axis shows the reaction at the column base and in the horizontal the time. For our purpose the useful data is the maximum column reaction that stands for the maximum capacity at ambient temperature. All of the analyses performed in order to get the maximum capacity for our study purpose are summarized in the table below.

	Frame 1	Frame 2	Frame 3
Steel	68	137	154
Concrete	2790	2790	2790

Table 17 - Maximum capacity at ambient temperature for each Frame modeled in kN

# LIST OF FIGURES

FIGURE 1 - PLASCO BUILDING BEFORE AND AFTER THE EVENT.	1
FIGURE 2 - ISO STANDARD FIRE CURVE EN1991-1-2	4
FIGURE 3 - PARAMETRIC FIRE CURVE APPENDIX A OF EN1991-1-2 (3)	4
FIGURE 4 - CALCAREOUS CONCRETE COMPRESSIVE STRENGTH BEHAVIOR DURING HEATING ACCORDING TO EN1992-1-2 (5)	5
FIGURE 5 - COMPARISON BETWEEN HOT AND RESIDUAL COMPRESSIVE STRENGTH, FROM (4)	6
FIGURE 6 - TEST GEOMETRY, IMAGE TAKES FROM (10)	10
FIGURE 7 - MASS DISTRIBUTION, IMAGES TAKEN FROM (10)	11
FIGURE 8 - FIRE CURVE TESTED FRAME I	12
FIGURE 9 - FIRE CURVE TESTED FRAME II	12
FIGURE 10 - FIRE CURVE TESTED FRAME III	13
FIGURE 11 - THERMOCOUPLES LOCATION, IMAGE TAKES FROM (10)	14
FIGURE 12 - TEMPERATURE EVOLUTION HEATED COLUMN FRAME I, IMAGE TAKES FROM (10)	15
FIGURE 13 - TEMPERATURE EVOLUTION HEATED COLUMN FRAME II, TAKES FROM (10)	16
FIGURE 14 - TEMPERATURE EVOLUTION HEATED COLUMN FRAME III, TAKES FROM (10)	16
FIGURE 15 - DISPLACEMENT GAUGES, TAKES FROM (10)	17
FIGURE 16 - VERTICAL DISPLACEMENT FRAME I, FROM (10)	18
FIGURE 17 - VERTICAL DISPLACEMENT FRAME II, TAKES FROM (10)	18
FIGURE 18 - VERTICAL DISPLACEMENT FRAME III, TAKES FROM (10)	19
FIGURE 19 - STRAIN GAUGES, TAKES FROM (10)	20
FIGURE 20 - STRAINS AT FOOT COLUMN $S_{c2}$ , FRAME I, TAKES FROM (10)	21
FIGURE 21 - STRAINS AT FOOT COLUMN $S_{c2}$ , FRAME II, TAKES FROM (10)	21
FIGURE 22 - STRAINS AT FOOT COLUMN $S_{c2}$ , FRAME III, FROM (10)	22
FIGURE 23 - RECTANGULAR HOLLOW SECTION	24
FIGURE 24 - VOID CONDITION	25
FIGURE 25 - BEAM CROSS-SECTION	26
FIGURE 26 - HEATED COLUMN CROSS-SECTION	26
FIGURE 27 - E.I. MATERIAL PROPERTIES	27
FIGURE 28 - FRAME CONSTRAINTS	28
FIGURE 29 - LOAD CASES FOR EACH DIFFERENT TEST FRAME	30
FIGURE 31 - COMPARISON OF TEMPERATURE EVOLUTION, HEATED COLUMN FRAME I	32
FIGURE 32 - COMPARISON OF TEMPERATURE EVOLUTION, HEATED COLUMN FRAME II	32
FIGURE 33 - COMPARISON OF TEMPERATURE EVOLUTION, HEATED COLUMN FRAME III	33
FIGURE 34 - COMPARISON OF VERTICAL DISPLACEMENT V4 FRAME I	34
FIGURE 35 - COMPARISON OF VERTICAL DISPLACEMENT V4 FRAME II	35
FIGURE 36 - COMPARISON OF VERTICAL DISPLACEMENT V4 FRAME III	35
FIGURE 37 - VERTICAL REACTION, FRAME I, TIME 20 SECONDS	37
FIGURE 38 - VERTICAL REACTIONS, FRAME I, TIME 2100 SECONDS	37
FIGURE 39 - VERTICAL REACTIONS, FRAME II,	38
FIGURE 40 - REFERENCE MODEL - GEOMETRY	39
FIGURE 41 - EXAMPLE SIMILAR TO FRAME 2, PICTURES TAKES FROM (18)	41
FIGURE 42 - EXAMPLE SIMILAR TO FRAME 3, A PICTURE TAKES FROM (19)	42
FIGURE 43 - PARAMETRIC FIRE CURVES ADOPTED	43
FIGURE 44 - DHP INDICATORS, FRAME 1	46

FIGURE 45 - BEHAVIOR DURING THE TEST, RELEVANT CASE 1, FRAME 1	47
FIGURE 46 - REACTIONS-DISPLACED CONFIGURATION	48
FIGURE 47 - DHP INDICATORS FRAME 2	49
FIGURE 48 - COMPARISON DHP INDICATORS, FRAME 1 & 2	50
FIGURE 49 - GENERAL BEHAVIOR, RELEVANT CASE 2 FRAME 2	51
FIGURE 50 - REACTIONS-DISPLACED CONFIGURATION	52
FIGURE 51 - DHP INDICATORS, FRAME 3	54
FIGURE 52 - GENERAL BEHAVIOR, RELEVANT CASE 3, FRAME 3	55
FIGURE 53 - EVOLUTION OF THE AXIAL FORCE DURING THE FIRE, RELEVANT CASE 3, FRAME 3	56
FIGURE 54 - GENERAL BEHAVIOR, RELEVANT CASE 3, FRAME 3, NON-REVERSIBLE TENSILE STRENGTH BEHAVIOR	57
FIGURE 55 - EVOLUTION OF THE AXIAL FORCE DURING THE FIRE, RELEVANT CASE 3, FRAME 3 NON REVERSIBLE BEHAVIOR.	58
FIGURE 56 - GENERAL BEHAVIOR, RELEVANT CASE 4, FRAME 3	59
FIGURE 57 - REACTIONS - DISPLACED CONFIGURATION	61
FIGURE 58 - FRAME RESPONSE OVERVIEW	63
FIGURE 59 - FRAME RESPONSE OVERVIEW	64
FIGURE 60 - FRAME RESPONSE OVERVIEW	65
FIGURE 61 - REINFORCED CONCRETE GEOMETRY	66
FIGURE 62 - COLUMN & BEAM MODEL	68
FIGURE 63 - LOAD APPLIED	70
FIGURE 65 - DHP INDICATOR, TIME OF LOCAL FAILURE, FRAME1	74
FIGURE 66 - GAS TEMPERATURE OVER TIME	75
FIGURE 67 - GENERAL BEHAVIOR, BASE REACTION - HORIZONTAL DISPLACEMENT.	75
FIGURE 68 - DHP INDICATORS AND FAILURE TIME, FRAME	77
FIGURE 69 - DHP INDICATORS AND FAILURE TIME FOR FRAME 3	77
FIGURE 70 - GAS TEMPERATURE OVER THE TIME - MAIN PHASES	78
FIGURE 71 - GENERAL OVERVIEW	79
FIGURE 72 - FIXED FIRE CURVE ITERATIVE METHOD TO OBTAIN DHP, PICTURE TAKES FROM (20)	85
FIGURE 73 - OUTPUT EXAMPLE MAXIMUM LOAD CAPACITY	86

# Lists of Tables

TABLE 1 - DETAILS OF MEMBER SECTIONS (MM)	10
TABLE 2 - MATERIAL PROPRIETIES	10
TABLE 3 - DETAILS OF WEIGHT CARRIED BY THE TEST FRAME	11
TABLE 4 THERMAL AND MECHANICAL PROPRIETIES	40
TABLE 5 - BEAMS SECTION	41
TABLE 6 – TEST RESULTS, GENERAL OVERVIEW	44
TABLE 7 – RELEVANT CASE CLASSIFICATION	62
TABLE 8 - COLUMNS SECTIONAL PROPRIETIES	67
TABLE 9 - BEAMS PROPRIETIES	67
TABLE 10 – FRAME MODELS	67
TABLE 11 - MATERIAL PROPRIETIES	69
TABLE 12 - DISTRIBUTED LOADS ON THE BEAMS	70
TABLE 13 - CONVERGENCE CRITERIA SETTINGS, MATERIAL PROPRIETIES	72
TABLE 14 – TEST RESULTS, GENERAL OVERVIEW	73
TABLE 15 - COMPARISON BETWEEN DIFFERENT DATA SETTINGS	76
TABLE 16 - COMPARISON BETWEEN DIFFERENT DATA SETTINGS	80
TABLE 17 - MAXIMUM CAPACITY AT AMBIENT TEMPERATURE FOR EACH FRAME MODELED IN kN	86

## BIBLIOGRAPHY

- [1] SwissInfo.ch; Seven firefighters killed; <https://www.swissinfo.ch/eng/seven-firefighters-killed/4222382> >[Accessed 05.10.17]
- [2] aljazeera.com., 20 dead in Plasco building collapse: <http://www.aljazeera.com/news/2017/01/tehran-fire-170119082905960.html> >[Accessed 8.5.17]
- [3] EN 1991-1-2. Eurocode 1: actions on structures - Part 1-2 general actions - actions on structures exposed to fire. (2002). Brussels: CEN.
- [4] Yi-Hai L, Franssen J. M. Test results and model for the residual compressive strength of concrete after a fire. Journal of Structural Fire Engineering. (2011).
- [5] EN1992 -1 -2 .Eurocode 2 : Design of concrete structures, part 1-2: General rules - Structural fire design. Brussels: CEN. (2004).
- [6] EN1994-1-2. Eurocode 4 : Design of composite composite steel and concrete structures – Part 1-2: General rules - Structural fire design. Brussels: CEN. (2004).
- [7] Kirby BR, Lapwood D.G., Thomson G. The reinstatement of fire damaged steel and iron framed structures. London, UK: B.S.C. (1986).
- [8] A performance indicator for structures under natural fire. T. Gernay, J.M. Franssen. Liege, Belgium: Elsevier Ltd. (2015).
- [9] Mao X, Kodur VKR. Fire resistance of concrete encased steel columns under 3-and 4-side standard heating. Michigan: Journal of Constructional Steel Research. (2011).
- [10] Binhui Jiang, Guo-qiang Li, Liulian Li, B.A. Izzuddin - Experimental studies on progressive collapse resistance of steel moment frames under localized fire. Journal of Structural Engineering. (In press).
- [11] [http://www.uee.ulg.ac.be/cms/c\\_2383458/en/safir](http://www.uee.ulg.ac.be/cms/c_2383458/en/safir) > [Accessed 16.5.17]
- [12] J.M. Franssen, T. Gernay; Users manual of SAFIR 2016 - Thermal. (Vers.2016.c.0).
- [13] J.M. Franssen, T. Gernay; Users manual of SAFIR 2016 - mechanical. (2016).

- [14] EN 1992-1-1. Eurocode 2:Design of concrete structures - Part 1-1: General rules and rules for buildings. Brussels: CEN. (2004).
- [15] EN 1993-1-2. Eurocode 3 : Design of steel structures - Part 1-2: General rules-Structural fire design. Brussels. (2005).
- [16]. J.M.Franssen, T.Gernay. SAFIR manual - Material propieties. Liege. (2016).
- [17] T.Gernay, M.S.Dimia. Structural behavior of concrete columns under natural fires (Vol. 30). EMERALD. (2012).
- [18] <http://www.understandconstruction.com/steel-frame-structures.html> >[Accessed 13.5.17]
- [19] Alibaba.com; [https://www.alibaba.com/product-detail/ISO9001-High-rise-steel-structure building\\_1060159932.html](https://www.alibaba.com/product-detail/ISO9001-High-rise-steel-structure-building_1060159932.html) >[Accessed 13.5.17]
- [20] T.Gernay ; A method for measuring the sensitivity of building structural members to fire decay phases. Vol.56 NO.4/2016 ;Acta Polytechnica 56(4):344-352,2016